LBL-18727
c.2

Lawrence Berkeley Laboratory

UNIVERSITY OF CALIFORNIA

RECEIVED
LAWRENCE
BERKELEY LABORATORY
JAN 7 1985
LIBRARY AND
DOCUMENTS SECTION

Materials & Molecular Research Division

[8]ANNULENE COMPLEXES OF THE LANTHANIDES

S.A. Kinsley
(Ph.D. Thesis)

November 1984

TWO-WEEK LOAN COPY
This is a Library Circulating Copy
which may be borrowed for two weeks

LBL-18727
c.2

Prepared for the U.S. Department of Energy under Contract DE-AC03-76SF00098

DISCLAIMER

This document was prepared as an account of work sponsored by the United States Government. While this document is believed to contain correct information, neither the United States Government nor any agency thereof, nor the Regents of the University of California, nor any of their employees, makes any warranty, express or implied, or assumes any legal responsibility for the accuracy, completeness, or usefulness of any information, apparatus, product, or process disclosed, or represents that its use would not infringe privately owned rights. Reference herein to any specific commercial product, process, or service by its trade name, trademark, manufacturer, or otherwise, does not necessarily constitute or imply its endorsement, recommendation, or favoring by the United States Government or any agency thereof, or the Regents of the University of California. The views and opinions of authors expressed herein do not necessarily state or reflect those of the United States Government or any agency thereof or the Regents of the University of California.

LBL-18727

[8]ANNULENE COMPLEXES OF THE LANTHANIDES

Steven Anthony Kinsley

Ph.D. Thesis

Lawrence Berkeley Laboratory
University of California
Berkeley, California 94720

November 1984

This work was supported by the Director, Office of Energy Research, Office of Basic Energy Sciences, Chemical Sciences Division of the U.S. Department of Energy under Contract No. DE-AC03-76SF00098.

Acknowledgement

I wish to thank Allan Zalkin for his helpful discussions and for his solving of the crystal structures presented in this thesis. Thanks also to John Rigsbee, Scott Gronert and Kelly Moran for their contributions to some of the work presented in this thesis.

I have had the good fortune to have worked with two excellent advisors and teachers, Andrew Streitwieser and John Forsberg. Their guidance and understanding is greatly appreciated. Finally, I also thank Ken Smith, Jon Swanson and Steve Bachrach for their many interesting and enjoyable chemical discussions.

This work was supported by the Director, Office of Energy Research, Office of Basic Energy Sciences, Chemical Sciences Division of the U.S. Department of Energy under Contract No. DE-AC03-76SF00098.

Table of Contents

I. A REVIEW OF THE [8]ANNULENE COMPLEXES OF THE ACTINIDES AND LANTHANIDES

Introduction.....1

Bis([8]annulene)actinide(IV) complexes.....3

Bis([8]annulene)actinate(III) anions.....16

Bis([8]annulene)lanthanate(III) anions.....16

Mono([8]annulene)actinate(IV) complexes.....23

Mono([8]annulene)lanthanate(III) complexes.....26

References and Notes.....31

II. [8]ANNULENE COMPLEXES OF YTERBIUM(II) AND CALCIUM(II)

Introduction.....37

Results and Discussion.....52

Experimental.....96

Appendix A.....105

Appendix B.....111

Appendix C.....117

References and Notes.....121

III. NEW STUDIES ON BIS([8]ANNULENE)CERIUM(IV)

Introduction.....127

Synthesis and Characterization.....143

Further Studies on bis([8]annulene)cerium(IV).....159

Experimental.....168

References and Notes.....175

IV. VIBRATIONAL SPECTRA OF BIS([8]ANNULENE) COMPLEXES

Introduction.....181

Applications.....191

References and Notes.....201

CHAPTER ONE

A Review of the [8]Annulene Complexes of the Actinides and Lanthanides

Introduction

Bis([8]annulene)uranium(IV)[1], uranocene, was prepared as an expected f-orbital analoque to d-transition metal metallocenes. In d-transition metal complexes such as ferrocene, an important amount of ring-metal covalency is achieved by the interaction of the highest occupied ligand MOs (e_{1g}) of two cyclopentadienyl anions with the unoccupied $3d_{\pm 1}$ orbitals on Fe^{2+}. By analogy, a ring-metal interaction is symmetry permitted between the interaction of the highest occupied MOs of two [8]annulene dianions with two lanthanide or actinide metal f-orbitals ($l = \pm 2$). An empirical model depicting this interaction is shown in Figure 1.1. In this example, the central metal ion shown, uranium(IV), has two electrons remaining in metal f-orbitals; thus, the HOMO of uranium(IV) is located on the metal.

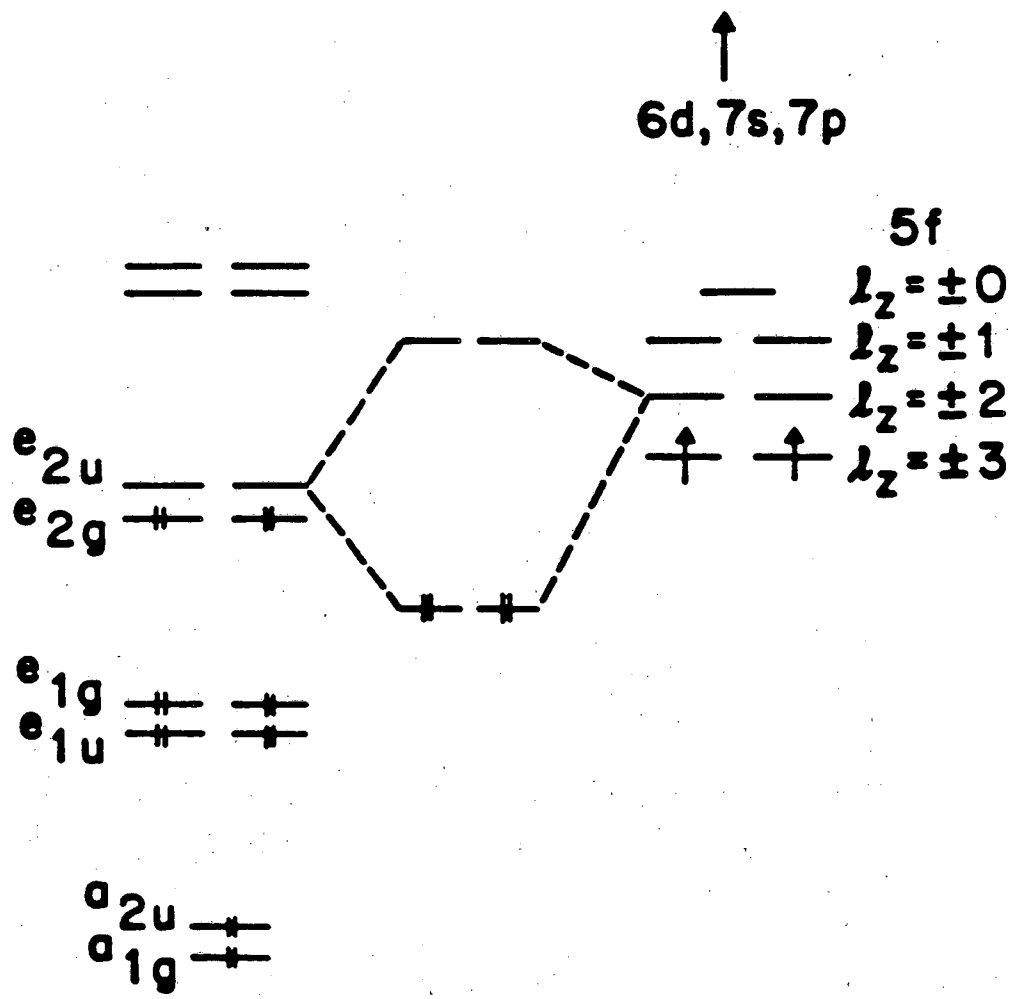

Figure 1.1: e_{2u} orbital interactions in and bis([8]annulene)uranium(IV).

Since the synthesis of bis([8]annulene)uranium(IV),[2] there have been many other complexes synthesized involving a lanthanide or actinide element and one or more [8]annulene dianions. All of these complexes are unstable towards air (most are pyrophoric) and water; all handling of these complexes must be carried out in an inert atmosphere.

This chapter reviews the synthesis and structures of the f-block metal [8]annulene dianion complexes. For the purpose of this chapter, the [8]annulene dianion complexes of the actinides and lanthanides have been classified as bis- or mono-[8]annulene complexes and are further classified by oxidation state of the f-block metal (+3 and +4 for actinides, +2, +3, and +4 for lanthanides).

Bis([8]annulene)actinide(IV) complexes

Bis([8]annulene)uranium(IV) and its ring alkylated,[3-7] arylated[8-10] and annulated[11-13] derivatives constitute the majority of the [8]annulene complexes known for the tetravalent actinides. The synthesis of the other bis([8]annulene)-actinide(IV) complexes is similar to that of the uranium systems.

The most utilized reaction for the synthesis of bis([8]annulene)actinide(IV) complexes is the reaction of a tetrahydrofuran (THF) solution of [8]annulene dianion with a stoichiometric

amount of the actinide tetrachloride in THF (1.1). This method has been employed for the synthesis of bis([8]annulene)-thorium(IV) (thorocene),[14] -protactinium(IV) (protactinocene),[15] -uranium(IV)[2] and -neptunium(IV) (neptunocene),[16] however, the yield of bis([8]annulene)protactinium by this method is low. Bis-([8]annulene)plutonium(IV), plutonocene, is synthesized by the reaction of tetraethylammonium hexachloroplutonate(IV) suspended in THF with a stoichiometric amount of [8]annulene dianion in THF (1.2).[16]

$$2\ K_2C_8H_8 + AnCl_4 \xrightarrow[\text{THF}]{} An(C_8H_8)_2 + 4\ KCl \qquad [1.1]$$

$$2\ K_2C_8H_8 + (C_5H_5NH)_2PuCl_6 \xrightarrow[\text{THF}]{} Pu(C_8H_8)_2 + 4\ KCl + 2\ C_5H_5N^+Cl^- \qquad [1.2]$$

Curiously, attempts to synthesize bis([8]annulene)plutonium(IV) using cesium- or pyridinium hexachloroplutonate(IV), Cs_2PuCl_6 or $(C_5H_5NH)_2PuCl_6$, were unsuccessful, but the synthesis of bis([8]-annulene)uranium(IV) from $(C_5H_5NH)_2UCl_6$ was successful.[16]

Bis([8]annulene)thorium(IV), -uranium(IV) and -plutonium(IV) can also be synthesized by the reaction of cyclooctatetraene with the finely divided metals obtained by heating the metal hydrides (1.3).[17] In this reaction, a sealed Pyrex tube containing the actinide-cyclooctatetraene mixture is heated in a tube furnance

at 150-160° C. The reaction product is isolated by sublimation. This preparative method provides demonstration of the thermodynamic stability of the bis([8]annulene)actinide complexes.

[1.3]

$$An^{\circ} + C_8H_8 \text{ ------> } An(C_8H_8)_2$$

The bis(1,3,5,7-tetramethyl[8]annulene)actinide(IV) complexes made from 1,3,5,7-tetramethyl-cyclooctatetraene have been synthesized for many of the actinide elements. The synthesis of 1,3,5,7-tetramethyl-cyclooctatetraene is shown in Figure 1.2.[18, 19]

Figure 1.2: Synthetic scheme for 1,3,5,7-tetramethyl-cyclooctatetraene

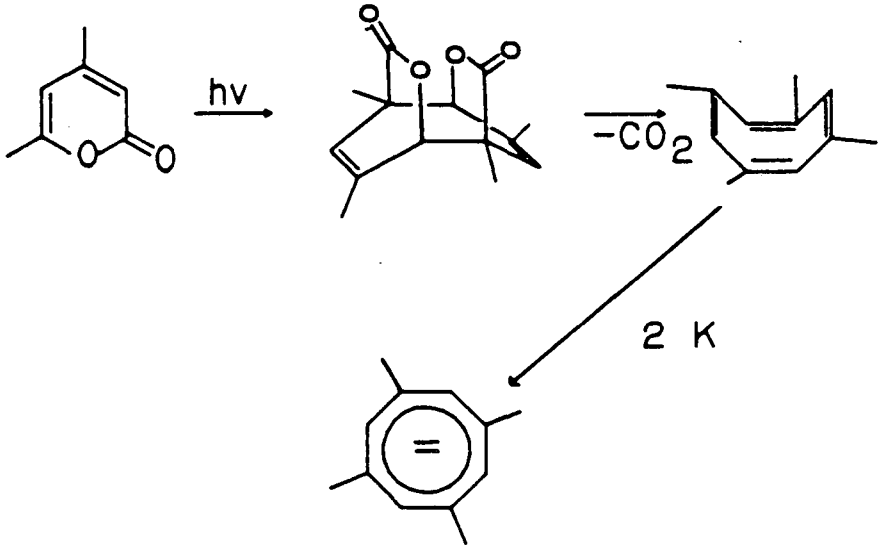

Treatment of 1,3,5,7-tetramethyl-cyclooctatetraene with two equivalents of potassium gives the corresponding [8]annulene dianion. Bis(1,3,5,7,tetramethyl[8]annulene)thorium(IV),[20] -uranium(IV),[19] -neptunium(IV)[19, 21] and -protactinium(IV)[21] have all been synthesized by the addition of 1,3,5,7-tetramethyl[8]-annulene dianion to the appropriate actinide salt (1.4).

[1.4]

$$2\ K_2(Me_4C_8H_4) + AnCl_4 \xrightarrow[THF]{} An(Me_4C_8H_4) + 4\ KCl$$

Attempts to make the bis(1,3,5,7-tetramethyl[8]annulene)plutonium(IV) derivative by addition of tetramethyl[8]annulene dianion to plutonium tetrachloride resulted in the reduction of Pu(IV) by the tetramethyl[8]annulene dianion to Pu(III).[19] When the borohydride complexes of neptunium and plutonium are used in place of the halide salts acceptable yields of the bis(tetramethyl[8]annulene) complexes were obtained (1.5).[21]

[1.5]

$$2\ K_2(Me_4C_8H_4) + An(BH_4)_4 \xrightarrow[THF]{} An(Me_4C_8H_4) + 4\ KBH_4$$

Other substituted bis([8]annulene)actinide(IV) complexes for uranium[3-13] thorium[20], neptunium[4] and plutonium[4] have been prepared by the reaction of the substituted [8]annulene dianion with the appropriate actinide(IV) salt. X-ray diffraction data suggest that the alkyl-substituted neptunium(IV) and plutonium(IV) complexes are isomorphous with the corresponding

uranium(IV) complex;[4] none of the structures of these complexes have yet been determined from single crystal x-ray diffraction.

The mechanism of the reaction to form the bis([8]annulene) complexes is not known. It is clear, however, that there are differences in the mechanism in the formation of bis([8]annulene)-uranium(IV) vs. bis([8]annulene)thorium(IV). When the reaction of two equivalents of n-butyl[8]annulene dianion with thorium tetrachloride was carried out in an NMR tube and monitored by ^{1}H-NMR, a resonance was observed which cannot be attributed to the bis([8]annulene) complex.[22] Further experiments showed that this apparent intermediate in the reaction is the mono-ring complex, ([8]annulene)thorate(IV) dichloride.[22] The mechanism for the formation of bis([8]annulene)thorium(IV) evidently involves the stepwise substitution of [8]annulene dianion for two chloride ions (figure 1.3). In the analogous uranium system, however, no intermediate mono-ring complexes have been observed.

Figure 1.3: Reactions for the formation of bis([8]annulene)thorium(IV).

$$K_2C_8H_8 + ThCl_4 \text{ -----> } (C_8H_8)ThCl_2 + 2\ KCl$$

$$K_2C_8H_8 + (C_8H_8)ThCl_2 \text{ -----> } Th(C_8H_8)_2 + 2\ KCl$$

Uranium, unlike thorium, has an accesible trivalent oxidation state. It has been shown that bis([8]annulene)uranium(IV) can be reduced by lithium naphthalide to the bis([8]annulene)uranate(III) anion (1.6).[23] The same complex can be synthesized by the reaction of two equivalents of [8]annulene dianion with one equivalent of uranium trichloride (1.6).[23]

[1.6]

$$U(C_8H_8)_2 + Li(C_{12}H_{10}) \xrightarrow[THF]{} Li[U(C_8H_8)_2] + C_{12}H_{10}$$

or

$$2\ K_2C_8H_8 + UCl_3 \xrightarrow[THF]{} K[U(C_8H_8)_2] + 3\ KCl$$

It has been found that [8]annulene dianion reduces uranium tetrachloride to uranium trichloride when the reaction is carried out at -78° C.[24] When two equivalents of [8]annulene dianion in THF are added to one equivalent of uranium tetrachloride in THF at -78° C, the green color of uranium tetrachloride changes to the purple color of the trichloride. As this reaction mixture is warmed slowly to room temperature, the color of the reaction changes to the dark green color of bis-([8]annulene)uranium(IV). The yield of bis-([8]annulene)uranium(IV) is not affected in this method of reaction. These reactions indicate that the first step of the reaction to form bis([8]annulene)uranium(IV) is the reduction of the uranium tetrachloride.

Based on the existence of the bis([8]annulene)uranate(III) anion and the reduction of U(IV) to U(III) by [8]annulene

dianion, the following mechanism (Figure 1.4) has been proposed, as an alternative to simple ligand substitution, for the formation of bis([8]annulene)uranium(IV):[24]

Figure 1.4: A Proposed Mechanism for the Formation of Bis-([8]annulene)uranium(IV).

$$UCl_4\ L_x + K_2C_8H_8 \longrightarrow UCl_3\ L_x + KC_8H_8^-$$

$$UCl_3\ L_x + K_2C_8H_8 \longrightarrow (C_8H_8)UCl\ L_x$$

$$(C_8H_8)UCl\ L_x + K_2C_8H_8 \longrightarrow (C_8H_8)_2U(III)$$

$$(C_8H_8)_2U(III) + UCl_4\ L_x \longrightarrow (C_8H_8)_2U + UCl_3\ L_x$$

$$(C_8H_8)_2U(III) + C_8H_8 \longrightarrow (C_8H_8)_2U + KC_8H_8^-$$

Clearly, more work is needed on the mechanism of the formation of bis([8]annulene)actinide(IV) complexes.

Structures of the Bis([8]annulene)actinide(IV) complexes

The crystal structures of some of the bis([8]annulene)actinide complexes are known. Bis([8]annulene)uranium(IV)[25,26] and -thorium(IV)[26] are isostructural (Figure 1.5) with the only major difference observed in the metal-to-carbon bond lengths; this difference reflects the larger crystal radius for thorium(IV) vs. uranium(IV).[27] Both of the molecules have D_{8h} symmetry; the carbon atoms of the [8]annulene rings are eclipsed. X-ray diffraction data and infrared spectra data on bis([8]annulene)neptunium and -plutonium suggest that these complexes are isostructural with bis([8]annulene)uranium and -thorium.[15]

The crystal structure of bis(1,3,5,7-tetramethyl[8]annulene)-uranium(IV) is also known.[28] This complex crystallizes as molecules in two rotomeric configurations (Figure 1.6).

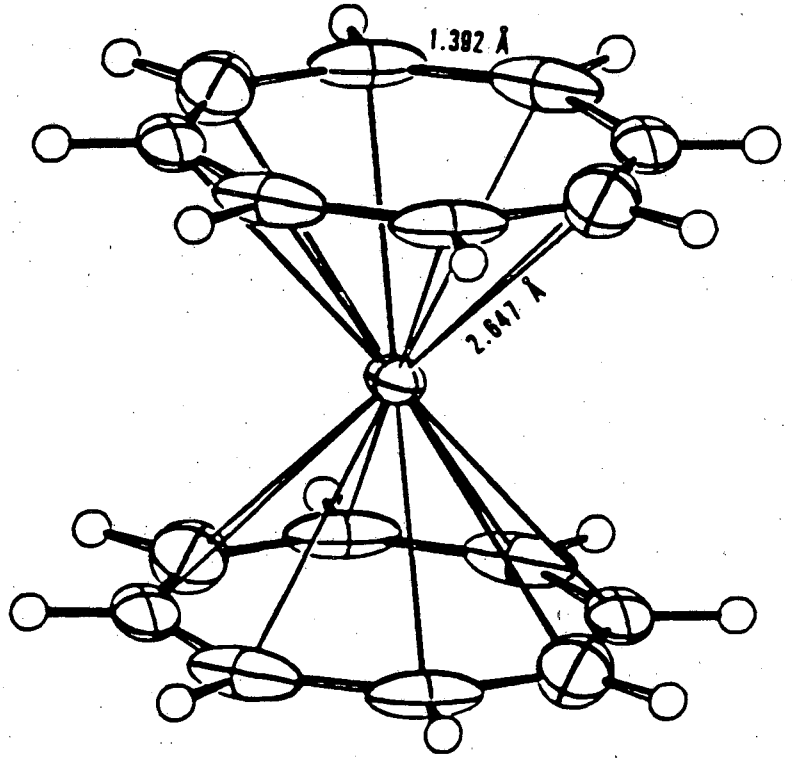

Figure 1.5: Structure of Bis([8]annulene)uranium(IV).

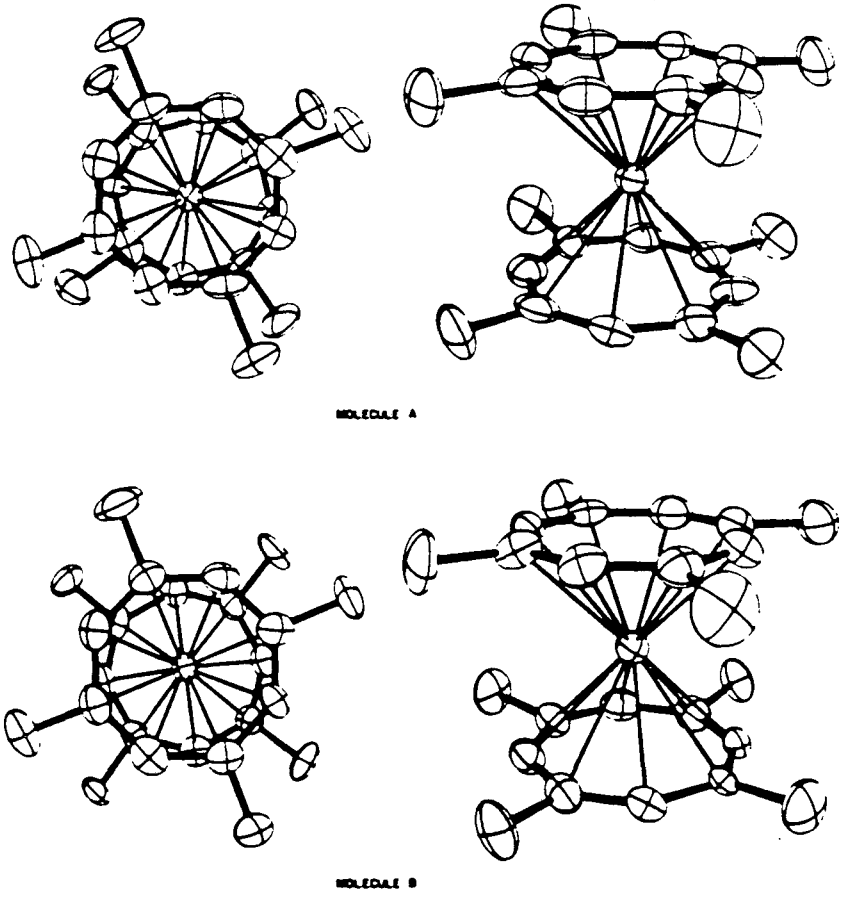

Figure 1.6: Structure of Bis(1,3,5,7-tetramethyl[8]annulene)-uranium(IV) (hydrogen atoms omitted).

In the A form the methyl groups are essentially eclipsed and in the B form the methyl groups are essentially staggered. The methyl groups on the [8]annulene rings are bent out of the plane of the ring by angles ranging from 0.8° to 6.5°. In the A form of this molecule, the methyl groups are separated by 3.76 Å as a result of this bending; this distance is within the Van der Waals contact distance for two methyl groups (4.0 Å).[29] One possible explanation for the bending of the methyl groups is the change in hybridization of the ring carbons to achieve better orbital overlap with the uranium 6d and 5f orbitals. This bending of the methyl group toward the uranium would result from such a change in hybridization (Figure 1.7).

Figure 1.7: Methyl Group Bending in Bis(1,3,5,7-tetramethyl[8]-annulene)uranium(IV).

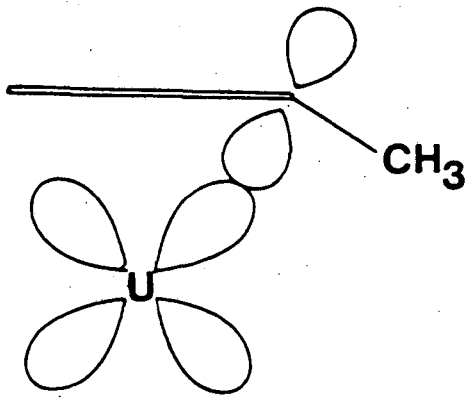

X-ray powder pattern data on bis(1,3,5,7-tetramethyl[8]annulene)protactinium(IV), -neptunium(IV) and -plutonium(IV) indicates that these complexes are isostructural with the uranium complex.[21]

Bis([8]annulene)lanthanide(IV) complexes

There are two reports of the tetravalent lanthanide complex, bis([8]annulene)cerium(IV). This work is discussed, in detail, in the third chapter of this thesis and will not be discussed here.

Theory of Bis([8]annulene)metal(IV) complexes

The existence of bis([8]annulene)actinide(IV) complexes does not by itself establish the existence of a ring-metal bond formed from the interaction of metal d and/or f orbitals with the ligand π orbitals. One method of establishing the importance of d and f orbital participation of bonding in these complexes is to compare experimental results, for example, photoelectron spectra, with predictions from calculational methods.

Early MO calculations (LCAO) by Hayes and Edelstein[30] on bis([8]annulene)actinide(IV) complexes did indeed indicate that there was significant interaction between the ligand e_{2u} orbitals and the metal $5f_{\pm 2}$ orbitals. In these calculations, only the ligand π orbitals and the metal f orbitals were used, since it was considered that the metal d-orbitals of the actinides were

too high in energy to have significant interaction with the ligand MOs.

One important consequence of the early model of bonding is that the interaction of the metal $f_{\pm 2}$ orbitals with the e_2 ligand π-MOs leads to the energy level ordering $e_{2g} > e_{2u}$ (as shown in figure 1.1) for the bis([8]annulene) sandwich complexes. The first photoelectron spectra (PES) bis([8]annulene)thorium(IV) and -uranium(IV)[31, 32] were interpreted on this basis, but later work by Clark and Green,[33] in which the spectral changes due to He-I or He-II ionizing light were compared, led to the assignment of $e_{2u} > e_{2g}$. This assignment suggests that there is participation of the metal d orbitals in the bonding scheme.

A more complete bonding model from the Xα scattered-wave (SW) treatment of bis([8]annulene)uranium(IV) and -thorium(IV) was proposed by Rösch and Streitwieser.[34] Agreement with the PES was remarkably good, considering that relativistic effects had not been included in the calculations. These calculations supported the assignment of ionization potentials by Clark and Green and verified that the contribution of the metal d orbitals to the ring metal bond in these complexes is at least as important as the contribution of the metal f orbitals.

Recently, the quasirelativistic Xα SW MO calculations on bis-([8]annulene)uranium(IV), -thorium(IV) and -cerium(IV) were reported.[35] These calculations show remarkably good agreement

with the PES spectra of bis([8]annulene)uranium(IV) and -thorium(IV). As is the case for non-relativistic calculations, the calculated level ordering ($e_{2u} > e_{2g}$) from quasirelativistic calculations confirms the PES interpretation of Clark and Green. A more detailed discussion of the results of the SCF-Xα calculations of Rösch and Streitwieser is in chapter three of this thesis.

The calculations by Rösch and Streitwieser indicate that bis([8]annulene)thorium(IV) is more ionic than bis([8]annulene)uranium(IV).[34, 35] One experiment that supports this idea is the slow reaction of bis(*n*-butyl[8]annulene)thorium(IV) with uranium tetrachloride to form bis(*n*-butyl[8]annulene)uranium(IV).[20] The reverse reaction does not occur. As an indication of the relative ionicity of bis([8]annulene)thorium(IV) as compared to bis([8]annulene)uranium(IV), the slow formation of bis([8]annulene)uranium(IV) in the above examples can be contrasted with the immediate reaction of the highly ionic bis([8]annulene)cerate(III) anion with UCl_4 to form bis([8]annulene)uranium(IV).[36]

<u>Figure 1.8</u>: Reactions of Bis([8]annulene) complexes with UCl_4.

$$Th(n\text{-}BuC_8H_7)_2 + UCl_4 \xrightarrow[k]{} U(n\text{-}BuC_8H_7)_2 + ThCl_4$$

$$K[Ce(C_8H_8)_2] + UCl_4 \xrightarrow[k']{} U(C_8H_8)_2 + CeCl_3 + KCl$$

where $k' >> k$

Bis([8]annulene)actinate(III) anions

When two [8]annulene dianion rings complex a trivalent metal atom, the result is a bis([8]annulene) sandwich anion. There is one class of complexes involving the actinides and two classes of complexes for the lanthanide(III) ions that contain two [8]annulene dianions sandwiching a trivalent central metal ion.

The potassium salts of bis([8]annulene)uranate(III),[23] -neptunate(III),[37] -plutonate(III)[37] and -americate(III)[38] have all been reported. These complexes have been synthesized by the reaction of two equivalents of [8]annulene dianion with one equivalent of the actinide trihalide (1.7).

$$2\ K_2C_8H_8 + AnX_3 \xrightarrow[THF]{} K[An(C_8H_8)_2] + 3\ KCl \qquad [1.7]$$

The physical properties of these complexes are similar to those of the class $K[Ln(C_8H_8)_2]$.[36, 39] Small amounts of oxidizing agents oxidize the trivalent central metal complexes to the corresponding tetravalent central metal complex (1.8).[37]

$$K[An(C_8H_8)_2] \xrightarrow[[O]]{} An(C_8H_8)_2 \qquad [1.8]$$

Bis([8]annulene)lanthanate(III) anions

The two classes of complexes containing a bis([8]annulene)lanthanate(III) anion are those that contain an alkali cation and

those that contain the complex ([8]annulene)lanthanate(III) cation. One of the classes, the alkali salts of the bis([8]annulene)lanthanate(III) anions, have been prepared by a variety of methods. The first of the methods, and the one which is of the most synthetic utility, is the direct reaction of the di-alkaline salt of [8]annulene dianion with the anhydrous lanthanide trichloride (1.9). The synthesis can be accomplished by the addition of a suspension of the lanthanide salt in THF to a THF solution of the dianion,[36, 39]

$$2\ K_2C_8H_8 + LnCl_3 \xrightarrow[THF]{} K[Ln(C_8H_8)_2] + 3\ KCl \qquad [1.9]$$

The bis([8]annulene)lanthanate(III) anion complexes from 1,3,5,7-tetramethyl-cyclooctatetraene have also been prepared the reaction of the substituted dianion with the lanthanide trichloride.[40]

Although the mechanism for the formation of the bis([8]annulene)lanthanate(III) complexes is not known, the following equilibria (figure 1.9) have been established involving the lanthanide trichlorides, [8]annulene dianion, the ([8]annulene)-lanthanate(III) chloride and the bis([8]annulene)lanthanate(III) anion.[36] It is postulated from these equilibria that in the reaction of [8]annulene dianion with a lanthanide trichloride the ([8]annulene)lanthanate(III) chloride is formed initially as a isolable intermediate of the reaction. The mono-ring intermediate

then reacts with additional [8]annulene dianion to form the bis-([8]annulene) complexes.

Figure 1.9: Equilibrium equations involving ([8]annulene)lanthanate(III) complexes and lanthanide trichlorides.

$$2\ K_2C_8H_8 + 2\ LnCl_3 \rightleftharpoons [C_8H_8LnCl\cdot 2THF]_2 + 4\ KCl$$

$$[C_8H_8LnCl\cdot 2THF]_2 + 2\ K_2C_8H_8 \rightleftharpoons 2\ K[Ln(C_8H_8)_2] + 2\ KCl$$

$$K[Ln(C_8H_8)_2] + LnCl_3 \rightleftharpoons [C_8H_8LnCl.2THF]_2 + KCl$$

The other preparations of the alkali bis([8]annulene)-lanthanate(III) salts are methods which are useful only for specific lanthanide elements. For example, the bis([8]annulene)-cerate(III) anion can be prepared by the reduction of bis([8]-annulene)cerium(IV) with one equivalent of potassium (1.10).[41]

$$Ce(C_8H_8)_2 + K \longrightarrow K[Ce(C_8H_8)_2] \qquad [1.10]$$

This method is only feasible for complexes that contain lanthanide ions that can exist in a 4+ oxidation state and thus only the cerium complex can be made in this manner.

The bis([8]annulene)lanthanate(III) anions which are complexed by an ([8]annulene)lanthanate(III) cation are the only other class of complexes which contain two [8]annulene dianions in a sandwich arrangement about a lanthanide(III) ion. This class was

first reported for the cerium(III) ion, from the reduction of cerium(IV) isopropoxide with triethylaluminum in the presence of cyclooctatetraene (1.11).[41]

[1.11]

$$Ce(OR)_4 + Al(C_2H_5)_3 \xrightarrow[C_8H_8]{} Ce_2(C_8H_8)_3$$

The green cerium complex was characterized by elemental analysis and infrared spectrum. The structure of this complex is not known, but its infrared spectrum indicates that all of the ligands are present as the planar [8]annulene. Reaction of $Ce_2(C_8H_8)_3$ with cyclooctatetraene using a catalytic amount of triethylaluminum gave bis([8]annulene)cerium(IV) (1.12).[41]

[1.12]

$$Ce_2(C_8H_8)_3 \xrightarrow[C_8H_8]{(C_2H_5)_3Al} Ce(C_8H_8)_2$$

A more general synthetic procedure for the synthesis of $Ln_2(C_8H_8)_3$ is by the reaction of neutral cyclooctatetraene with lanthanide atom vapor at -198 °C (1.13).[42]

[1.13]

$$Ln^\circ + C_8H_8 \longrightarrow Ln_2(C_8H_8)_3$$

Crystallization of $Ln_2(C_8H_8)_3$ from THF gives the complex as its bis-THF adduct, $[(C_8H_8)Ln(OC_4H_8)_2][Ln(C_8H_8)_2]$.[42] The crystal

structure of the THF adduct of the neodymium complex (discussed later) clearly shows that the bis([8]annulene)neodymate(III) anion is present in this structure.[42]

The structures of both classes of compounds involving bis([8]-annulene)lanthanate(III) anions have been elucidated from single crystal x-ray diffraction studies on etherate adducts of the complexes. The structure of the diglyme adduct of $K[Ce(C_8H_8)_2]$[43] shows a bis([8]annulene)cerate(III) anion which has the [8]annulene rings parallel planar and with a local symmetry of D_{8d} about the central metal atom. The anion is in a tight ion pair with a diglyme solvated potassium cation.

The symmetry of $[K(diglyme)][Ce(C_8H_8)_2]$ is C_s; the potassium ion, cerium ion, two ring carbons and the central oxygen of the diglyme all lie on the mirror plane of this molecule.

The structure of the bis-THF adduct of $Nd_2(C_8H_8)_3$[42] shows a bis([8]annulene)neodymate(III) anion where the local symmetry of the anion is C_1. The carbon atoms of the two [8]annulene rings (A and B) are almost eclipsed, but the rings are not parallel planar and these planes intersect at an angle of 7.28 °. The complex anion is an ion pair with a bis-THF solvated [8]annulene)neodymate cation. The metal-ring carbon distances shown in Figure 1.11 illustrate the effect of the presence of two trivalent atoms in this molecule.

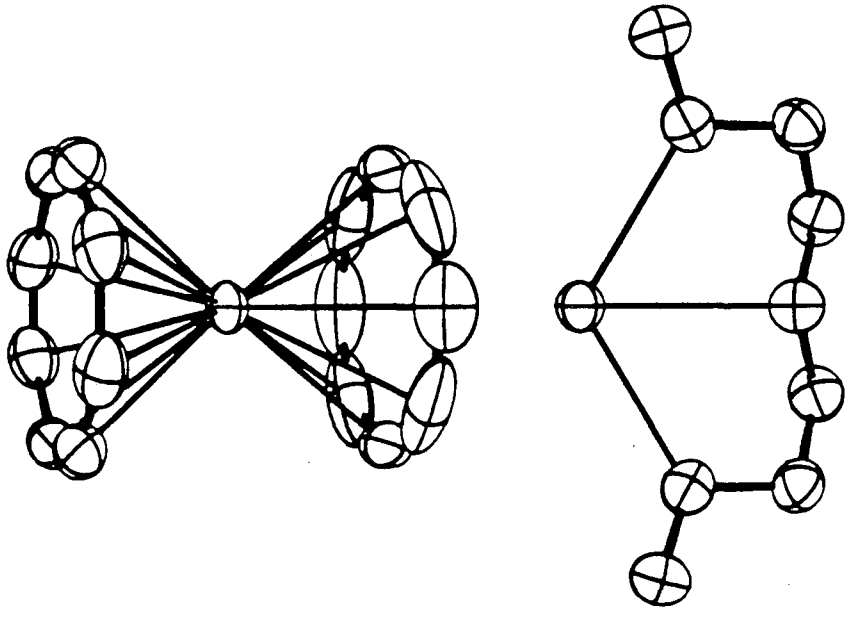

Figure 1.10: Structure of $[K(C_6H_{14}O_3)][Ce(C_8H_8)_2]$ (hydrogen atoms omitted).

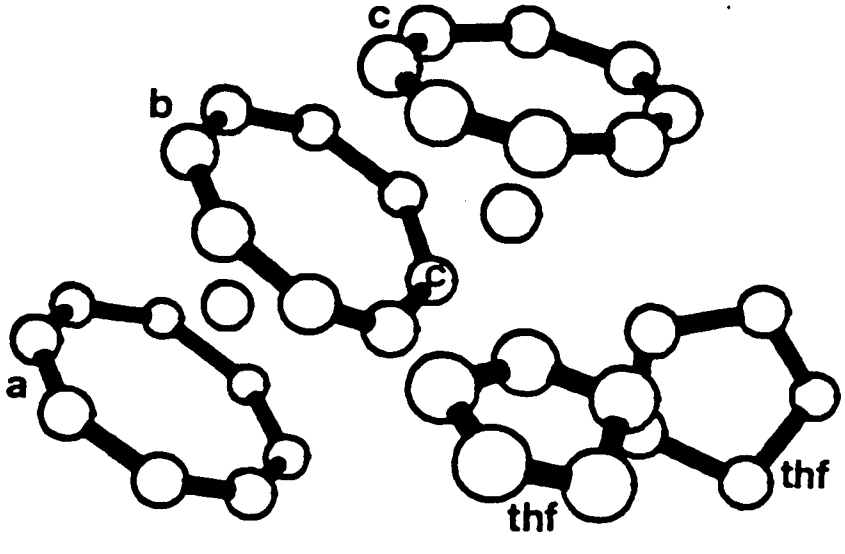

Figure 1.11: Structure of $[(C_8H_8)Nd^{\cdot}\ 2THF][Nd(C_8H_8)_2]$ (hydrogen atoms omitted).

The carbon atom indicated on ring B (in the structure of $[(C_8H_8)Nd^{\cdot}\ 2THF][Nd(C_8H_8)_2]$ is within bonding distance of both neodymiums. The presence of two neodymium atoms does not break the planarity of the rings, but it does cause distortions in the bis([8]annulene)neodymate anion.

The structure of $[(C_8H_8)Nd(OC_4H_8)_2]\ [Nd(C_8H_8)_2]$ can be contrasted with the structure of $Ti_2(C_8H_8)_3$.[44,45] In the titanium structure, both titaniums are complexed by one [8]annulene, but they share a third cyclooctatetraene (Figure 1.12).

<u>Figure 1.12</u>: Structure of $Ti_2(C_8H_8)_3$ (hydrogen atoms omitted).

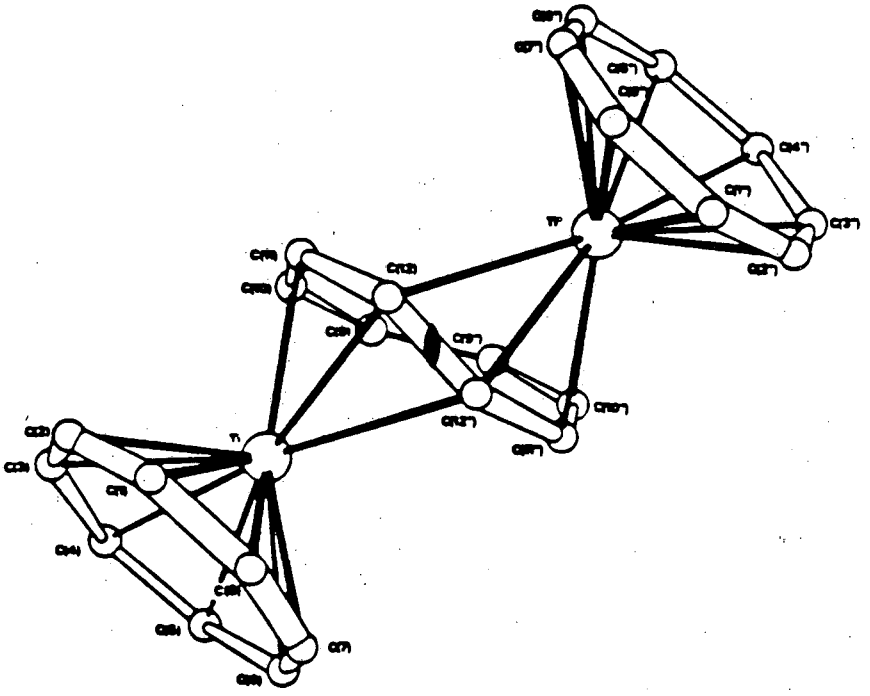

In the neodymium complex, the presence of a second lanthanide(III) only distorts the bis([8]annulene)lanthanate(III) ion. The thermodynamic driving force for neodymium to form a covalent π-bond with cyclooctatetraene is not sufficient to overcome the coulombic attraction between [8]annulene dianion and a lanthanide(III) ion.

Bis([8]annulene)lanthanate(II) dianions

Bis([8]annulene)lanthanate(II) dianions are the subject of the second chapter of this thesis and are not discussed in this chapter.

Mono([8]annulene)actinate(IV) complexes

The ([8]annulene)thorate(IV) "half-sandwich" complexes are by far the most extensivly studied of the mono([8]annulene) complexes. ([8]Annulene)thorate(IV) dichloride can be synthesized as a bis-THF adduct by the stoichiometric reaction of [8]annulene dianion with thorium tetrachloride (1.14) or by the reaction equilibrium reaction between $ThCl_4$ and $Th(C_8H_8)_2$ (1.15).[22, 46]

$$K_2C_8H_8 + ThCl_4 \xrightarrow[THF]{} (C_8H_8)ThCl_2 + 2\ KCl \qquad [1.14]$$

$$ThCl_4 + Th(C_8H_8)_2 \xrightarrow[THF]{} 2\ (C_8H_8)ThCl_2 \qquad [1.15]$$

The related compounds from alkyl substituted cyclooctatetraenes can be best prepared by refluxing bis(alkyl[8]annulene)-thorium(IV) with excess thorium tetrachloride in THF or DME until the yellow color of the bis(alkyl[8]annulene)thorium(IV) disappears. ([8]Annulene)thorate(IV) dichlorides can also be prepared by reaction of bis([8]annulene)thorium(IV) with anhydrous hydrogen chloride (1.16).[22]

[1.16]

$$Th(C_8H_8)_2 + 2\ HCl \xrightarrow[THF]{} (C_8H_8)ThCl_4 + C_8H_{10}$$

The preparation of ([8]annulene)thorate(IV) bis-hydroborates have been achieved by several routes.[47] The alkyl substituted complex, (*n*-butyl[8]annulene)thorate(IV) bis-hydroborate, is prepared by the reaction of thorium tetrahydroborate with bis(*n*-butyl[8]annulene)thorium(IV) in refluxing THF (1.17). Due to the low solubility of the unsubstituted bis([8]annulene)-thorium(IV) in THF, the unsubstituted mono-ring complex is best prepared by the reaction of thorium tetrahydroborate with an equimolar amount of dipotassium [8]annulene in THF at room temperature (1.18).

[1.17]

$$Th(BH_4)_4 + Th(n\text{-}BuC_8H_7)_2 \longrightarrow 2\ (n\text{-}BuC_8H_7)ThCl_2$$

[1.18]

$$K_2C_8H_8 + Th(BH_4)_4 \longrightarrow (C_8H_8)Th(BH_4)_2 + 2\ KBH_4$$

Similar reactions to those shown above on the analogous uranium systems gives poorly characterized products which suggest the existence of ([8]annulene)uranate(IV) bis-borohydride.[47]

The structure of the bis-THF adduct of ([8]annulene)-thorate(IV) dichloride is known (Figure 1.13).[46]

<u>Figure 1.13</u>: Structure of $(C_8H_8)ThCl_2 \cdot 2THF$

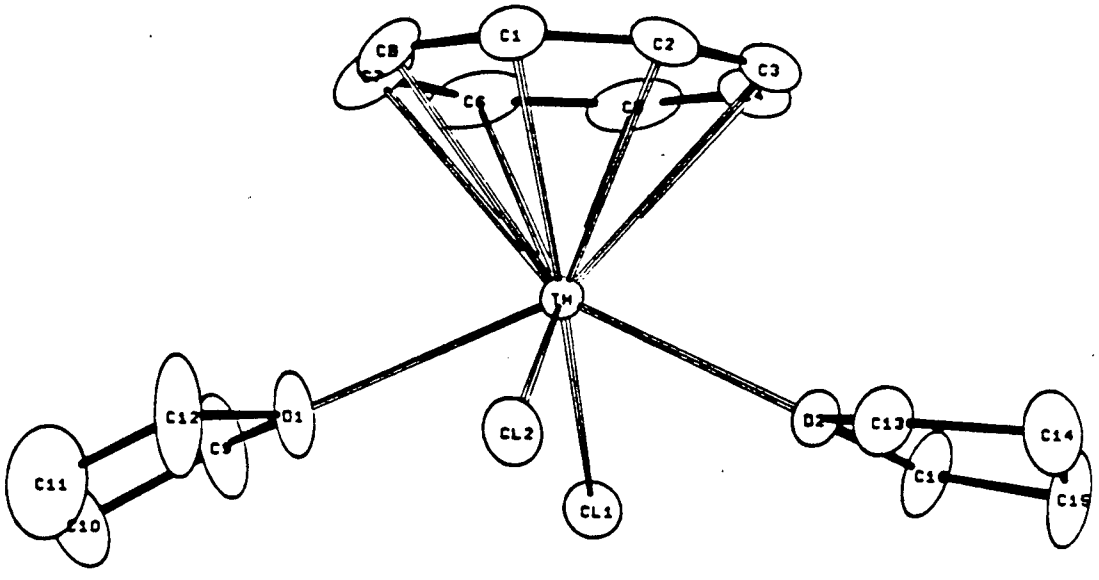

The mono-ring dichloride crystallizes in two modifications. In both the α and β forms the thorium atom is complexed by one [8]annulene ring, two chlorine atoms and two THF molecules. The [8]annulene ring is centrally located on the thorium atom. The chlorine atoms and THF molecules are in trans-configuration on the side of the thorium atom opposite the ring. The α form of the complex crystallizes in space group $P2_1/n$ and the β form crystallizes in space group $P2_1/c$. The only significant geometrical difference between these two forms is the larger Cl-Th-Cl and smaller O-Th-O angles that the α form exhibits relative to the β form. The existence of two forms of mono-ring thorium complex is adequately explained by crystal packing forces.

Mono([8]annulene)lanthanate(III) complexes

There are several types of lanthanide(III) complexes which contain only one [8]annulene ligand. The class of complexes $[(C_8H_8)LnCl^{\cdot}C_4H_8O]_2$, which was shown earlier as an isolable intermediate in the formation of the bis([8]annulene)-lanthanate(III) anion,[47] is made in good yield from the addition of one equivalent of [8]annulene dianion in THF to a suspension of one equivalent of anhydrous lanthanide trichloride in THF (1.19).[36, 48] Good yields of the mono-ring cerium complex product were obtained by the reaction of bis([8]annulene)cerate(III) anion with one equivalent of cerium trichloride (1.20).[36]

[1.19]

$$K_2C_8H_8 + LnCl_3 \xrightarrow[THF]{} 1/2\ [(C_8H_8)LnCl\cdot 2THF]_2$$

[1.20]

$$K[Ce(C_8H_8)_2] + CeCl_3 \xrightarrow[THF]{} [(C_8H_8)LnCl\cdot 2THF]_2 + KCl$$

The mono-THF adduct of ([8]annulene)scandate(III) chloride is obtained from the addition of [8]annulene dianion to scandium trichloride.[49] Reaction of ([8]annulene)scandate(III) chloride with one equivalent of [8]annulene dianion gives bis([8]annulene)scandate(III) anion.[49]

The structure $(C_8H_8)CeCl_3\cdot 2THF$ is known[50] and shows that ([8]annulene)cerate(III) chloride exists as a chloride bridged dimer of the THF adduct (Figure 1.14).

<u>Figure 1.14</u>: Structure of $[(C_8H_8)CeCl\cdot 2THF]_2$

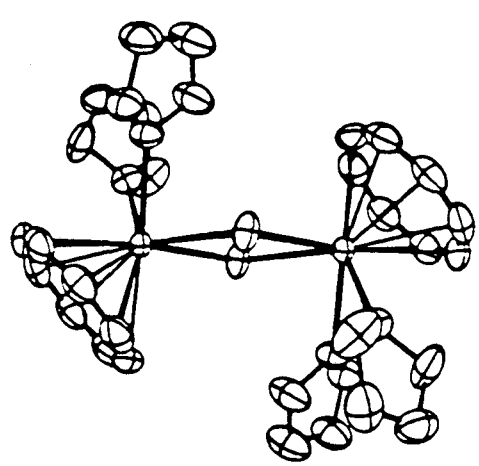

The ([8]annulene)lanthanate(III) alkyls have been prepared from the corresponding chlorides by reaction of the chloride with alkyllithium reagents (1.21).[51]

[1.21]

$$1/2\ [(C_8H_8)LnCl\cdot 2THF]_2 + LiR \longrightarrow (C_8H_8)LnR\cdot xTHF$$

The alkyl derivatives were characterized by elemental analysis, infrared, ^{1}H-NMR and ^{13}C-NMR. The infrared spectra of the alkyls indicate that the planar [8]annulene is present in these complexes. It is not known whether the ([8]annulene)lanthanate(III) alkyls exist as monomers, dimers or as polymers.

A bimetallic ([8]annulene) complex containing cerium(III) and aluminum(III) has been synthesized.[52] ([8]annulene)cerate(III)-di-μ-isopropoxydiethylaluminum was synthesized from the reaction of cerium(IV) isopropoxide with triethylaluminum in the presence of cyclooctatetraene and toluene as the solvent (1.22).

[1.22]

$$Ce(OR)_4 + Al(C_2H_5)_3 \xrightarrow[C_7H_8]{C_8H_8} (C_8H_8)Ce(OR)_2\cdot Al(C_2H_5)_2$$

This bimetallic complex is characterized by elemental analysis, infrared spectrum and mass spectrum. The infrared spectrum indicates that the eight-membered ring is present as [8]annulene. It was suggested from mass spectrum and ^{1}H-NMR studies that this complex exists with the isopropoxide ligands bridging between the cerium and aluminum ions. (Figure 1.15)[52]

Figure 1.15: Proposed structure of $(C_8H_8)Ce(OR)_2{\cdot}Al(C_2H_5)_2$

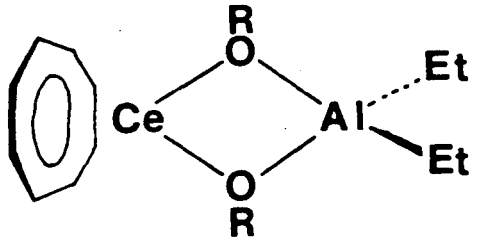

The bimetallic [8]annulene complex has also been made as its acetonitrile adduct.[52]

The only other class of compounds which contain a lanthanide(III) ion and one [8]annulene ligand is the "mixed sandwich" complex, ([8]annulene)lanthanate(III) cyclopentadienides.[53] This class of complexes can be made by either the addition of cyclopentadienide to the ([8]annulene)-lanthanate(III) chlorides of the addition of [8]annulene dianion to (cyclopentadienyl)lanthanate(III) dichloride (1.23). The yttrium[53] and scandium[49] members of this class have also been reported.

[1.23]

$$(C_5H_5)LnCl_2 + K_2C_8H_8 \text{ ------>}$$

$$(C_8H_8)Ln(C_5H_5)$$

$$(C_8H_8)LnCl + Na(C_5H_5) \text{ ------>}$$

These complexes are initially obtained as THF adducts, but lose THF, *in vacuo*, at 50 °C. The mass spectrum of the complexes contain the parent $[MC_{13}H_{13}]^+$ as well as the fragments $[MC_8H_8]^+$ and $[MC_5H_5]^+$. The infrared spectrum of each complex contains absorbances which are attributable to [8]annulene and cyclopentadienide anion and the ^{1}H-NMR of the diamagnetic yttrium complex of this series contains resonances which can be assigned to the protons of [8]annulene dianion and cyclopentadienide anion. In addition to characterization of the THF adduct, the complexes have also been characterized as 1:1 adducts with pyridine, ammonia, and cyclohexylisonitrile.[53]

([8]annulene)lanthanate(II) complexes

The ([8]annulene)lanthanate(II) complexes, $Ln(C_8H_8)$ (Ln = Eu, Yb), are discussed in the next chapter.

References and Notes

1. Controversy exists in naming sandwich organometallic actinide and lanthanide compounds of cyclooctatetraene dianion; [8]annulene dianion and [8]annulene-metal(X) complex are chosen here because these names properly describe the delocalization of charge in the ligand and also emphasize the formal oxidation state of the metal in the complex.

2. (a) Streitwieser, A., Jr.; Muller-Westerhoff, U. *J. Am. Chem. Soc.* 1968, *90*, 7364. (b) Streitwieser, A., Jr.; Muller-Westerhoff, U.; Sonnichsen, G.; Mares, F.; Morrell, D.G.; Hodgson, K.O. *J. Am. Chem. Soc.* 1973, *95*, 8644.

3. Streitwieser, A., Jr.; Harmon, C.A. *Inorg. Chem.* 1973, *12*, 1102.

4. Karraker, D.G. *Inorg. Chem.* 1973, *12*, 1105.

5. Harmon, C.A.; Bauer, D.P.; Berryhill, S.R.; Hagiwara, K.; Streitwieser, A., Jr. *Inorg. Chem.* 1977, *16*, 2143.

6. Streitwieser, A., Jr.; Burghard, H.P.G.; Morrell, D.G.; Luke, W.D. *Inorg. Chem.* 1980, *19*, 1863.

7. Miller, M.F.; Lyttle, M.H.; Streitwieser, A., Jr. *J. Org. Chem.* 1981, *46*, 1977.

8. Streitwieser, A., Jr.; Wang, H.-K.; Lyttle, M.H.; Solar, J.P., manuscript in preparation.

9. Moore, R.M.; Streitwieser, A., Jr.;Wang, H.-K., manuscript in preparation.

10. Streitwieser, A., Jr.; Walker, R. *J. Organometal. Chem.* 1975, *97*, C41.

11. Luke, W.D.; Berryhill, S.R.; Streitwieser, A., Jr. *Inorg. Chem.* 1981, *20*, 3086.

12. Zalkin, A.; Templeton, D.H.; Luke, W.D.; Streitwieser, A., Jr. *Organometallics* 1982, *1*, 618.

13. Streitwieser, A., Jr.; Kluttz, R.Q.; Smith, K.A.; Luke, W.D. *Organometallics* 1983, *2*, 1873.

14. (a) Streitwieser, A., Jr.; Yoshida, N. *J. Am. Chem. Soc.* 1969, *91*, 7528. (b) Goffart, F.; Fuger, J.; Gilbert, B.; Kanellakopulos, B.; Duyckaerts, G. *Inorg. Nucl. Chem. Lett.* 1972, *8*, 403.

15. (a) Starks, D.F.; Parsons, T.C.; Streitwieser, A., Jr.; Edelstein, N. *Inorg. Chem.* 1974, *13*, 1307. (b) Goffart, F.; Fuger, J.; Brown, D.; Duyckaerts, G. *Inorg. Nucl. Chem. Lett.* 1974, *10*, 413.

16. Karraker, D.G.; Stone, J.A.; Jones, E.R., Jr.; Edelstein, N. *J. Am. Chem. Soc.* 1970, *92*, 4841.

17. Starks, D.F.; Streitwieser, A., Jr. *J. Am. Chem. Soc.* 1973, *95*, 3423.

18. de Mayo, P.; Yip, R.W. *Proc. Chem. Soc.* 1964, 84.

19. Streitwieser, A., Jr.; Dempf, D.; LaMar, G.N.; Karraker, D.G.; Edelstein, N. *J. Am. Chem. Soc.* 1971, *93*, 7343.

20. Le Vanda, C.; Streitwieser, A., Jr. *Inorg. Chem.* 1981, *20*, 656.

21. Solar, J.P.; Berghard, H.P.G.; Banks, R.H.; Streitwieser, A., Jr.; Brown, D. *Inorg. Chem.* 1980, *19*, 2186.

22. Le Vanda, C.; Solar, J.P.; Streitwieser, A., Jr. *J. Am. Chem. Soc.* 1980, *102*, 2128.

23. Billiau, F.; Folcher, G.; Marquet-Ellis, H.; Rigny, P.; Saito, E. *J. Am. Chem. Soc.* 1981, *103*, 5603.

24. Smith, K.A. Doctoral Thesis, University of California, Berkeley, 1984

25. Zalkin, A.; Raymond, K.N. *J. Am. Chem. Soc.* 1969, *91*, 5667.

26. Avdeef, A.; Raymond, K.N.; Hodgson, K.O.; Zalkin, A. *Inorg. Chem.* 1972, *11*, 1083.

27. Raymond, K.N.; Eigenbrot, C.W.,Jr. *Acc. Chem. Res.* 1980, *13*, 276; Baker, E.C.; Halstead, G.W.; Raymond, K.N. *Struct. & Bonding* (Berlin) 1976, *25*, 23.

28. Hodgson, K.O.; Raymond, K.N. *Inorg. Chem.* 1973, *12*, 458.

29. Pauling, L. "The Nature of the Chemical Bond," 3rd. Ed., Cornell University Press, Ithaca, New York, 1960, p. 260.

30. Hayes, R.G.; Edelstein, N. *J. Am. Chem. Soc.* 1972, *94*, 8688.

31. Clark, J.P.; Green, J.C. *J. Organometal. Chem.* 1976, *112*, C14.

32. Fragalà, I.; Condorelli, G.; Zanella, P.; Tondello, E. *J. Organometal. Chem.* 1976, *122*, 357.

33. Clark, J.P.; Green, J.C. *J. Chem. Soc. Dalton Trans.* 1977, 505.

34. Rösch, N.; Streitwieser, A., Jr. *J. Organometal. Chem.* 1978, *145*, 195.

35. Rösch, N.; Streitwieser, A., Jr. *J. Am. Chem. Soc.* 1983, *105*, 7237.

36. Hodgson, K.; Mares, F.; Starks, D.; Streitwieser, A., Jr. *J. Am. Chem. Soc.* 1973, *95*, 8650.

37. Karraker, D.G.; Stone, J.A. *J. Am. Chem. Soc.* 1974, *96*, 6885.

38. Karraker, D.G. *J. Inorg. Nucl. Chem.* 1977, *39*, 87.

39. Mares, F.; Hodgson, K.; Streitwieser, A., Jr. *J. Organometal. Chem.* 1970, *24*, C68.

40. Harmon, C.A. Ph.D. Thesis, University of California, Berkeley, 1975.

41. Greco, A.; Cesca, S.; Bertolini, G. *J. Organometal. Chem.* 1976, *113*, 321.

42. DeKock, C.W.; Ely, S.R. Hopkins, T.E.; Brault, M.A. *Inorg. Chem.* 1978, *17*, 625.

43. Hodgson, K.O.; Raymond, K.N. *Inorg. Chem.* 1972, *11*, 3030.

44. Breil, H.; Wilke, G. *Angew. Chem.* 1966, *78*, 942; *Angew. Chem. Int. Ed. Eng.* 1966, *4*, 898.

45. Dierks, H.; Dietrich, H. *Acta Crystallogr. Sect. B.* 1968, *24*, 59.

46. Zalkin, A.; Templeton, D.H.; Le Vanda, C.; Streitwieser, A., Jr. *Inorg. Chem.* 1980, *19*, 2560.

47. Solar, J.P.; Streitwieser, A., Jr.; Edelstein, N. in "Lanthanide and Actinide Chemistry and Spectroscopy" ACS Symposium Series No. 131, 1980, 81.

48. Mares, F.; Hodgson, K.; Streitwieser, A., Jr. *J. Organometal. Chem.* 1971, *28*, C24.

49. Westerhof, A.; De Liefde Meijer, H.J. *J. Organometal. Chem.* 1976, *116*, 319.

50. Hodgson, K.O.; Raymond, K.N. *Inorg. Chem.* 1972, *11*, 171.

51. Wayda, A.L. *Organometallics* 1983, *2*, 565.

52. Greco, A.; Bertolini, G.; Cesca, S. *Inorg. Chim. Acta* 1977, *21*, 245.

53. Jamerson, J.D.; Masino, A.P. Takats, J. *J. Organometal. Chem.* 1974, *65*, C33.

CHAPTER TWO

[8]Annulene Complexes of Ytterbium(II) and Calcium(II)

Introduction

The lanthanide elements are the series of fourteen elements with atomic numbers 58-71. They constitute half of the "f-block" transition metal elements in the periodic table; the fourteen actinide elements constitute the other half. Lanthanum (Z = 57) is not, strictly, a lanthanide;[1] in its ground state lanthanum contains no f-electrons (Ln° = $[Xe]5d6s^2$).[2] However, the chemistry and physical properties of lanthanum and the fourth row element, yttrium (Y° = $[Kr]4d5s^2$), are lanthanide-like; these elements are almost always treated as lanthanides. Scandium (Sc° = $[Ar]3d4s^2$), due to its small ionic radii (relative to the lanthanides), has properties intermediate between the lanthanides and aluminum, yet the chemistry of scandium is often included in reviews of the lanthanides.

The common oxidation state for the lanthanides is the trivalent state. In fact, all of the lanthanides have the trivalent state as the most thermodynamically stable oxidation state. The chemistry of trivalent lanthanide compounds and organometallic complexes[3,4] is well reviewed, and is not reviewed in this work.

The Divalent Lanthanides

One might expect that the thermodynamically stable oxidation state of the lanthanides is the divalent state, noting the similarity of the ground state configuration of most of the lanthanides ($[Xe]f^n s^2$ for Pr-Eu, Tb-Yb), and the ground state configuration of the alkaline earth elements ($[core]s^2$). In fact, the divalent state of nearly all the lanthanides has been reported. Table 2.1 gives the oxidation potentials for the Ln(III)/Ln(II) couple.[5]

As one can conclude from inspection of Table 2.1, the trivalent state of the lanthanides is more stable than the divalent state. Consideration of ionization energies, atomization energies, solvation energies and/or lattice energies of the lanthanide elements in, for example, Born-Haber cycles, show that the trivalent state is the most stable state for the lanthanides in both solids and solutions.[1,6] The values for Ln(III)/Ln(II) in

Table 2.1: Standard Oxidation Potential of Ln(III)/Ln(II)[a]

Ln	Ln(III)/Ln(II)[b]	Ln	Ln(III)/Ln(II)[b]
Ce	-2.92	Tb	-2.83
Pr	-2.84	Dy	-2.56
Nd	-2.62	Ho	-2.79
Pm	-2.44	Er	-2.87
Sm	-1.50	Tm	-2.22
Eu	-0.34	Yb	-1.18
Gd	-2.85	Lu	unknown

(a) ref. 5. (b) in volts.

Table 2.1 are determined from the energy of the third ionization potentials (ΔG°_{ip})and the energies of hydration (ΔG°_{hyd}) for the divalent and trivalent state for the lanthanides (2.1).[5]

$$F(E^\circ_{(III)/(II)} + 4.43) = \Delta G^\circ_{ip} + \Delta G^\circ_{hyd}(Ln^{3+}) - \Delta G^\circ_{hyd}(Ln^{2+}) \quad [2.1]$$

where 4.43 is the standard thermodynamic electrode potential of the hydrogen electrode.[7]

As one might predict, the divalent lanthanides are similar to the alkaline earth elements. Europium and ytterbium compare with the alkaline earth elements strontium and calcium, respectively. In Table 2.2, various comparisons are shown between these elements.

Table 2.2: Comparisons of Some Divalent Metal Ions (Ca,Eu,Sr,Yb).

M	Ionic Radius[a,b] (C.N.=8)	Ionization Potentials[c,d] (1st, 2nd)	M°/M(II) couple[e]
Eu	1.39	5.67, 11.25	-3.44[f]
Sr	1.40	5.70, 11.03	-2.91
Yb	1.28	6.25, 12.17	-2.80[f]
Ca	1.26	6.11, 11.87	-2.86

(a) in Å . (b) ref. 8. (c) in eV (d) ref. 9. (e) in volts. (f) calculated from M(III)/M(II) and M°/M(III) couples from ref. 6.

One important similarity of the divalent oxidation states of europium(II) and ytterbium(II) with the alkaline earth elements is the solubility of the metal in liquid ammonia. Warf and Korst were the first to observe that europium and ytterbium metals dissolve in liquid ammonia to give blue solutions.[10] Subsequent measurement of the electrical conductivity of these solutions led to the suggestion that ytterbium is divalent in liquid ammonia and can be considered as $Yb^{2+}(2e^{-})$.[11]

Organometallic Complexes of the Divalent Lanthanides

Organometallic complexes involving divalent lanthanide metals are now known for samarium, europium and ytterbium involving a variety of organic ligands. These complexes have been recently reviewed by Schumann[4] and by the Gmelin series[3] and will not be reviewed here. Following is a brief review emphasizing complexes which are pertainent to [8]annulenelanthanide(II) complexes.

Cyclopentadienide Complexes

The solubility of europium and ytterbium in liquid ammonia was utilized in the synthesis of the first organometallic complexes involving divalent lanthanides. Fischer and Fischer reported $Eu(C_5H_5)_2$ and $Yb(C_5H_5)_2$ from the addition of two equivalents of neutral cyclopentadiene to one equivalent of lanthanide metal in liquid ammonia.[12] The lanthanide complexes were compared with their alkaline earth analogs. The comparison of the infrared spectra of $Eu(C_5H_5)_2$ with $Sr(C_5H_5)_2$ and $Yb(C_5H_5)_2$ with $Ca(C_5H_5)_2$ (Table 2.3) suggest that the complexes have similar structures.

Comparison of the x-ray powder pattern of $Eu(C_5H_5)_2$ with $Sr(C_5H_5)_2$ also indicates that the divalent lanthanide and alkaline earth cyclopentadienides have similar structure.[12]

Table 2.3: Comparison of Infrared Spectra of $M(C_5H_5)_2$ (M=Eu,Sr,Yb,Ca).[a,b,c]

$Eu(C_5H_5)_2$	$Sr(C_5H_5)_2$	$Yb(C_5H_5)_2$	$Ca(C_5H_5)_2$
3077 m	3077 m	3086 m	3049 m
		2933 m	
2681 w	2667 w	2681 w	
1724 w	1724 w		
1621 w	1621 w	1658 w	
1590 w	1590 w	1590 w	1590 w
1435 m	1435 m	1433 m	1433 m
1346 w		1344 w	1362 w
1119 w	1119 w	1120 w	1119 2
1057 m	1057 m	1053 m	
1007 s	1008 s	1006 s	1006 s
880 m	891 w	890 w	889 w
863 m	865 m	870 m	
838 m	840 m	841 m	
782 s	784 s	774 s	778 s
739 vs	739 vs	752 vs	750 vs

(a) ref. 12.
(b) vs, very strong; s, strong; m, medium; w, weak.
(c) nujol/fluorolube mulls.

Since the ring-metal interaction in the alkaline earth complexes is surely ionic, then the similarity of structures suggests that the ring-metal interaction in the lanthanide complexes is also ionic. Additional support for the ionicity of the ring-metal bond in $Eu(C_5H_5)_2$ is from Mössbauer spectroscopy. The Eu^{131} shift (δ= -1.32 cm/s relative to EuF_3) in $Eu(C_5H_5)_2$ is comparable to the shift measured for the ionic species $EuCl_2$ (δ=-1.34 cm/s).[12]

The crystal structure of the class $LnCp_2$ is not known, but the structure of $CaCp_2$ has been reported.[13] This molecule exists as a polymer, with each calcium atom associated with four cyclopentadienide rings (figure 2.1).

Subsequent work on the bis(cyclopentadienyl)lanthanide complexes has led to the synthesis and structural characterization of many substituted cyclopentadienide complexes. Most of these divalent lanthanide complexes exist as monomers of their base-adducts; the base is coordinated to the lanthanide atom.[3] Recently, Evans has synthesized and characterized the first base-free, non-polymeric complex of a divalent lanthanide with a cyclopentadienide ligand, bis(pentamethyl-cyclopentadienide)samarate(II).[14] The structure of this complex is similar to the structure shown in figure 2.2.

There is no explanation at this time for the non-coplanarity of the ligands in this complex; however, it is unlikely that

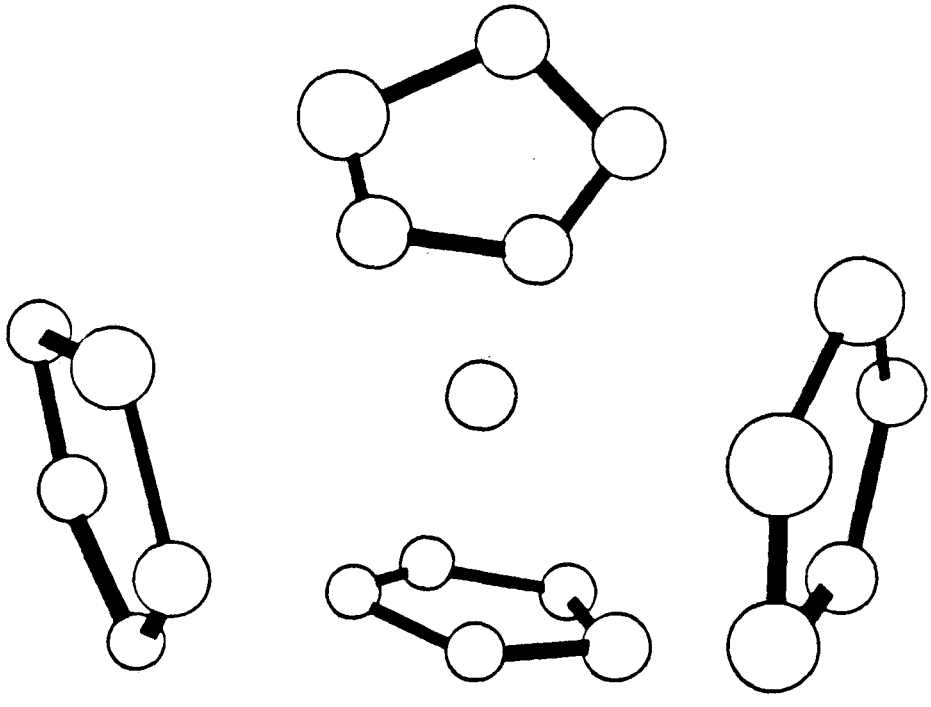

Figure 2.1: Structure of Bis(cyclopentadienyl)calcate(II) (hydrogen atoms omitted).

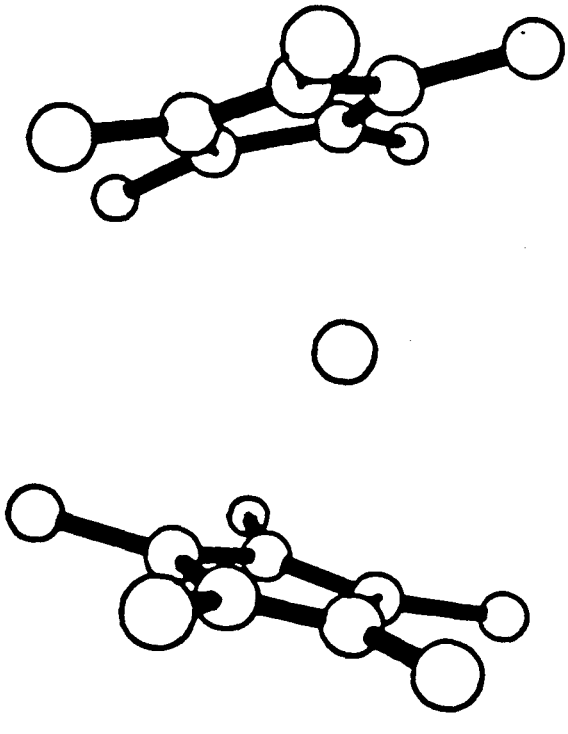

Figure 2.2: Structure of Bis(pentamethylcyclopentadienide)-samarate(II) (hydrogen atoms omitted).

orbital interactions between the rings and the metals play a major role in the ring-tilting.

[8]Annulene Dianion Complexes

The first lanthanide [8]annulene complexes reported, $Ln(C_8H_8)$ (Ln = Eu, Yb),[15] are the only [8]annulene complexes which have been shown to contain a divalent lanthanide. These complexes were synthesized by the addition of one equivalent of neutral cyclooctatetraene to one equivalent of europium or ytterbium metal in liquid ammonia (2.2).

[2.2]

$$C_8H_8 + M\ (M{=}Eu,Yb) \xrightarrow[NH_3]{} M(C_8H_8)$$

The pyrophoric powders, $Ln(C_8H_8)$ (green, Ln=Eu; pink, Ln=Yb) are insoluble in hydrocarbons, ethers and liquid ammonia; the ytterbium complex gives a dark red solution in equilibrium with a dark solid in pyridine. $Yb(C_8H_8)$ has also been synthesized by the reaction of cyclooctatetraene vapor with ytterbium metal atoms (2.3).[16]

[2.3]

$$C_8H_8 + Yb^{\circ} \longrightarrow Yb(C_8H_8)$$

The crude reaction product was purified by Soxhlet extraction with pyridine for three days.

Further characterization of the [8]annulenelanthanide complexes is limited. The divalent nature of the metal in the complexes was illustrated by EPR [15] ($Eu(C_8H_8)$ has an EPR spectrum at 77 K which is consistent with the presence of Eu^{2+}) or magnetic susceptibility[15] (Yb^{2+} is diamagnetic). No reactions of the divalent lanthanide complexes have been reported, except for their violent reaction with oxygen.[15]

The structure of the class $Ln(C_8H_8)$ has not been elucidated. The infrared spectrum of $Yb(C_8H_8)$[17] (figure 2.3) suggests a highly symmetric complex involving the [8]annulene dianion[18] (the only bands present between 1000 and 600 cm^{-1} occur at 888 and 678 cm^{-1}), and the low solubility of the complexes in hydrocarbons, ethers and liquid ammonia suggests that the class $Ln(C_8H_8)$ is polymeric.

The report of synthesis of $K_2[Ce(C_8H_8)_2]$ from the reduction of $Ce(C_8H_8)_2$ by two equivalents of potassium in 1,2-dimethoxyethane[19] is the only example of a bis([8]annulene) compound with a central metal atom in a formal 2+ oxidation state. The cerium complex as its di(1,2-dimethoxyethane) adduct was characterized by elemental analysis and infrared spectrum. The structure of $[K(C_4H_{10}O_2)]_2[Ce(C_8H_8)_2]$ is not known, but the infrared spectrum of the cerium complex does contain bands (887 and 682 cm^{-1}) which are consistent with the presence of an [8]annulene dianion.[18] Although there are reports of Ce(II) from the

Figure 2.3: Infrared specta (nujol mull) of $Yb(C_8H_8)$.

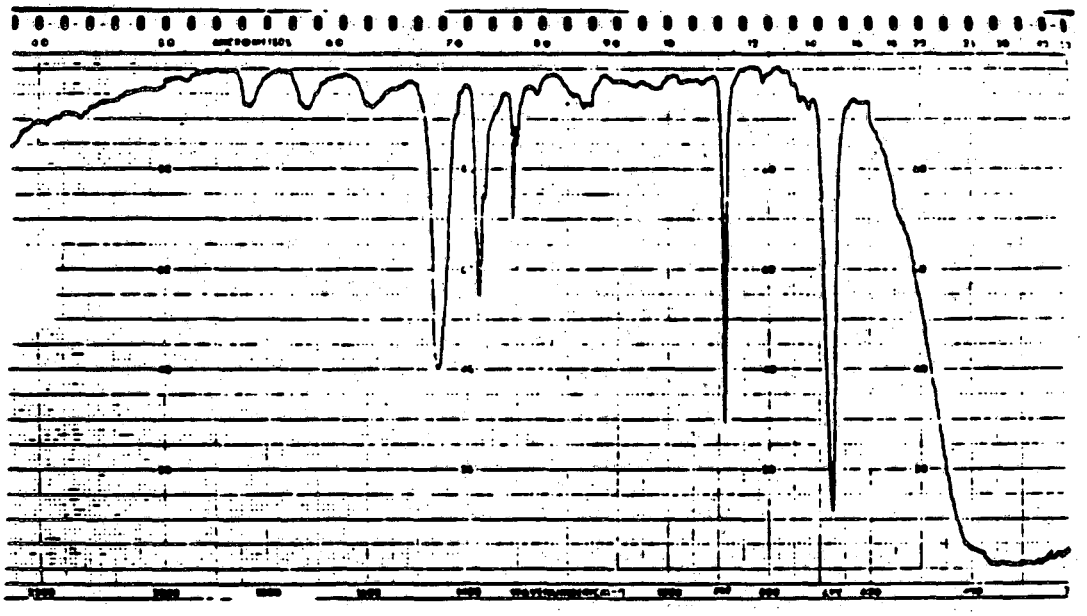

reduction of Ce(III) in other systems,[5] the presence of the cerium(II) ion in $[K(C_4H_{10}O_2)]_2[Ce(C_8H_8)_2]$ has not been shown by chemical or spectroscopic methods.

In order to study a bis-[8]annulene compound with a divalent central metal atom, the divalent ytterbium complex, $K_2[Yb(C_8H_8)_2]$, and its calcium analogue, $K_2[Ca(C_8H_8)_2]$ have now synthesized and characterized. The determination of the structure of the di(1,2-dimethoxyethane) adduct of $K_2[Yb(C_8H_8)_2]$ by single crystal x-ray diffraction is the first structure solved for a complex of [8]annulene dianion with a divalent lanthanide. The crystal structure and characterization of the bis([8]annulene)lanthanate(II) complexes is in the Results and Discussion section of this chapter.

Electron Exchange in Sandwich Complexes

Along with the information obtained on the nature of the ring-metal interaction in the bis([8]annulene)metal(II) complexes, the ^{1}H-NMR studies on bis([8]annulene)ytterbate(II) and bis([8]annulene)ytterbate(III) indicate that a dynamic electron exchange is occuring between these two complexes on the NMR timescale. The observation of a dynamic electron exchange between bis([8]annulene) complexes has no literature precedence. There is only one example of dynamic electron exchange (measurable by ^{1}H-NMR) between two sandwich complexes that differ only in the formal

oxidation state of their central metal atoms and that is the dynamic electron exchange between ferrocene and ferricenium ion.[20]

Bis(cyclopentadienyl)iron(II), ferrocene, can undergo a one electron oxidation to form bis(cyclopentadienyl)iron(III), ferricenium ion (2.4). These two complexes can equilibrate by the exchange of an electron.

$$Fe(C_5H_5)_2 \underset{+e^-}{\overset{-e^-}{\rightleftharpoons}} Fe(C_5H_5)_2^+ \qquad [2.4]$$

Due to the position of the rings, the iron atom in the sandwich complexes is shielded from interaction with the solvent.[21] Thus, the ferrocene/ferricenium system is close to the the simple model for electron exchange proposed by Marcus.[22] Marcus' theoretical model predicts that:

$$k = \kappa \rho Z(\exp(-\Delta G^* RT)) \qquad [2.5]$$

and

$$\Delta G^* = w_r + \Delta G_o^* + \Delta G_i^* \qquad [2.6]$$

where

$$\Delta G_o^* = \frac{e^2}{4R^*}(1/D_{op} - 1/D_s) \qquad [2.7]$$

The coulombic repulsion between the reactants is small (the work required to bring the reactants together (w_r is minimal) and the structures of $Fe(C_5H_5)_2$[24] and $Fe(C_5H_5)_2^+$[25] are similar so that the energy involved in rearrangement (ΔG_i^*) after electron transfer is small. The free energy of activation for the electron exchange should then be ΔG_o^* (the terms in the Marcus equation are defined in footnote 23).

The study, by ^{1}H-NMR, of the electron exchange in the ferrocene/ferricenium system was first reported by Wahl in 1963. In this study it was found that the addition of a small amount of ferricenium ion (or more precisely, the addition of a small amount of oxidizing agent) caused the ferrocene resonance to broaden. Assumming that the electron exchange reaction was first order with respect to each reactant (2.8).[20]

$$\text{rate} = k[Fe(C_5H_5)_2][Fe(C_5H_5)_2^+] \qquad [2.8]$$

and that the electron exchange is fast relative to the spin-spin relaxation of the paramagnetic species, it was found that $k > 1\times10^5\ M^{-1}s^{-1}$ at 25° C.

In further studies by Wahl,[26] it was found that the line width of the coalescence peak in the ferrocene/ferricenium system (W_{DP}) was given by equation 2.9.

[2.9]

$$W_{DP} = f_P W_P + (1-f_P)W_D + f_P(1-f_P)4\pi(\delta v)^2/kc$$

where W_D and W_P are the linewidths of the individual species, f_P is the mole fraction of $FeCp_2^+$, δv is the difference in chemical shift between the two species, c is the total concentration and k is the second order rate constant given in equation 2.8. From equation 2.9 it is seen that the line width of the coalesced species arises from the line widths of the individual species and from a line-broadening dependent on the rate of exchange between the two species. In Wahl's experiments, the plotting of W_{DP} vs 1/c, for various concentrations of the sandwich complexes, gave a straight line whose slope gives $k = 5.3\times10^6\ M^{-1}s^{-1}$ at 25° C in acetonitrile-d_3. This rate constant is consistent with $k = 5.7\times10^6 M^{-1}s^{-1}$ from Marcus theory.[22,25] Subsequent studies[21] have shown that the solvent has little effect on the rate of electron exchange in the ferrocene/ferricenium system. Shown in table 2.4 are the rate constants for the electron exchange in various solvents.

Table 2.4: Rate of Ferrocene/Ferrocenium Electron Exchange at 25° C as a Function of Solvent.[a]

Solvent	k $(x10^{-6})M^{-1}s^{-1}$	Solvent	k $(x10^{-6})M^{-1}s^{-1}$
CD_3OD	6.0	$C_6D_5NO_2$	2.3
CD_3CN	5.3	CD_2Cl_2	4.3
CD_3NO_2	5.8	$(CD_2Cl)_2$	4.3
$(CD_3)_2CO$	4.6	CD_3CO_2D	7.0
$(CD_3)_2SO$	1.6		

(a) ref. 21

Results and Discussion

Synthesis of Bis([8]annulene)Metal(II) Complexes

The synthesis of dipotassium bis([8]annulene)ytterbate(II) and calcate(II) is straightforward in liquid ammonia. These complexes were synthesized by the addition of two equivalents of cyclooctatetraene to a blue liquid ammonia solution of two equivalents of potassium and one equivalent of ytterbium or calcium metal.

[2.10]

$$M_{(Ca,\ Yb)} + 2\ C_8H_8 + 2\ K \xrightarrow[NH_3]{} K_2[M(C_8H_8)_2]$$

When a 2:1:1 ratio of cyclooctatetraene:potassium:ytterbium was used in the liquid ammonia reaction, the ytterbium(III) complex $K[Yb(C_8H_8)_2]$ was obtained (2.11). In this reaction a ytterbium(II) species is probably formed first, followed by oxidation to the ytterbium(III) by cyclooctatetraene.

[2.11]

$$Yb + 2\ C_8H_8 + K \xrightarrow[NH_3]{} K[Yb(C_8H_8)_2]$$

Bis(t-butyl[8]annulene)ytterbate(II) dianion and -ytterbate(III) anion were prepared from t-butyl-cyclooctatetraene[27] in reactions similar to 2.10 and 2.11

The utility of the ytterbium in liquid ammonia reaction is illustrated by the synthesis of (2-cyclopentadienylethyl)[8]annuleneytterbate(III). (2-Cyclopentadienylethyl)cyclooctatetraene, synthesized by Halpern,[28] is a ligand involving both a cyclopentadiene and cyclooctatetraene moiety bridged by an ethyl group. Addition of a THF solution of the one equivalent of the neutral ligand to a blue liquid ammonia solution containing one equivalent of ytterbium metal resulted in an instant color change of the solution, followed by a vigorous evolution of bubbles. Apparently, the $Yb^{2+}(2e^{-})$ in liquid ammonia reacts with the cyclooctatetraene moiety of the ligand (the color change) to form a ytterbium(II) species which can undergo oxidation (with the evolution of hydrogen) to the ytterbium(III) species by reaction with the cyclopentadiene moiety (figure 2.4).

Figure 2.4: Reaction of (2-cyclopentadienylethyl)cyclooctatetraene with ytterbium in liquid ammonia.

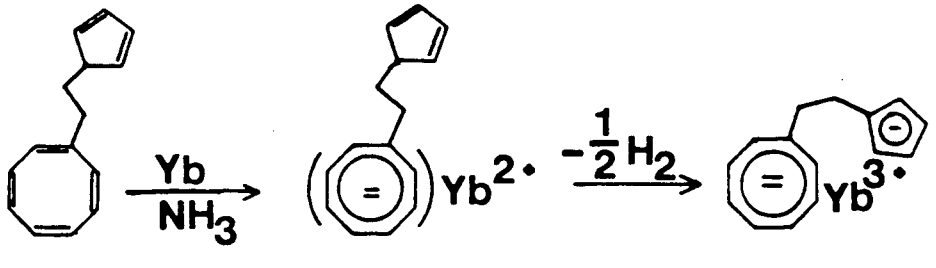

The liquid ammonia system was also used in the attempted synthesis of bis(benzo-[8]annulene)calcate(II) dianion. When a THF solution of two equivalents of benzocyclooctatetraene[29] was added to a liquid ammonia solution of two equivalents of potassium and one equivalent calcium, a pyrophoric red powder was formed. The diffusion of hexane into a diglyme solution of this red powder caused two distinct compounds to crystallize; the analysis of these two complexes indicated that they are the diglyme adducts of (benzo[8]annulene)calcate(II) and dipotassium benzo[8]annulene.

The unsuccessful attempt to prepare $K_2[Ca(benzo\text{-}C_8H_6)]$ can be rationalized by considering the equilibrium shown in equation 2.12.

$$[KS_x]_2[ML_2] \rightleftharpoons [KS_x]L + S_yML \qquad [2.12]$$

where L = [8]annulene ligand
M = divalent metal
S = ethereal solvent

In the benzo-[8]annulene system, the solvent coordinated (benzo-[8]annulene)calcate(II) is favored over the bis(benzo-[8]annulene)calcate(II) dianion.

In the unsubstituted [8]annulene system in ethereal solvents, the equilibrium shown in equation 2.12 does not exist. $Yb(C_8H_8)$ is insoluble in ethereal solvents, so that if the bis-[8]annulene

dianion were in equilibrium with the mono-[8]annulene complex, the insolubility of ML would drive the equilibrium totally to the right.

Physical Properties:

The physical properties for $K_2[Yb(C_8H_8)_2]$ and $K_2[Ca(C_8H_8)_2]$ are similar to the properties reported for the trivalent lanthanide complexes, $K[Ln(C_8H_8)_2]$.[30] The most noticeable similarity is the air-sensitivity of the compounds $K_2[M(C_8H_8)_2]$; $K_2[Yb(C_8H_8)_2]$ and $K_2[Ca(C_8H_8)_2]$ enflame in contact with air.

Compounds $K_2[Yb(C_8H_8)_2]$ and $K_2[Ca(C_8H_8)_2]$ are thermally stable, showing no sign of decomposition when heated to 360 °C sealed under one atm of argon or to 200 °C *in vacuo*. A mass spectrum of $K_2[Yb(C_8H_8)_2]$ shows no *m/z* that can be attributed to the ionization of the sandwich compound.

In THF solution, $K_2[Yb(C_8H_8)_2]$ is oxidized to $K[Yb(C_8H_8)_2]$ by O_2, CCl_4, COT, and $U(C_8H_8)_2$; the presence of the bright blue ytterbium(III) complex was indicated by its visible spectrum. Compound $K[Yb(C_8H_8)_2]$ is thermally unstable and is converted to $K_2[Yb(C_8H_8)_2]$ (by the loss of COT, eq. 2.13) when heated at 310 °C sealed under one atm of argon, or to 200 °C *in vacuo*.

[2.13]

$$2\ K[Yb(C_8H_8)_2] \longrightarrow K_2[Yb(C_8H_8)_2] + Yb(C_8H_8) + C_8H_8$$

Surprisingly, the reaction of $K[Yb(C_8H_8)_2]$ with potassium in refluxing THF failed to produce any $K_2[Yb(C_8H_8)_2]$. This result makes the reduction of $Ce(C_8H_8)_2$ by potassium to form the divalent cerium complex $K_2[Ce(C_8H_8)_2]$ unlikely.[19]

Bis([8]annulene)ytterbate(II) and -ytterbate(III) can be separated by crystallization. Diffusion of hexane into an ether solution of a mixture of $K_2[Yb(C_8H_8)_2]$ and $K[Yb(C_8H_8)_2]$ results in the formation of blue crystals of the ytterbium(III) complex and a red-orange solution of the ytterbium(II) complex. However, if an ether solution of $K_2[Yb(C_8H_8)_2]$ and $K[Yb(C_8H_8)_2]$ is cooled, orange crystals form out of the dark blue solution. The difference in conditions for the crystallization of the ytterbium(II) or ytterbium(III) complex can be readily rationalized. The symmetric $[KL]_2[Yb(C_8H_8)_2]$ (L = ethereal ligand or ligands) has a relatively higher lattice energy and will, as a result, crystallize at higher temperatures than the ytterbium(III) species. The ether adduct $[KL][Yb(C_8H_8)_2]$, however, is less soluble in a hexane-ether solution, and falls out of solution preferentially to the ytterbium(II) complex. These crystallization processes aid in obtaining the ytterbium(II) or ytterbium(III) complexes in pure form.

Compounds $K_2[Yb(C_8H_8)_2]$ and $K_2[Ca(C_8H_8)_2]$ have the same solubility properties; they are insoluble in hydrocarbon solvents such as hexane, toluene and benzene, but soluble in ethers such

as diethyl ether, THF, and DME. The slow cooling of a saturated solution of $K_2[Yb(C_8H_8)_2]$ or $K_2[Ca(C_8H_8)_2]$ in an ether gives crystals of the ether adduct. The THF adducts of $K_2[Yb(C_8H_8)_2]$ and $K_2[Ca(C_8H_8)_2]$ rapidly lose THF, *in vacuo*, or in an argon atmosphere (ca. one hour), but the DME adducts are stable at ambident temperatures. As with all of the lanthanide [8]annulene complexes, $K_2[Yb(C_8H_8)_2]$ and $K_2[Ca(C_8H_8)_2]$ exist as powders in the absence of coordinated ether molecules.

The t-butyl derivatives behave similarly to the unsubstituted complexes. One surprising result is that the bis-diglyme adduct of dipotassium bis(t-butyl[8]annulene)ytterbate(II) is relatively stable to air. When a crystal of $[K(C_6H_{14}O_3)]_2[Yb(t\text{-}BuC_8H_7)_2]$ was exposed to air, no signs of decomposition were detected for at least five minutes; the total decomposition of a small crystal took 30 min. The stability of $[K(C_6H_{14}O_3)]_2[Yb(t\text{-}BuC_8H_7)_2]$ is likely due to the steric bulk of the diglyme and the t-butyl group and clearly illustrates why air stability is not a good criterion for covalency in [8]annulene complexes.

Bis(t-butyl[8]annulene)ytterbate(III) proved difficult to purify, due to contamination of the ytterbium(II) complex. When the crude reaction product was crystallized from diglyme, both a blue powder and red crystals were formed. Repeated crystallization from hexane diffusion into diglyme solutions gave a sample which contained very little ytterbium(II) (as shown by

^{1}H-NMR at -70°C; see the NMR section of this chapter). The visible spectrum of this sample showed the same complex spectrum as for the unsubstituted bis([8]annulene)ytterbate(III) and was, therefore, pressumed to be bis(t-butyl[8]annulene)ytterbate(III).

The difficulty in purifying bis(t-butyl[8]annulene)ytterbate(III) is due to the greater reduction potential of t-butyl[8]annulene dianion relative the [8]annulene dianion.

The presence of a t-butyl group on cyclooctatetraene makes the compound harder to reduce (and the corresponding dianion more reducing). A good measure of the effect of the t-butyl group on the ability of cyclooctatetraene to hold a negative charge is the equilibrium between cyclooctatetraene radical anion and t-butyl-cyclooctatetraene. In the equilibrium, shown in equation 2.14, the equilibrium lies far to the left such that $K_{eq} = 2.8 \times 10^{-2}$. The same situation should occur for the equilibrium between [8]annulene dianion and t-butyl-cyclooctatetraene.

[2.14]

$$C_8H_8^- + t\text{-}BuC_8H_7 \rightleftharpoons C_8H_8 + t\text{-}BuC_8H_7^-$$

^{1}H-NMR of a system involving ytterbium(III) and t-butyl[8]annulene dianion does indicate that some reduction of the ytterbium(III) does occur.[31]

Visible Spectra

The bright orange $K_2[Yb(C_8H_8)_2]$ in THF solution has an intense, broad absorbance in the visible region at 504 nm. In THF solution, $K_2[Ca(C_8H_8)_2]$ has no absorbance in the visible region. The pale green color of $K_2[Ca(C_8H_8)_2]$ is due to trace impurities; repeated recrystallization of $K_2[Ca(C_8H_8)_2]$ from THF gives a pure white powder. The dark blue $K[Yb(C_8H_8)_2]$ in THF solution has a broad absorbance at 570 nm with a sharp shoulder at 649 nm.

The visible spectrum of $K_2[Yb(C_8H_8)_2]$ in THF can be readily interpreted. Earlier studies on the class $K[Ln(C_8H_8)_2]$ led to the conclusion that the broad absorption bands in the visible region of these complexes are due to ligand-to-metal charge transfer.[30] The visible absorbance of $K_2[Yb(C_8H_8)_2]$ can also be assigned to a ligand-to-metal charge transfer band. The visible spectrum of the di-t-butyl derivative of $K_2[Yb(C_8H_8)_2]$, $K_2[Yb(t\text{-}BuC_8H_7)_2]$, show the visible absorbance red-shifted to 520 nm.[26] Alkyl substituents on the [8]annulene dianion make the ligand more reducing and would shift a ligand-to-metal charge transfer band to lower energy. Since the Yb(II) ion in $K_2[Yb(C_8H_8)_2]$ has completely filled 4f orbitals, π-f charge transfer can be ruled out and the visible absorbance of $K_2[Yb(C_8H_8)_2]$ can be assigned as a ligand π-to-metal d charge transfer.

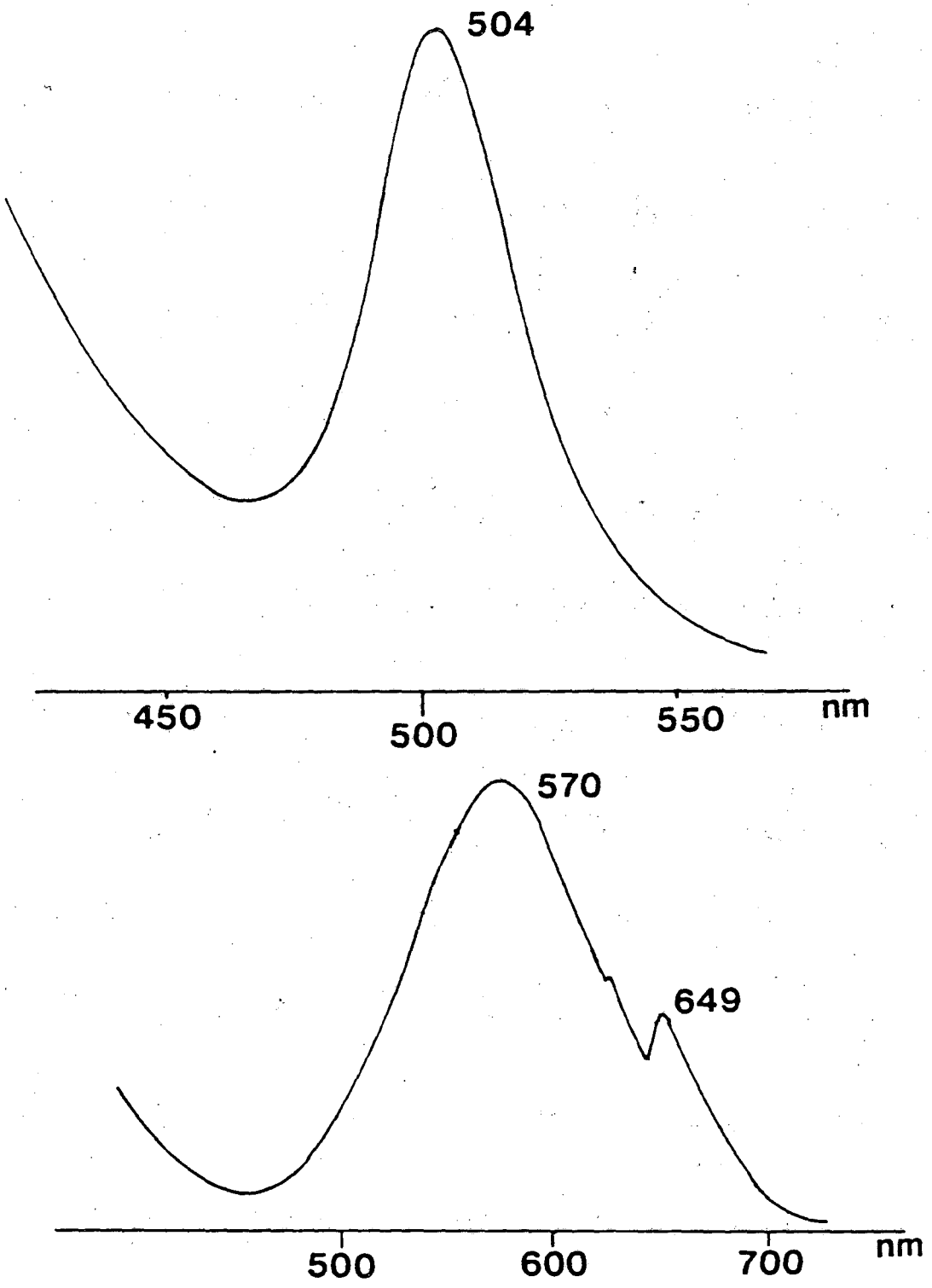

Figure 2.5: Visible spectra of $K_2[Yb(C_8H_8)_2]$ (top) and $K[Yb(C_8H_8)_2]$ (bottom) in THF.

X-ray Powder Pattern

The measured powder patterns of $K_2[Yb(C_8H_8)_2]\cdot 2DME$, $K_2[Ca(C_8H_8)_2]\cdot 2DME$ and the powder pattern calculated from the single crystal x-ray data of $K_2[Yb(C_8H_8)_2]\cdot 2DME$ are shown in Table 2.5. The powder pattern of $K_2[Yb(C_8H_8)_2]\cdot 2DME$ was calculated (by Dr. Allan Zalkin) using the cell dimensions and the structure factor of the single crystal structure determinations. Only two weak lines out of 21 lines calculated for $K_2[Yb(C_8H_8)_2]\cdot 2DME$ are not observed in the pattern of $K_2[Ca(C_8H_8)_2]\cdot 2DME$.[30] Since the ytterbium(II) complex contains 50 more electrons than the calcium complex, one expects and finds intensity differences in the measured powder patterns of $K_2[Yb(C_8H_8)_2]\cdot 2DME$ and $K_2[Ca(C_8H_8)_2]\cdot 2DME$. Nevertheless, the x-ray powder patterns are sufficiently similiar that $K_2[Yb(C_8H_8)_2]\cdot 2DME$ and $K_2[Ca(C_8H_8)_2]\cdot 2DME$ are clearly isostructural.

Infrared Spectra: The infrared spectra of $K_2[Yb(C_8H_8)_2]$ and $K_2[Ca(C_8H_8)_2]$ as Nujol mulls are shown in Figure 2.6 The infrared spectra of $K_2[Yb(C_8H_8)_2]\cdot 2DME$ and $K_2[Ca(C_8H_8)_2]\cdot 2DME$ are shown in figure 2.7.

The infrared spectra of $K_2[Yb(C_8H_8)_2]$ and $K_2[Ca(C_8H_8)_2]$ are identical; the infrared spectra of $K_2[Yb(C_8H_8)_2]\cdot 2DME$ and $K_2[Ca(C_8H_8)_2]\cdot 2DME$ are also identical. This similarity of

Table 2.5: X-ray powder diffraction data on $K_2[M(C_8H_8)_2]\cdot 2DME$

M = Yb calculated[a]		Yb found		Ca found	
d(Å)[b]	I	d(Å)[c]	I[d]	d(Å)[c]	I[d]
9.75	282	9.83(5)	w+		
8.81	140	8.80(4)	w	8.76(4)	w
7.31	747	7.31(3)	s-	7.33(3)	s-
6.76	1282	6.73(2)	s	6.74(2)	s
6.35	229	6.36(2)	w+	6.37(2)	w-
5.79	1125	5.76(2)	s-	5.76(2)	s-
5.46	77	5.45(2)	w-		
4.89	174	4.87(1)	w+	4.90(1)	w-
4.45	392	4.42(1)	m	4.47(1)	m
4.33	4			4.34(1)	w
4.14	99	4.15(1)	w-	4.15(1)	w-
4.06	119	4.07(1)	w-	4.07(1)	w-
3.95	13			3.93(1)	w-
3.85	273	3.85(1)	m	3.85(1)	m
3.65	17			3.61(1)	w-
3.51	19			3.52(1)	w-
3.41	235	3.43(1)	w+	3.43(1)	w
3.31	131	3.31(1)	w-	3.31(1)	w-
3.24	129	3.25(1)	w-	3.25(1)	w-
3.17	155	3.17(1)	w	3.17(1)	m
3.10	227	3.10(1)	w	3.10(1)	w

(a) The complete calculated powder pattern for M = Yb is at the end of this chapter. (b) Adjacent lines combined where 2θ values are less than 0.50° apart. The position of the combined line is calculated as

$$D = \frac{\Sigma(Di * Ii)}{\Sigma Ii}$$

(c) The number in brackets is the extimated error in the least significant digit. (d) Estimated relative intensity.

infrared spectra was anticipated, since ytterbium(II) and calcium(II) have almost identical ionic radii[8] and previous work had shown that the infrared spectra of $Ca(C_5H_5)_2$ and $Yb(C_5H_5)_2$ are similar,[12] even though the sample of $Yb(C_5H_5)_2$ may have been contaminated with $Yb(C_5H_5)_3$.[32]

Infrared spectra for the 600-1000 cm^{-1} region of some bis-[8]annulene complexes are compared in Table 2.6. It has been noted previously that the infrared spectra of all of the bis-[8]annulene sandwich complexes of the f-transition metals are similar as a result of their similar structures.[30] The assignment of the infrared absorbances of these complexes is still in question; a recent assignment[33] (shown in Table 2.6) is additionally consistent with the fact that $K_2[Yb(C_8H_8)_2]$ and $K_2[Ca(C_8H_8)_2]$ have the same infrared spectra. An earlier assignment attributed the strong band at 698 cm^{-1} to a ring-metal-ring tilt.[34] Such an assignment could not give identical spectra for $K_2[Yb(C_8H_8)_2]$ and $K_2[Ca(C_8H_8)_2]$, since the difference in mass of ytterbium and calcium would cause a difference in energy for any absorbances which involve the central metal. Since the infrared spectra of $K_2[Yb(C_8H_8)_2]$ and $K_2[Ca(C_8H_8)_2]$ are identical in the 400-4000 cm^{-1} region, then any absorbance involving the central metal must occur outside of this range. A further discussion of the infrared spectra of bis([8]annulene) sandwich complexes is in Chapter 4.

$K_2[Ca(C_8H_8)_2]$ - top,

$K_2[Yb(C_8H_8)_2]$ - bottom.

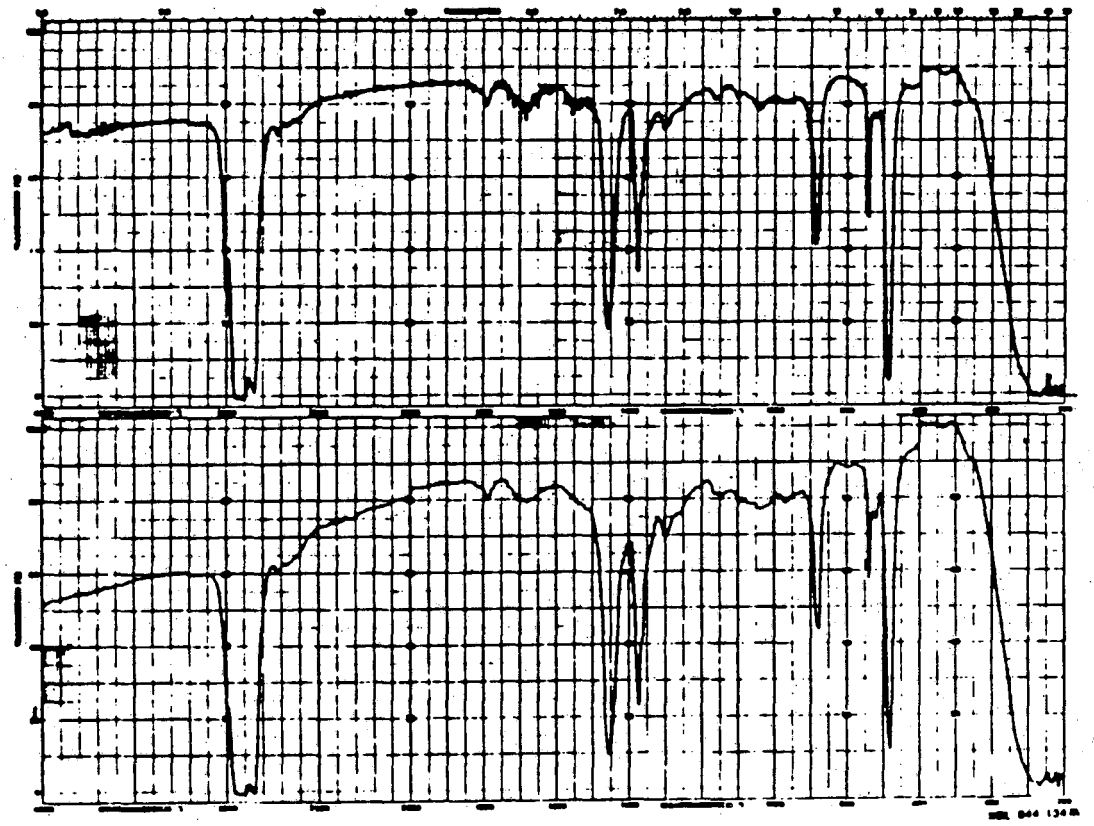

Figure 2.6: Infrared Spectra (nujol mull) of $K_2[M(C_8H_8)_2]$ (M=Ca, Yb)

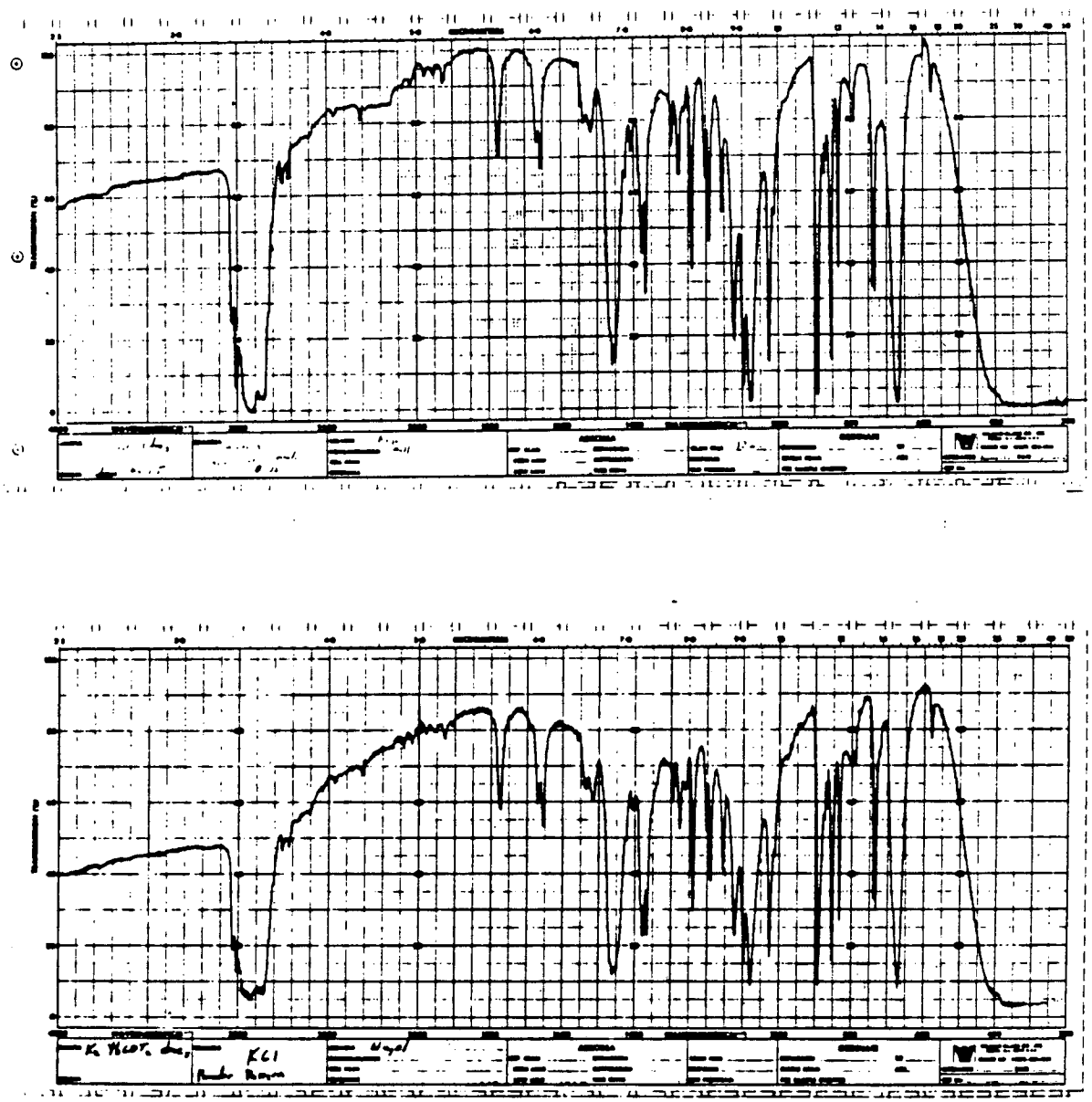

Figure 2.7: Infrared Spectra (nujol mull) of $[K(C_4H_{10}O_2)]_2[M(C_8H_8)_2]$ (M=Ca, Yb).

Table 2.6. Comparison of infrared spectra[a,b]

$U(C_8H_8)_2$[c]	$K[La(C_8H_8)^2]$[d]	$K[Yb(C_8H_8)_2]$[e]	$K_2[Yb(C_8H_8)_2]$[e,f]	Assignment[f]
698 vs	680 vs	690 vs	683 vs	p(CH), A_{2u}
746 s	740 m	741 s	740 m	v(CC), A_{2u}
777 m	771 w	770 w		p(CH), E_{1u}
792 m				
			879 s	
900 s	892 s	899 s	888 s	β(CH), E_{1u}

(a) vs, very strong; s, strong; m, medium; w, weak. (b) nujol mulls. (c) Ref. 34. (d) Ref. 33. (e) This work. (f) Infrared of $K_2[Yb(C_8H_8)_2]$ and $K_2[Ca(C_8H_8)_2]$ are identical.

Discussion of the Structure of $[K(C_4H_{10}O_2)]_2[Yb(C_8H_8)_2]$: The atomic parameters and distances are listed in Tables 2.7 and 2.8. Figure 2.8 shows an ORTEP view of a formula unit with the numbering scheme used for the atoms in Table II. Additional atomic distances are given at the end of this chapter.

The [8]annulene rings of $K_2[Yb(C_8H_8)_2]\cdot 2DME$ are planar with all the carbon-carbon bond lengths equivalent. The maximum deviation from the least squares plane of the ring for any carbon atom is 0.01 Å . The carbon-carbon distances within the ring range from 1.40 to 1.42 Å with an average of 1.41 ± .01 Å . The bond angles within the ring are all within their standard deviations of 135°.

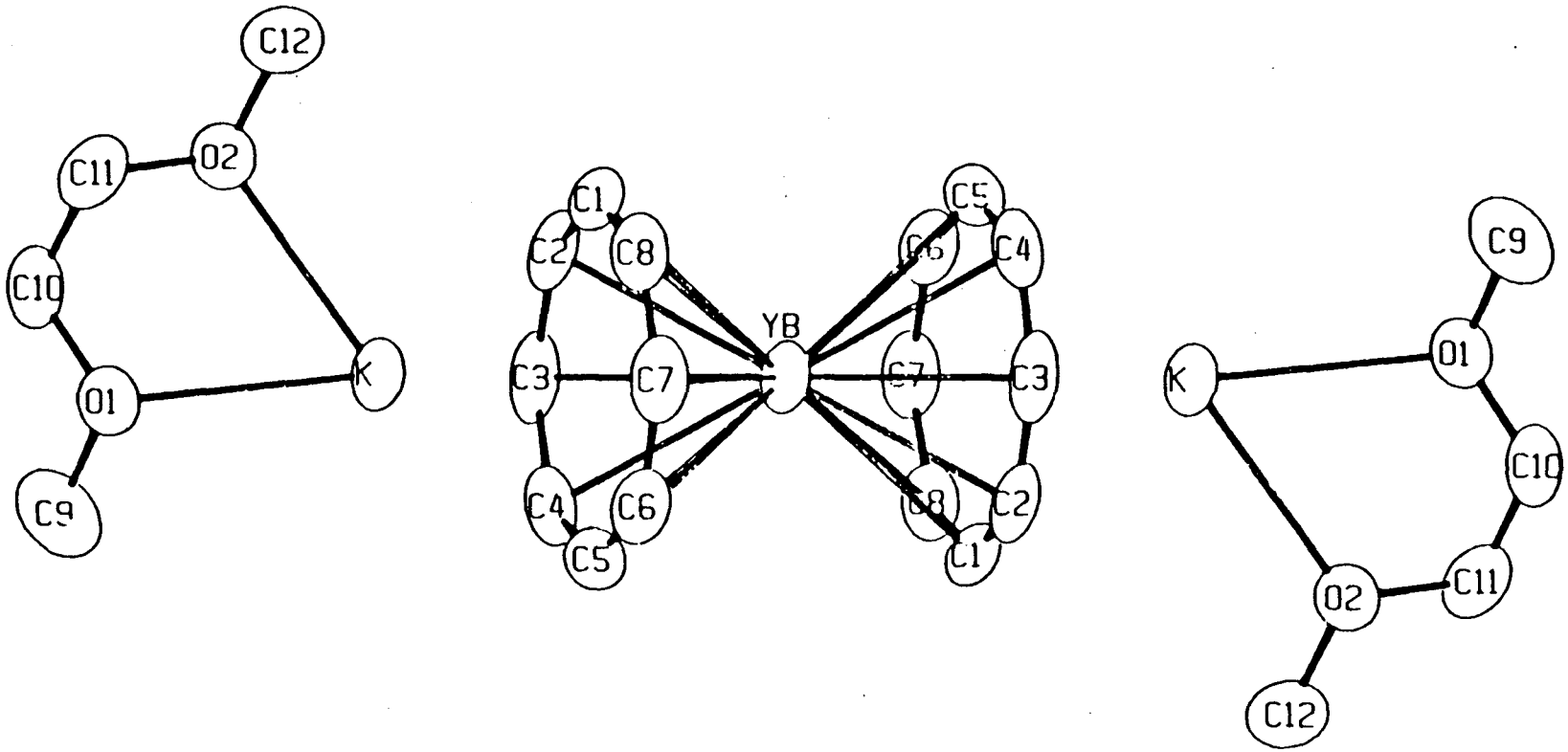

(hydrogen atoms omitted for clarity)

Figure 2.8: ORTEP drawing and atomic numbering scheme for $[K(C_4H_{10}O_2)]_2[Yb(C_8H_8)_2]$

Table 2.7: Positional parameters for $[K(C_4H_{10}O_2)]_2[Yb(C_8H_8)_2]$[a]

Atom	x	y	z
Yb	0	0	0
K	0.35199(13)	-0.34073(12)	0.09645(17)
O(1)	0.5266(4)	-0.5865(4)	0.2003(5)
O(2)	0.6346(4)	-0.3377(4)	0.3517(6)
C(1)	0.2982(6)	-0.0479(6)	0.1970(8)
C(2)	0.2208(7)	-0.1188(6)	0.2916(7)
C(3)	0.1084(7)	-0.2140(6)	0.2420(8)
C(4)	0.0252(7)	-0.2787(6)	0.0758(10)
C(5)	0.0200(6)	-0.2717(6)	-0.1077(9)
C(6)	0.0944(7)	-0.1982(6)	-0.2010(7)
C(7)	0.2084(6)	-0.1027(6)	-0.1517(8)
C(8)	0.2936(6)	-0.0416(6)	0.0138(9)
C(9)	0.4371(9)	-0.7001(7)	0.1946(12)
C(10)	0.6448(7)	-0.5787(6)	0.3691(8)
C(11)	0.7322(7)	-0.4573(7)	0.3771(9)
C(12)	0.7098(8)	-0.2143(7)	0.3748(10)

(a) In this Table and in Table 2.8, 2.9, 2.10 and 2.11, the number in parentheses is the estimated standard deviation in the least significant digits.

Table 2.8: Selected interatomic distances (Å)

Atom 1-Atom 2	*Distance*	*Atom 1-Atom 2*	*Distance*
Yb-C(1)	2.719(5)	K-C(1)	2.998(6)
-C(2)	2.736(5)	-C(2)	3.026(6)
-C(3)	2.760(5)	-C(3)	3.036(6)
-C(4)	2.783(5)	-C(4)	3.027(6)
-C(5)	2.773(5)	-C(5)	3.025(6)
-C(6)	2.729(5)	-C(6)	3.025(6)
-C(7)	2.711(5)	-C(7)	3.012(6)
-C(8)	2.715(5)	-C(8)	2.989(6)
O(1)-C(9)	1.425(8)	K-O(1)	2.796(4)
-C(10)	1.411(7)	-O(2)	2.731(4)
O(2)-C(11)	1.415(7)	K-O(1)[a]	2.928(4)
-C(12)	1.414(8)		
C(11)-C(10)	1.481(10)		

(a) Atom at position 1-x, -1-y, -z.

The ytterbium atom is on the center of symmetry and is sandwiched by two planar [8]annulene ligands; the potassium atoms are each coordinated to one dimethoxyethane ligand and a $[Yb(C_8H_8)_2]$ dianion. The average ytterbium-to-carbon distance is 2.74 ± 0.03 Å ; the distance of the ytterbium atom to the least squares plane of the [8]annulene is 2.03 Å . The two sandwiching [8]annulene rings are parallel-planar and exactly eclipsed (being related to each other through the center of symmetry), making the symmetry of the $[Yb(C_8H_8)_2]$ dianion D_{8h}. $K_2[Yb(C_8H_8)_2]$ is the only bis-[8]annulene complex of a lanthanide that exhibits eclipsed rings. In $K(C_6H_{14}O_3)][Ce(C_8H_8)_2]$[35] the [8]annulene rings are in a staggered conformation (i.e., the symmetry of the $[Ce(C_8H_8)_2]$ anion is D_{8d}) and in $[Nd(THF)_2(C_8H_8)][Nd(C_8H_8)_2]$[16] the [8]annulene rings are nearly eclipsed, but not parallel-planar. The eclipsed vs. staggered arrangement of bis-[8]annulene rings is not considered to be indicative of the type of ring-metal bond for these complexes. Wideline NMR studies on crystals of $U(C_8H_8)_2$ indicate that the barrier to ring rotation is essentially 0 kcal $mole^{-1}$.[36] Any conformational preference for the rings in the bis-[8]annulene complexes is more than likely due to crystal packing forces, and not due to orbital interactions between the metal and ligands.

The average potassium-to-carbon distance is 3.02 ± 0.02 Å ; the distance of the potassium atom to the least squares plane of the [8]annulene ring is 2.39 Å . The potassium atom is also coordinated to two oxygen atoms of a DME ligand at 2.796(4) Å and

2.731(4) Å and to an oxygen atom of an adjacent DME ligand at a distance of 2.928(4) Å .

The average Yb-C distance (2.74 ± .03 Å) in 1 2DME is the same as the average Ce-C distance (2.74 ± .02 Å) in $[K(C_6H_{14}O_3)][Ce(C_8H_8)_2]$.[35] These equal distances are consistent with Raymond's arguments on the ionic nature of the metal-carbon bond in [8]annulenelanthanide complexes,[37] since the ionic radii of Ce(III) and Yb(II) are the same.[38] Note that the addition of the calculated ionic radius of carbon in [8]annulene dianion, 1.49 Å ;[23] to the extrapolated ionic radius for a 10-coordinate divalent ytterbium cation, 1.25 Å ;[39] gives a Yb-C distance of 2.74 Å .

Discussion of the Structure of $[K(C_6H_{14}O_3)]_2[Yb(t\text{-}BuC_8H_7)_2]$. The ORTEP drawing of this molecule and the atomic numbering scheme is given in figure 2.9. The positional parameters are given in table 2.9. Selected interatomic distances and distances of selected atoms from the least squares plane of the ring are given in tables 2.10 and 2.11 respectively.

The ytterbium atom is centrally sandwiched between the two substituted [8]annulene rings at a distance of 2.055 Å from the ring centers. The potassium atoms are also centered on the substituted [8]annulene rings, opposite the ytterbium atom, at a

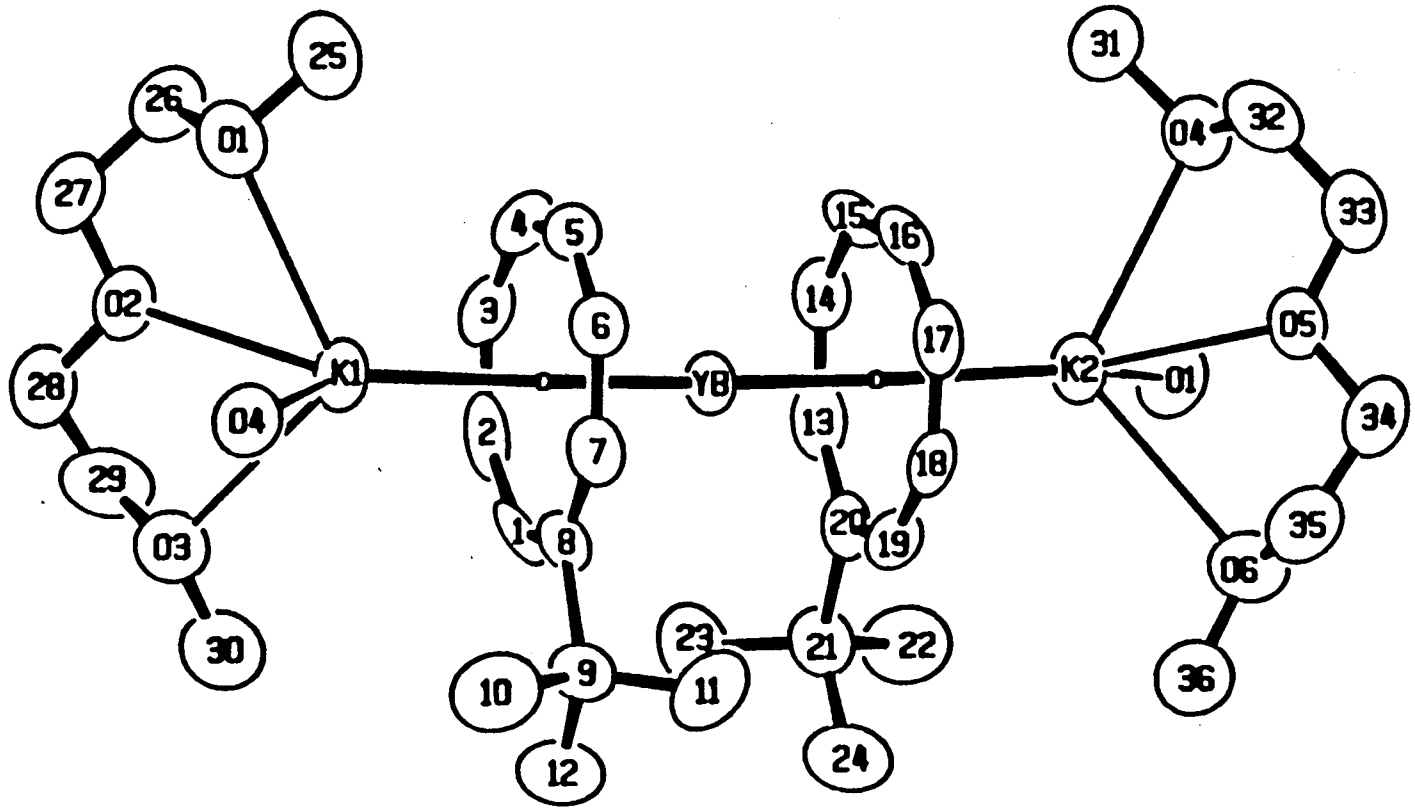

Figure 2.9: ORTEP drawing and atomic numbering scheme for $[K(C_6H_{14}O_3)]_2[Yb(tBuC_8H_7)_2]$.

Table 2.9: Positional parameters for $[K(C_6H_{14}O_3)]_2[Yb(t\text{-}BuC_8H_7)_2]$.

ATOM	X	Y	Z
YB	.04544(3)	.18694(2)	.24563(2)
K(1)	.34906(18)	.19628(10)	.44746(8)
K(2)	-.26406(16)	.18968(10)	.04465(8)
O(1)	.4529(5)	.3275(3)	.50844(29)
O(2)	.3451(6)	.2295(3)	.57997(28)
O(3)	.3212(7)	.0963(4)	.5509(3)
O(4)	-.3663(5)	.3170(3)	-.01679(28)
O(5)	-.2526(6)	.2208(3)	-.08799(27)
O(6)	-.2512(7)	.0862(3)	-.0605(3)
C(1)	.1471(9)	.1051(5)	.3523(4)
C(2)	.0682(9)	.1533(6)	.3786(4)
C(3)	.0602(10)	.2214(6)	.3804(5)
C(4)	.1246(11)	.2731(6)	.3546(5)
C(5)	.2251(10)	.2748(5)	.3177(4)
C(6)	.3045(8)	.2284(5)	.2949(4)
C(7)	.3165(8)	.1602(5)	.2945(4)
C(8)	.2532(8)	.1067(4)	.3175(4)
C(9)	.3093(9)	.0382(4)	.3015(4)
C(10)	.4548(10)	.0321(5)	.3429(6)
C(11)	.3052(11)	.0317(5)	.2245(5)
C(12)	.2329(12)	-.0209(5)	.3196(6)
C(13)	-.2241(8)	.1565(5)	.1990(4)
C(14)	-.2159(8)	.2258(5)	.1979(4)
C(15)	-.1388(10)	.2717(5)	.1732(5)
C(16)	-.0375(10)	.2681(5)	.1353(5)
C(17)	.0264(9)	.2162(6)	.1090(4)
C(18)	.0173(9)	.1479(5)	.1125(4)
C(19)	-.0568(9)	.1014(5)	.1401(4)
C(20)	-.1589(9)	.1022(5)	.1767(4)
C(21)	-.2120(9)	.0356(4)	.1947(4)
C(22)	-.3623(10)	.0285(5)	.1541(5)
C(23)	-.2045(10)	.0297(5)	.2712(5)
C(24)	-.1424(11)	-.0239(5)	.1726(6)
C(25)	.4333(10)	.3749(5)	.4539(5)
C(26)	.3646(9)	.3408(5)	.5541(5)
C(27)	.3941(9)	.2908(5)	.6097(5)
C(28)	.3351(11)	.1813(6)	.6293(5)
C(29)	.2546(14)	.1262(6)	.5956(6)
C(30)	.2563(16)	.0378(7)	.5240(6)
C(31)	-.3517(10)	.3642(5)	.0379(5)
C(32)	-.2846(9)	.3319(4)	-.0633(5)
C(33)	-.3034(9)	.2815(5)	-.1177(5)
C(34)	-.2393(10)	.1725(5)	-.1372(4)
C(35)	-.1686(10)	.1152(5)	-.1000(5)
C(36)	-.2009(14)	.0265(6)	-.0324(5)

Table 2.10: Selected Interatomic distances.

Atom 1-Atom 2	*Distance*	*Atom 1-Atom 2*	*Distance*
Yb-C(1)	2.733(8)	Yb-C(13)	2.788(8)
-C(2)	2.710(8)	-C(14)	2.758(8)
-C(3)	2.762(10)	-C(15)	2.735(8)
-C(4)	2.786(10)	-C(16)	2.746(8)
-C(5)	2.747(9)	-C(17)	2.766(8)
-C(6)	2.758(8)	-C(18)	2.737(8)
-C(7)	2.791(8)	-C(19)	2.767(8)
-C(8)	2.821(7)	-C(20)	2.836(8)

Table 2.11: Selected interatomic distances and distances of selected atoms from the least squares plane of the ring.

Plane 1: C(1) - C(8)		Plane 2: C(13) - C(20)	
Atom	Distance	Atom	Distance
Yb	-2.054	Yb	2.056
K(1)	2.456	K(2)	-2.468
C(1)	-0.022	C(13)	-0.022
C(2)	-0.004	C(14)	-0.011
C(3)	0.025	C(15)	0.024
C(4)	0.003	C(16)	0.009
C(5)	-0.030	C(17)	-0.024
C(6)	0.007	C(18)	-0.005
C(7)	0.018	C(19)	0.018
C(8)	0.003	C(20)	0.011
C(9)	0.007	C(21)	0.010

mean potassium-ring distance of 2.46 Å . The K-Yb-K angle is 176° and the planes of the two [8]annulene rings intersect at an angle of 2.7°. In addition to coordination to the [8]annulene ring, each potassium atom is coordinated by four oxygen atoms from the diglyme. Both O(1) and O(4) are involved in coordinating to two potassium atoms from two adjacent molecules; in the crystaline state the compound is polymeric.

The central carbon atoms of the t-butyl groups (C9 and C21) are in the plane of the [8]annulene ring. One methyl group (C12 or C24) is nearly in the plane of the ring such that the other methyl carbons (C10,11 or C22,23) are nearly equidistant above and below the plane of the ring (see figure 2.10). This orientation for a t-butyl group on an [8]annulene ring was predicted by calculations by Schilling.[40]

The conformation of the two rings is nearly eclipsed (figure 2.10); the distance between C12 and C24 is 4.21 Å .

The distance for a Van der Waal's interaction between methyl groups is ≈ 4.0 Å .[41] The question arises whether the closeness of the two t-butyl groups in the crystal structure of $[K(diglyme)]_2[Yb(t\text{-}BuC_8H_7)_2]$ is due to a Van der Waal's attraction between the alkyl groups or due to crystal packing forces. Since there are no other crystal stuctures determined for any other bis(alkyl[8]annulene) sandwich complexes, it is impossible,

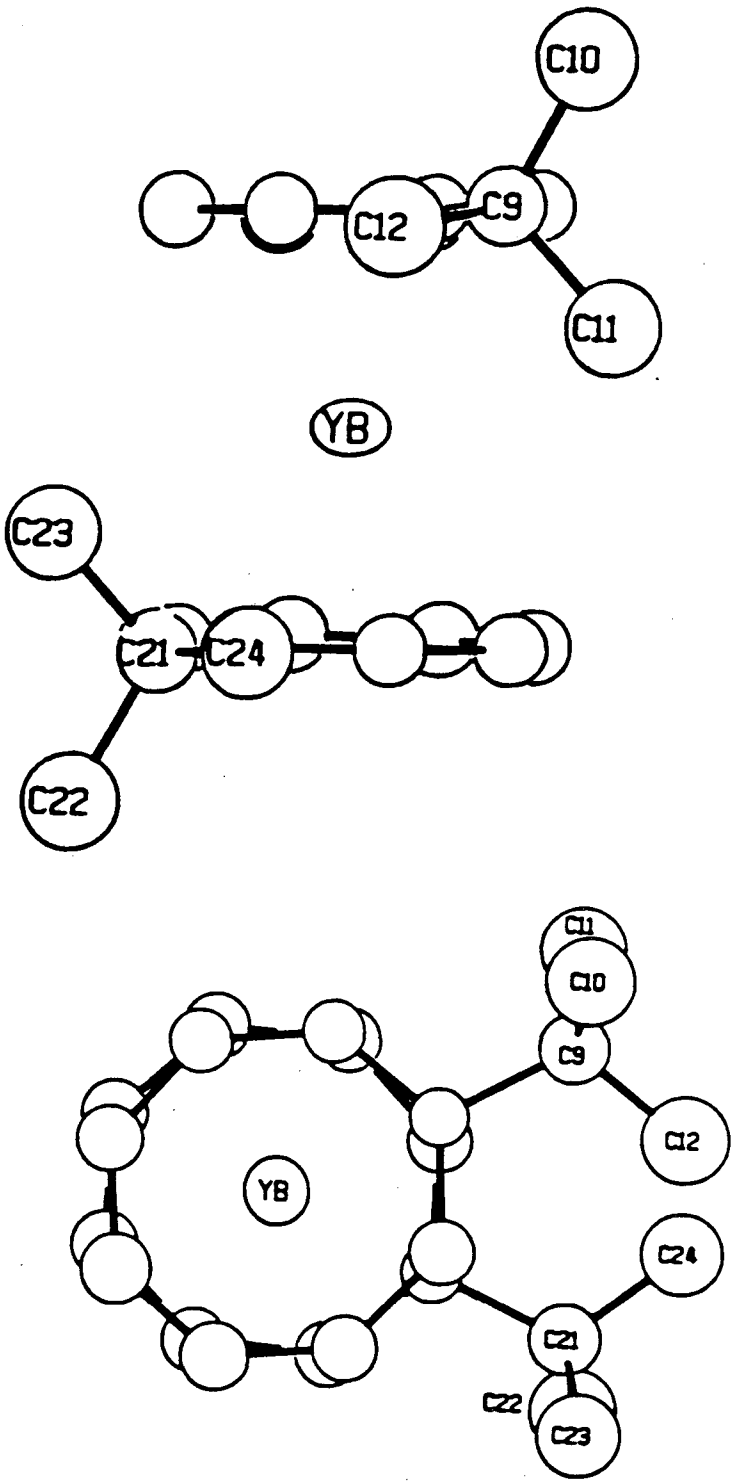

Figure 2.10: ORTEP of the "Side" and "Top" View of $[Yb(t\text{-}BuC_8H_7)_2]$ Dianion.

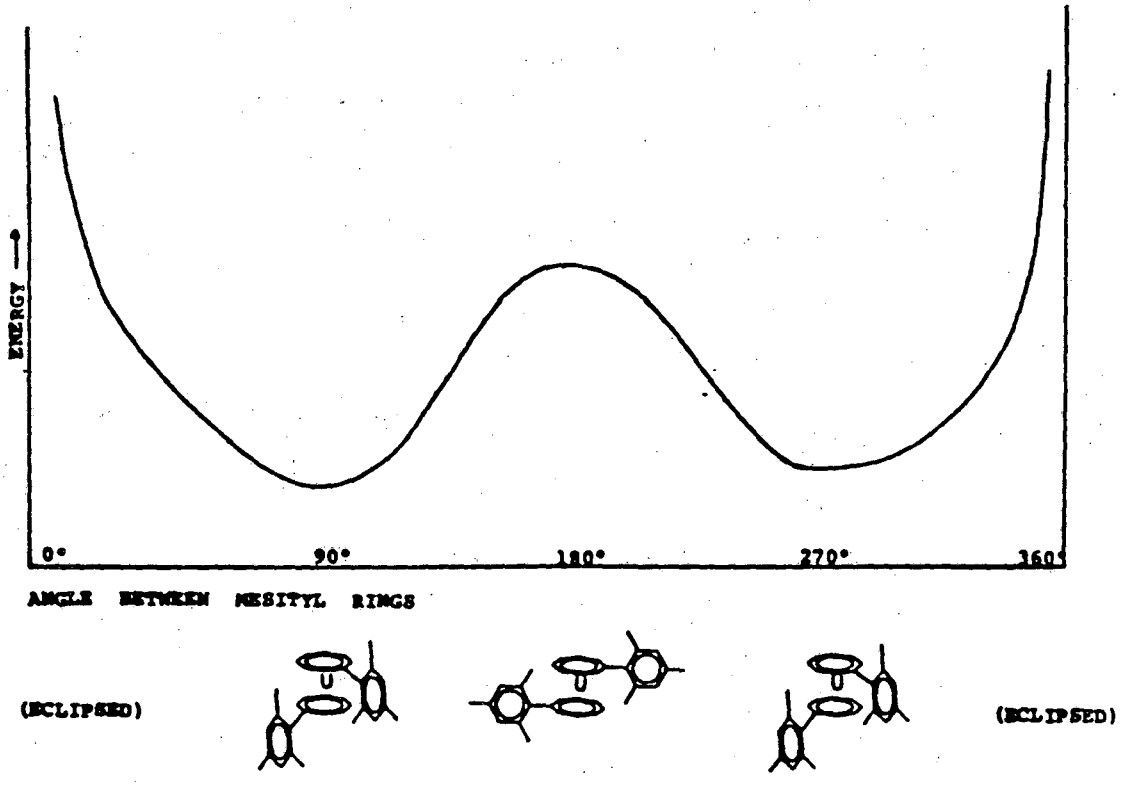

Figure 2.11: Energy diagram for the ring rotation in bis(mesityl[8]annulene)uranium(IV).

at this time, to determine the forces responsible for the conformation found in $[K(diglyme)]_2[Yb(t\text{-}BuC_8H_7)_2]$. It is, however, interesting to note that in bis(mesityl[8]annulene)uranium(IV), an unusual temperature-dependent ^{1}H-NMR spectrum has been explained by the preference of the mesityl groups on the two [8]annulene rings to be close to each other (figure 2.11).[42]

^{1}H-NMR: The ^{1}H-NMR of $K_2[Yb(C_8H_8)_2]$ and $K_2[Ca(C_8H_8)_2]$ were determined in THF-*d8* solutions. The sixteen equivalent protons of $K_2[Ca(C_8H_8)_2]$ occur as a singlet at δ = 5.47 ppm. This resonance is observed upfield from the resonances reported for $K[Y(C_8H_8)_2]$ and $K[La(C_8H_8)_2]$ which occur at 5.75 and 5.90 ppm, respectively, relative to external TMS.[30] The ring proton resonance of $K_2[Yb(C_8H_8)_2]$ is observed at δ = 5.47 ppm (figure 2.12). In its ground state, the ytterbium(II) ion has no unpaired electrons[43] and is diamagnetic; the lack of a shift in the observed ring proton resonance of $K_2[Yb(C_8H_8)_2]$ relative to $K_2[Ca(C_8H_8)_2]$ shows that $K_2[Yb(C_8H_8)_2]$ contains the diamagnetic lanthanide(II) ion. No resonance is observed for the paramagnetic $K[Yb(C_8H_8)_2]$ (Yb(III) is $4f^{13}$ and has one unpaired electron), due to paramagnetic line-broadening.

The ^{1}H-NMR of $K_2[Yb(t\text{-}BuC_8H_7)_2]$ in THF-*d8* is straightforward (figure 2.13). The seven ring protons occur as a multiplet at δ=5.26. The nine equivalent t-butyl methyl group protons occur as a sharp singlet at δ=1.52. For the analogous ytterbium(III)

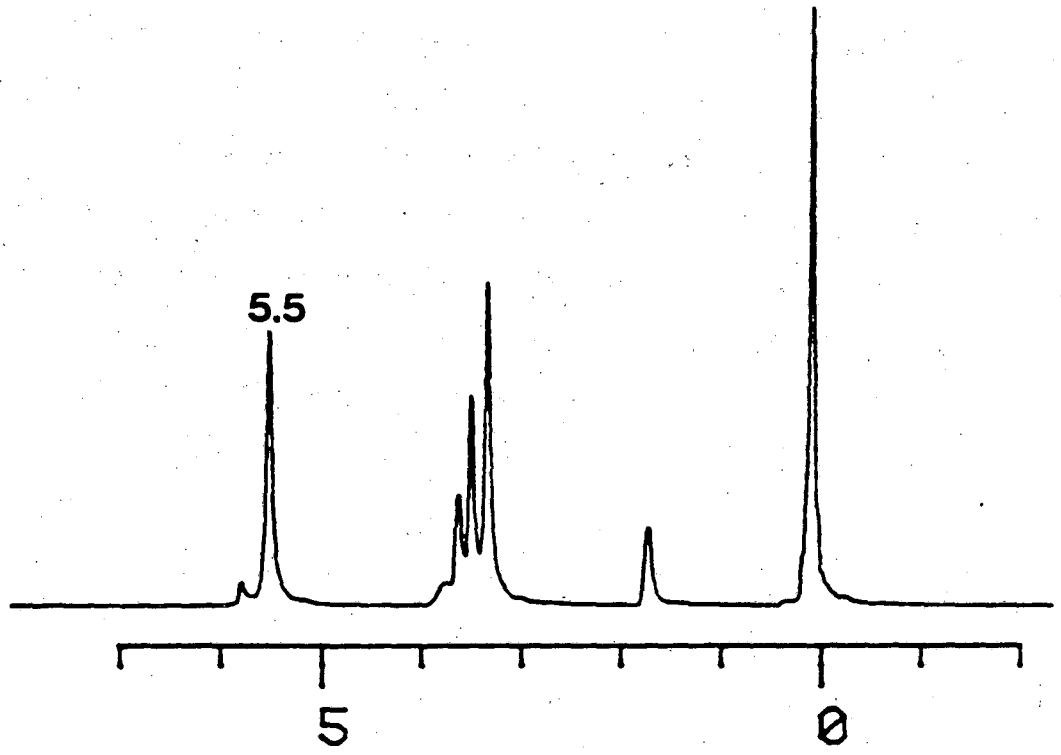

Figure 2.12: ^{1}H-NMR of $[K(DME)]_2[Yb(C_8H_8)_2]$ in THF-*d8*.

$K_2[Yb(C_8H_7(t\text{-}C_4H_9))_2]/THF_{d8}$
(a) (b)

H	δ (ppm)
a	5.31
b	1.54

XBL 844-1302

Figure 2.13: ^{1}H-NMR of $[K(C_6H_{14}O_3)]_2[Yb(t\text{-}BuC_8H_7)_2]$ in THF-*d8*.

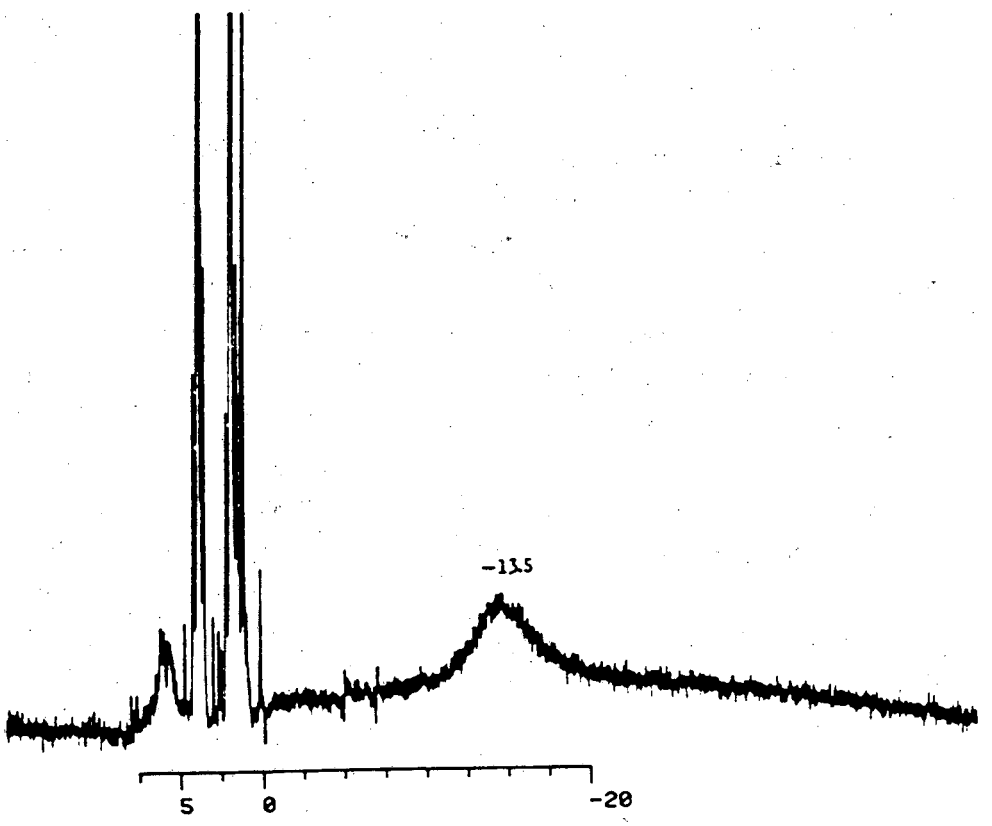

Figure 2.14: ^{1}H-NMR of $[K(C_6H_{14}O_3)][Yb(t\text{-}BuC_8H_7)_2]$ in THF-*d8*.

complex, the ring proton resonances are again too broad to be located, but the t-butyl methyl protons are far enough removed from the paramagnetic central atom that their resonance occurs as a broad singlet at $\delta \approx -14$ (line-width ≈ 300 Hz, figure 2.14).

Electron Exchange between $[Yb(C_8H_8)_2]^{=}$ *and* $[Yb(C_8H_8)_2]^{-}$.

When the ^{1}H-NMR spectrum of $K_2[Yb(C_8H_8)_2]$ was first recorded, there was no signal found at δ=5.47 at room temperature. The only major peaks observed could be assigned as stopcock grease, and the residual proton peaks of THF-*d8*. Upon cooling the solution, a resonance at $\delta \approx 5.5$ appeared and sharpened as the sample became colder (figure 2.15). It was postulated at that time that the temperature-dependent phenomenon observed was an exchange process involving the diamagnetic $K_2[Yb(C_8H_8)_2]$ and the paramagnetic $K[Yb(C_8H_8)_2]$. At room temperature, this exchange process was occurring at a rate such that the ring-proton resonance was time-averaged between the Yb(II) and the Yb(III) environment and was too broad to be observed due to the combination of exchange and paramagnetic broadening effects. At colder temperatures, the exchange was slow enough that the resonance for the diamagnetic species could be observed. Later experiments were successful at isolating pure $K_2[Yb(C_8H_8)_2]$ and the ^{1}-NMR of this complex was as expected for the diamagnetic complexes. Addition of $K[Yb(C_8H_8)_2]$ to THF-*d8* solution of the diamagnetic ytterbium(II) complex

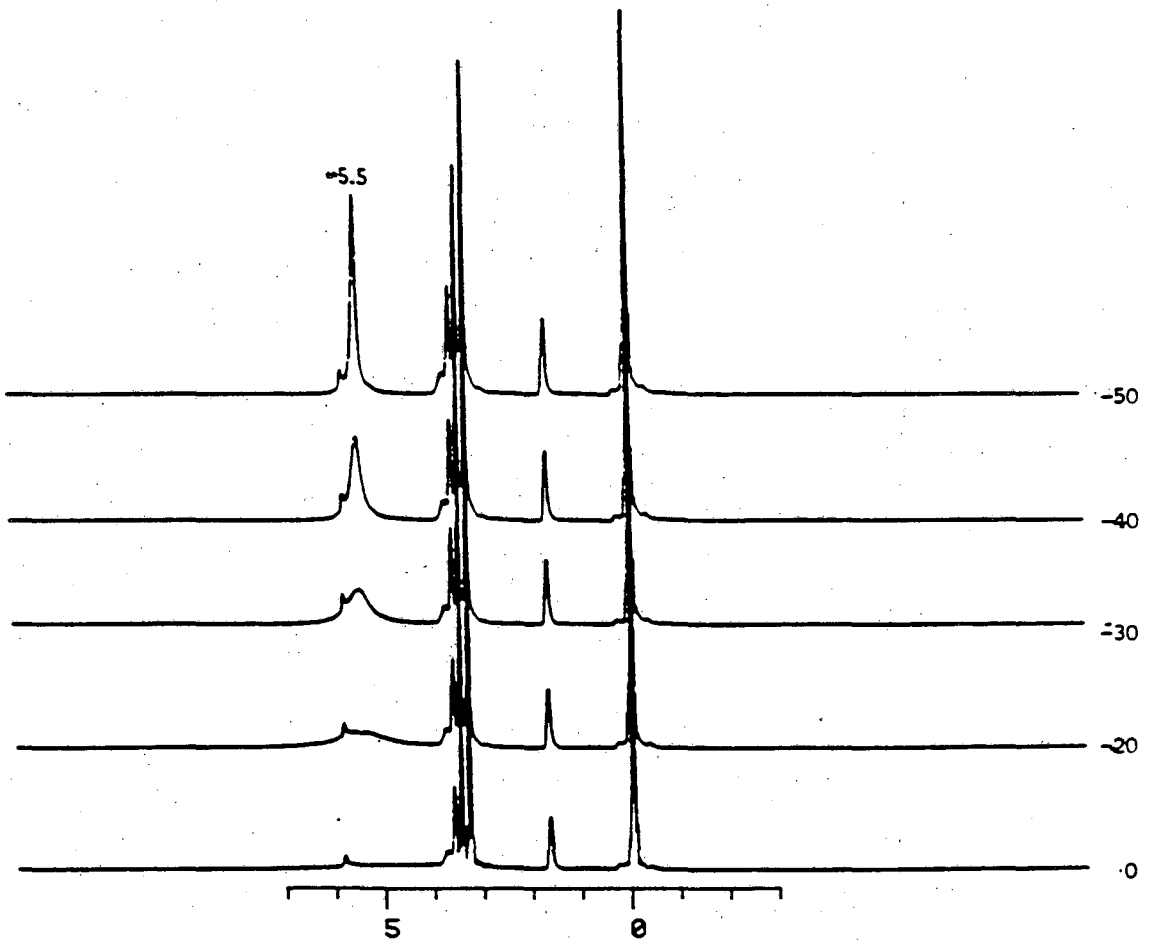

Figure 2.15: Temperature dependent ^{1}H-NMR of bis([8]annulene)-ytterbate(II) and -ytterbate(III) anions (potassium-DME adducts).

verified that the phenomenon observed in the earlier experiment was due to the presence of $[Yb(C_8H_8)_2]^-$ in the $K_2[Yb(C_8H_8)_2]$ sample.

There are two processes which can occur which will average the ring-protons' environment between Yb(II) and Yb(III). One such process is the [8]annulene ring exchange between $[Yb(C_8H_8)_2]^=$ and $[Yb(C_8H_8)_2]^-$. From experiments involving the reaction of $[Ce(C_8H_8)_2]^-$ with UCl_4 or $CeCl_3$,[30] it is known that the [8]annulene rings of the lanthanide(III) complexes are quite labile (2.15, 2.16). No experiments had been performed to determine if the ring exchange was fast on the NMR timescale.

[2.15]

$$K[Ce(C_8H_8)_2] + UCl_4 \text{ ------> } U(C_8H_8)_2 + CeCl_3 + KCl$$

[2.16]

$$K[Ce(C_8H_8)_2] + CeCl_3 \text{ ------> } [(C_8H_8)CeCl\cdot THF]_2 + KCl$$

The other process that can time-average the ring environment between the Yb(II) and Yb(III) atoms is an electron exchange between the two sandwich complexes, by a process analogous to the ferrocene/ferricenium exchange illustrated earlier in this chaptern (2.17).

[2.17]

$$[Yb(C_8H_8)_2]^- \underset{-e^-}{\overset{+e^-}{\rightleftharpoons}} [Yb(C_8H_8)_2]^=$$

The temperature-dependent ^{1}H-NMR of the bis([8]annulene)ytterbate(II) and -ytterbate(III) system could be due to either or both of the exchange processes discussed above.

The calcium analog of the ytterbium(II) complex served as an excellent tool for determining the exchange process responsible in the observed ^{1}H-NMR of the $[Yb(C_8H_8)_2]^=/[Yb(C_8H_8)_2]^-$ mixture. Since $K_2[Ca(C_8H_8)_2]$ had been shown to be identical in structure and physical properties to the ytterbium(II) analog and since calcium does not have a trivalent oxidation state, the only process that can result in a time averaging of the ring protons' environment in a mixture of $[Ca(C_8H_8)_2]^=$ and $[Yb(C_8H_8)_2]^-$ is [8]annulene ring exchange.

The temperature-dependent ^{1}H-NMR spectrum of approximately equal ammounts of $K_2[Ca(C_8H_8)_2]$ and $K[Yb(C_8H_8)_2]$ indicate that ring exchange does not occur between these two complexes on the NMR timescale. Figure 2.16 shows that the ring resonance of $K_2[Ca(C_8H_8)_2]$ remains sharp and unshifted throughout a temperature range between -60 to 40 °C.

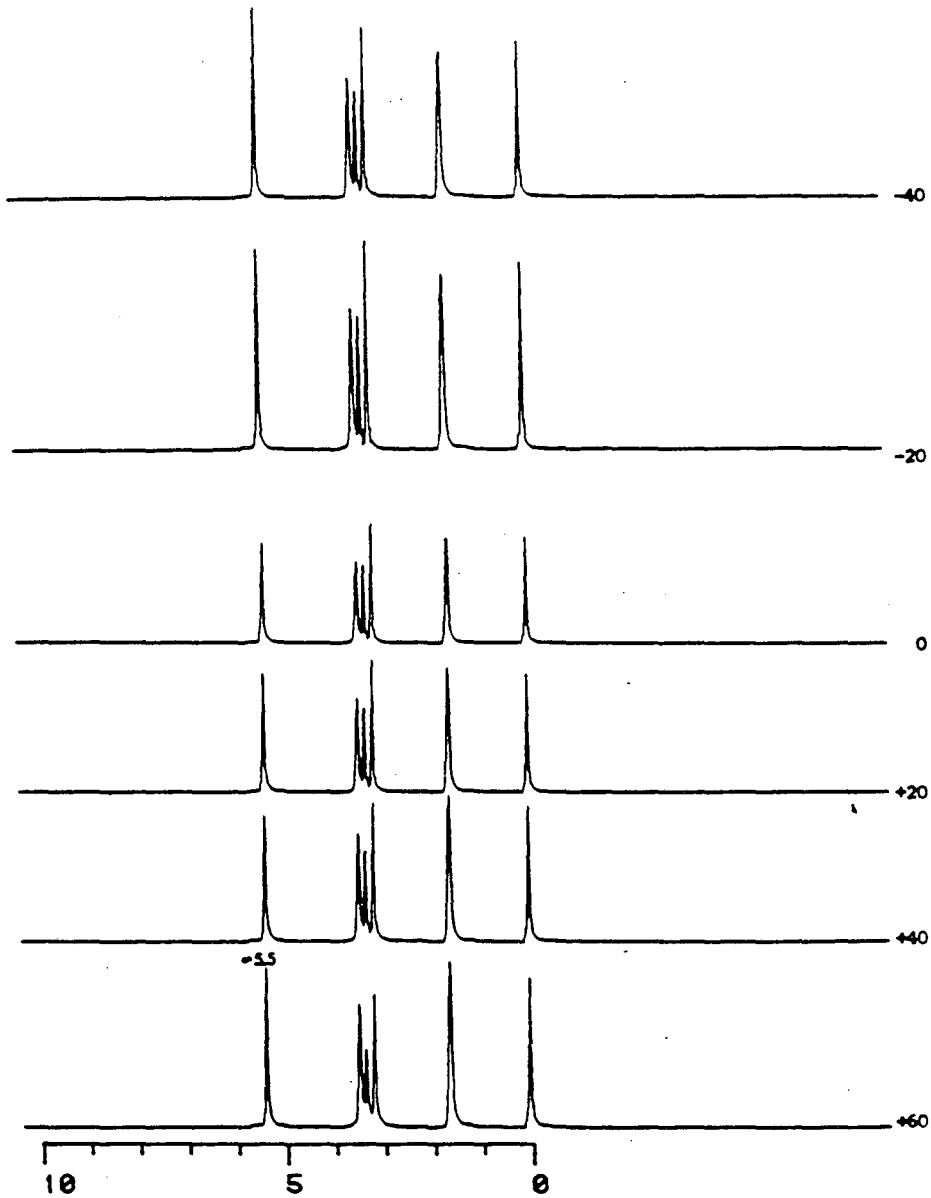

Figure 2.16: Temperature Dependent ^{1}H-NMR Spectrum of a Mixture of $[K(DME)]_2[Ca(C_8H_8)_2]$ and $[K(DME)][Yb(C_8H_8)_2]$ in THF-d8.

The NMR experiment shown above indicates that the ring exchange between $K_2[Ca(C_8H_8)_2]$ and $K[Yb(C_8H_8)_2]$ in THF-*d8* is either slow on the NMR timescale or does not occur at all. In order to show whether or not the [8]annulene rings of $K_2[Ca(C_8H_8)_2]$ are as labile as the [8]annulene rings on the class $K[Ln(C_8H_8)_2]$, $K_2[Ca(C_8H_8)_2]$ and $K[Yb(t\text{-}BuC_8H_7)_2]$ were mixed in THF-*d8*. Although slow compared to the NMR timescale, ring exchange does occur between the calcium(II) and ytterbium(III) bis-[8]annulene complexes. The ^{1}H-NMR of a THF-*d8* solution made from $K_2[Ca(C_8H_8)_2]$ and $K[Yb(t\text{-}BuC_8H_7)_2]$ has resonances that can be assigned as $K_2[Ca(C_8H_8)_2]$ and $K_2[Ca(t\text{-}BuC_8H_7)_2]$ (figure 2.17). The bis(*t*-butyl-[8]annulene)calcate(II) can come only as a result of ring exchange between the unsubstituted calcium complex with the substituted ytterbium(III) complex (2.18).

[2.18]

$$K_2[Ca(C_8H_8)_2] + K[Yb(t\text{-}BuC_8H_7)_2] \longrightarrow K_2[Ca(t\text{-}BuC_8H_7)_2] + K[Yb(C_8H_8)_2]$$

The sharpness of the resonances of the calcium complexes again indicate that ring exchange between the calcium(II) and ytterbium(III) species is slow on the NMR timescale; the above experiments clearly rule out ring-exchange as the source of the phenomenon observed in the bis([8]annulene)ytterbate(II) and -ytterbate(III) system.

In the NMR spectrum shown in figure 2.17, there is a resonance at δ=1.03 that can be assigned as the methyl proton resonance for

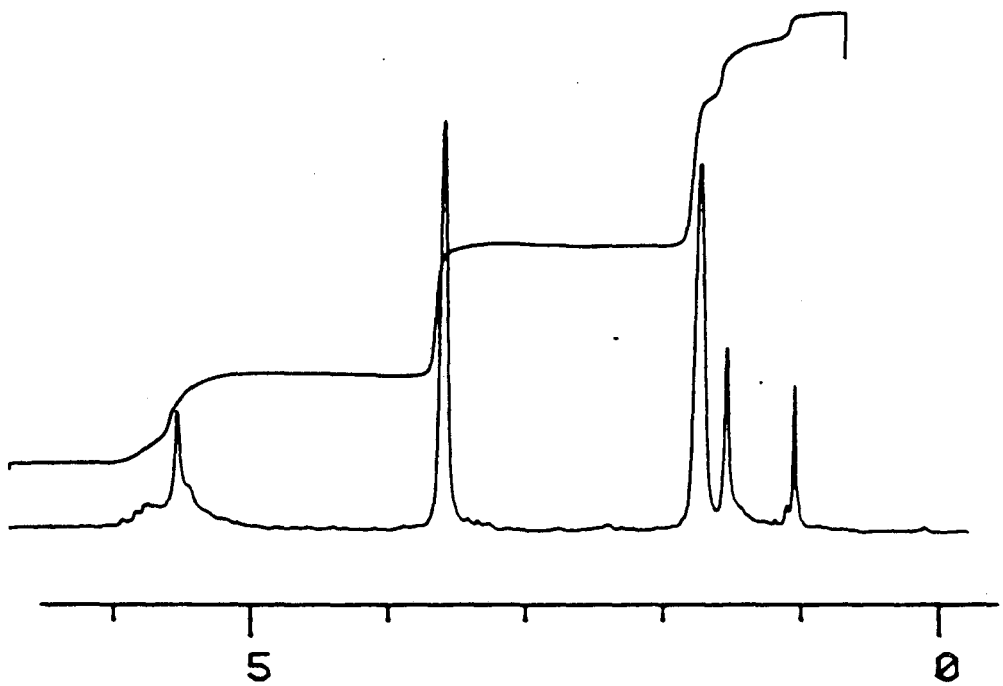

Figure 2.17: ^{1}H-NMR of $K_2[Ca(C_8H_8)_2]$ + $K[Yb(t\text{-}BuC_8H_7)_2]$.

neutral t-butyl-cyclooctatetraene. The presence of this neutral species (and the lack of any neutral unsubstituted cyclooctatetraene can be explained by the reducing ability of t-butyl[8]annulene dianion.

Since the ring environment in the $[Yb(C_8H_8)_2]^{=}/[Yb(C_8H_8)_2]^{-}$ system is not averaged by [8]annulene ring exchange, then the only other phenomenon possible to average the ring's environment between a ytterbium(II) and a ytterbium(III) atom is electron exchange of the type shown in equation 2.17.

The equation used by Warf[26] for the electron exchange (eq. 2.9) greatly simplifies when applied to a two-site exchange on one molecule at coalescence (for derivation of eq. 2.19 from the equation given by Warf, see the end of this chapter).

$$k_c = \pi(\delta v)/\sqrt{2} \qquad [2.19]$$

In the two-site exchange involving second order kinetics, the rate constant in the above expression is actually k_{app} such that the true rate constant for the system is k_{app} over some concentration.

In the $[Yb(C_8H_8)_2]^{=}/[Yb(C_8H_8)_2]^{-}$ system the rate law of the electron exchange reaction is

$$\text{rate} = k'[Yb(C_8H_8)_2^{=}][Yb(C_8H_8)_2^{-}] \qquad [2.20]$$

Since in the ^{1}H-NMR, the resonance of the diamagnetic species is monitored, it is useful to express the lifetime of the diamagnetic species, τ_D as:

$$\tau_D = 1/k'[Yb(C_8H_8)_2^-] \qquad [2.21]$$

At coalescence, the rate of exchange is then:

$$k_c' = \pi(\delta v)/\sqrt{2}[Yb(C_8H_8)_2^-] \qquad [2.22]$$

and

$$k_c'[Yb(C_8H_8)_2^-] = k_{app} \qquad [2.23]$$

Equation 2.23, however, neglects the effects of the concentrations of the two individual species in a two-site exchange involving two different molecules, such as the electron exchange between $[Yb(C_8H_8)_2]^=$ and $[Yb(C_8H_8)_2]^-$.

The equation for the rate of reaction at coalescence for the exchange between two molecules is somewhat more involved than equation 2.19. For the exchange between two molecules, the mole fractions of each component (f_x) are not equal, so that the individual mole fractions and the total concentration (c) of the NMR sample must be considered, since the exchange is second order (first order in each component). Deriving the rate of exchange for a second order reaction from equation 2.9, taking into account the individual component mole fractions (f_x) and total concentration (c) gives:

$$k_c' = \left(4\, f_{YbII} f_{YbIII}\, \frac{\pi^2 (\delta v)^2}{c[Yb(C_8H_8)_2^-]}\right)^{1/2} \qquad [2.24]$$

The derivation of equation 2.24 from equation 2.9 is also shown at the end of this chapter.

In order to estimate the rate constant at coalescence for the electron exchange between $[Yb(C_8H_8)_2]^=$ and $[Yb(C_8H_8)_2]^-$ an NMR sample tube was prepared containing a THF-*d8* solution that was 3.7×10^{-2} M in $K_2[Yb(C_8H_8)_2]$ and 3×10^{-3} M in $K[Yb(C_8H_8)_2]$. The temperature dependent ^{1}H-NMR of this sample indicated that the coalescence temperature for the $[Yb(C_8H_8)_2]^=$ and $[Yb(C_8H_8)_2]^-$ exchange was ≈ -10°C. At 30°C, a broad peak (line-width ≈ 300 Hz) peak was observed at $\delta \approx 2$ (figure 2.18). If this peak is assumed to be the time averaged resonance between $[Yb(C_8H_8)_2]^=$ and $[Yb(C_8H_8)_2]^-$, then the chemical shift of the paramagnetic species at 30°C is calculated as $\delta \approx -50$ from equation 2.25.

$$\delta_{YbIII} = \frac{\delta_c - f_{YbII}(\delta_{YbII})}{f_{YbIII}} \qquad [2.25]$$

Since the chemical shift of the ring proton resonance of $K[Yb(C_8H_8)_2]$ is for T = 30°C, then it is assumed that this resonance is ≈ -55 ppm at the coalescence temperature of the

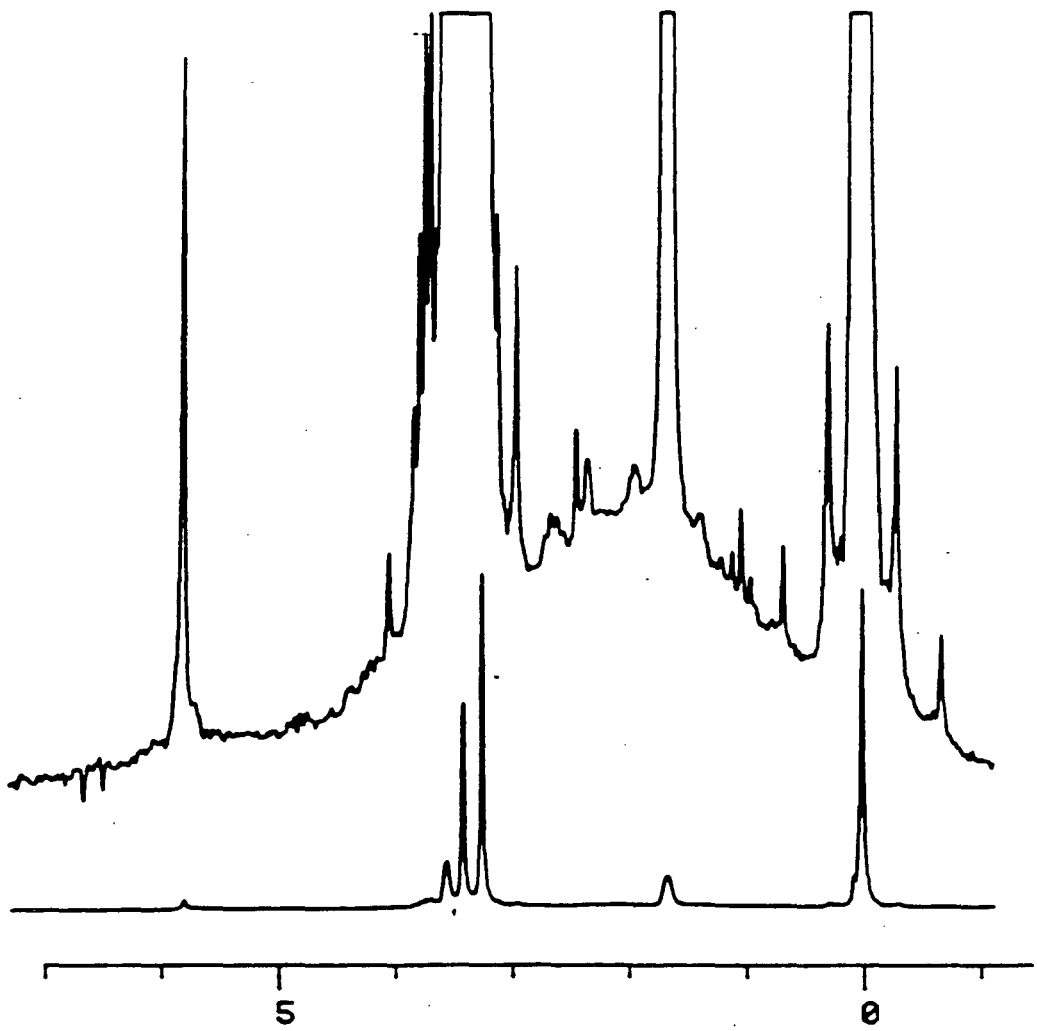

Figure 2.18: Time-averaged ^{1}H-NMR resonance peak in the $[Yb(C_8H_8)_2]^-/[Yb(C_8H_8)_2]$ spectrum (at 30°C).

system.[44] In this case, the δv for equations 2.19 and 2.24 is $\approx$ 5400 Hz and the rate of exchange at coalescence (which is the rate of the electron exchange reaction at -10°C) from equation 2.24 is $k' \approx 8 \times 10^5$ moles^{-1}s^{-1} (if the concentrations of the individual components are ignored, a rate of $k^1 \approx 5 \times 10^6$ moles^{-1}s^{-1} is calculated from eq. 2.19). A rate constant of $k' = 10^5$-10^6 moles^{-1}s^{-1} at -10°C for the exchange between bis([8]annulene)ytterbate(II) and -ytterbate(III) is consistent with a rate of 5.7×10^6 moles^{-1}s^{-1} (at 25°C) found for the electron exchange between ferrocene and ferricenium ion.

The addition of $NOBF_4$ to a THF-*d8* solution of $[K(diglyme)]_2[Yb(t\text{-}Bu(C_8H_7)_2]$ causes the resonance at δ=1.54 to disappear and a new, broad resonance to appear upfield of 1.54 ppm (experiment at RT). As this solution is cooled, the peak broadens and dissappears (at -10 - -20°C). By the time the solution is cooled to -40°C, a broad resonance appears at δ=1.54 which sharpens as the solution is cooled further (figure 2.18). It is apparent that the electron exchange between $[Yb(t\text{-}BuC_8H_7)_2]^{=}$ and $[Yb(t\text{-}BuC_8H_7)_2]^{-}$ occurs in this system. Since the coalesced t-butyl methyl proton peak is easily observable in this system, a study similar to Wahl's can be undertaken in future research.

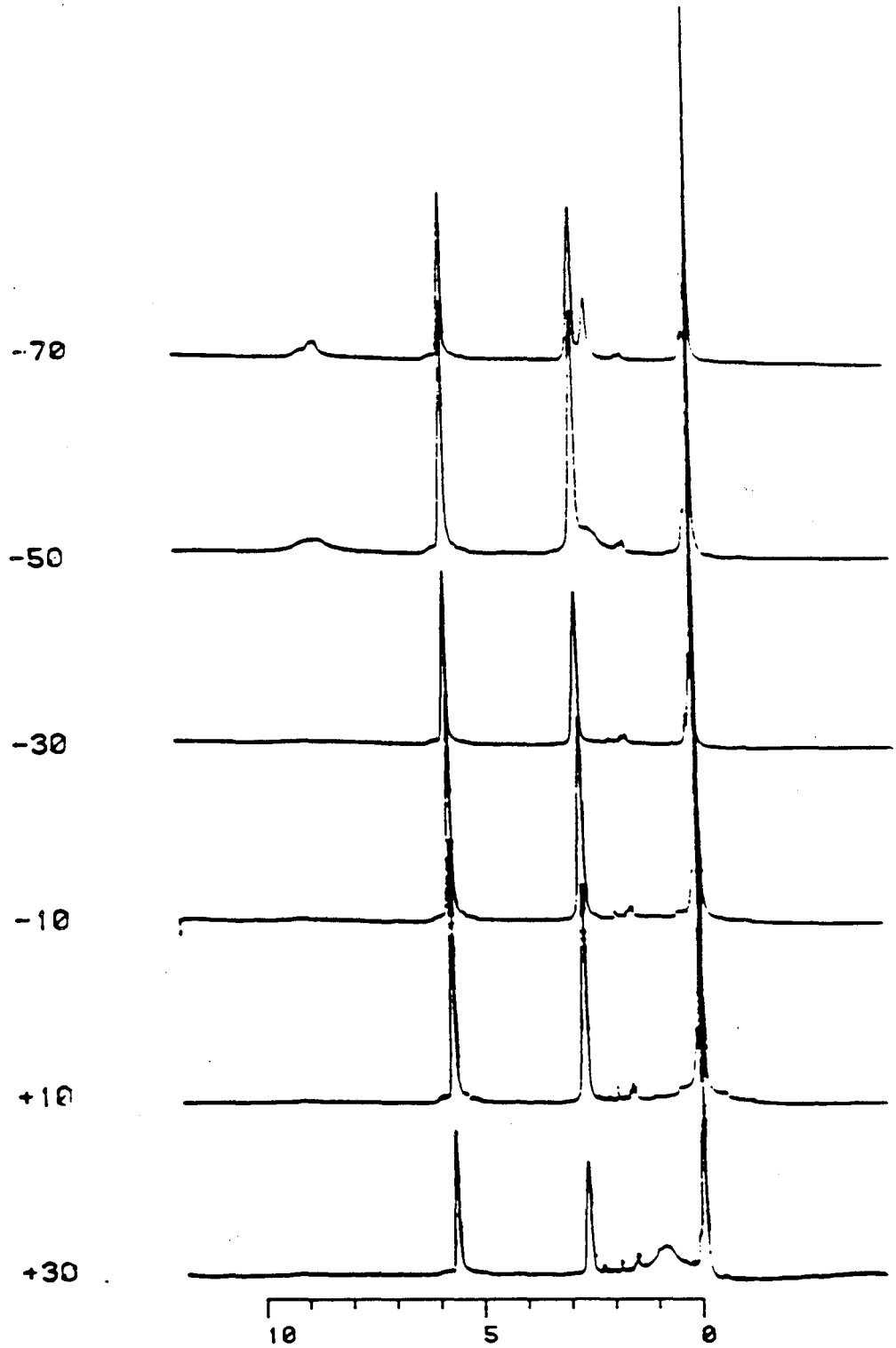

Figure 2.18: Temperature dependent ^{1}H-NMR of $[Yb(t\text{-}BuC_8H_7)_2]^{=}$ and $[Yb(t\text{-}BuC_8H_7)_2]^{-}$.

Conclusion

Except for the differences that can be attributed to either the difference in the number of electrons between ytterbium and calcium, or to the availability of a trivalent state for the ytterbium complex, $K_2[Yb(C_8H_8)_2]$ and $K_2[Ca(C_8H_8)_2]$ behave as identical complexes. Since it is highly unlikely that the 4f and 5d orbitals are involved in the ring-metal interaction of $K_2[Ca(C_8H_8)_2]$, these orbitals also play no major role in the ring-metal interaction of $K_2[Yb(C_8H_8)_2]$. The agreement of the ring-metal distance in $K_2[Yb(C_8H_8)_2]\cdot 2DME$ with the sum of the ionic radius of carbon in [8]annulene dianion and the ionic radius of 10-coordinate ytterbium(II) also suggests the lack of significant covalent interaction between the ring and metal in $K_2[Yb(C_8H_8)_2]$. The results reported in this paper further emphasize the unimportance of the 4f and 5d orbitals in ytterbium(II) chemistry; e.g., the ring-metal interaction in $K_2[Yb(C_8H_8)_2]$ is essentially ionic.

Although the ring-metal interaction in the bis([8]annulene) dianions is ionic and the [8]annulene rings are labile, the rings of the complexes do not exchange on the NMR timescale. However, a fast electron exchange ($k \approx 10^6$ moles^{-1} s^{-1}) occurs between bis([8]annulene)ytterbate(II) dianion and bis([8]annulene)ytterbate(III) anion. This is the first example of a dynamic electron exchange for a bis([8]annulene) complex and suggests that other

[8]annulene sandwich complexes, which contain a central metal atom that can exist in more than one oxidation state, will undergo the same type of electron exchange.

Experimental Section

General : Unless otherwise noted, materials were obtained from commercial suppliers and used without further purification. Ytterbium metal turnings were purchased from Alfa/Ventron. Tetrahydrofuran (THF) was distilled from sodium/benzophenone. 1,2-Dimethoxyethane (DME) was distilled from Na/K alloy. Cyclo-octatetraene (COT) (BASF) was vacuum distilled and stored over Molecular Sieves 3Å . Liquid ammonia was vacuum transferred into the reaction vessels from a solution of sodium in liquid ammonia. All air-sensitive compounds were handled in a helium or argon atmosphere glovebox or by standard Schlenk techniques. Unless otherwise indicated, all weights are ± .01 g. Infrared spectra were determined with a Perkin-Elmer Model 283 infrared recording spectrophotometer. Samples for infrared determination were prepared in a glovebox as Nujol mulls. Visible spectra of THF solutions of the organometallic compounds were determined with a Cary Model 118 spectrophotometer; results are expressed as λ_{max} in nm (ε). ^{1}H-NMR of the organometallic compounds were determined in sealed tubes of THF-*d8* solutions on a JOEL FX-90Q. The chemical shifts of the proton resonances are referenced to the low field residual proton resonance of THF-*d8* (set as 3.58 ppm). Samples for x-ray powder pattern determination were prepared by grinding the crystalline sample to a fine powder and sealing the powder into a quartz capillary under argon. X-ray powder pattern data were taken with a Debye-Scherrer camera using nickel filtered copper Kα x-rays.

Elemental analyses were performed by the Microanalytical Laboratory of the College of Chemistry, University of California, Berkeley.

Reactions in liquid ammonia: The reaction vessel used for the syntheses in liquid ammonia was a two-necked 100 mL round bottom flask with sidearm. During the reactions, the flask was connected through one neck to a Schlenk line and cooled in a Dry Ice/isopropanol bath. While transferring the liquid ammonia into the reaction vessel and during the course of the reaction, the vacuum manifold was isolated from the vacuum pump. The vacuum manifold was protected from developing high ammonia pressure by a mercury bubbler. After the metals were added to the ammonia, a septum was placed on the free neck of the flask (under argon purge) and cyclooctatetraene was added to the blue solution via syringe. Since cyclooctatetraene freezes on contact with liquid ammonia at that low temperature, the Dry Ice bath was removed to facilitate reaction. When the reaction was complete, the ammonia was allowed to evaporate through the mercury bubbler, leaving the pyrophoric material behind.

Preparation of $K_2[Yb(C_8H_8)_2]$ and $K_2[Ca(C_8H_8)_2]$. The procedure for the synthesis of the divalent ytterbium complex follows with differences for the procedure for the calcium complex noted. Cyclooctatetraene (1.79 g, 17 mmol) was added to a Dry-Ice/isopropanol-cooled liquid ammonia solution of 0.67 g

(17 mmol) of potassium metal and 1.49 g (8.6 mmol) of ytterbium metal. The Dry-Ice/isopropanol bath was removed from the reaction vessel at this time to allow the ammonia solution to warm. As the reaction began, the solution turned green as a bright orange precipitate appeared (the solution and precipitate were bright yellow for the calcium reaction). The ammonia was allowed to evaporate and a bright orange solid was left in the reaction vessel (bright yellow for calcium). When the reaction vessel was warmed with a heat gun, the solid turned bright pink (pale green for calcium). The yield of the solid was 3.57 g (90%). Yields from the liquid ammonia reactions were typically about 90%. Crystals of the THF adducts of $K_2[Yb(C_8H_8)_2]$ and $K_2[Ca(C_8H_8)_2]$ were obtained by the slow cooling of a saturated solution of $K_2[Yb(C_8H_8)_2]$ or $K_2[Ca(C_8H_8)_2]$ in the ether. The THF adducts of $K_2[Yb(C_8H_8)_2]$ and $K_2[Ca(C_8H_8)_2]$ rapidly lost THF of solvation (ca. one hour in an argon atmosphere or ca. 5 minutes, *in vacuo*) and decomposed to unsolvated powders. Analysis of $K_2[Ca(C_8H_8)_2]$ as a THF complex was not satisfactory, but the analysis does suggest that there are two THF molecules per potassium atom. Anal. of $K_2[Ca(C_8H_8)_2]\cdot 4THF$: Calcd. for $C_{32}H_{48}O_4K_2Ca$: C, 62.49; H, 7.87; K, 12.71. Found: C, 61.73; H, 7.40; K, 11.8.

The unsolvated powders were heated at 200°C, *in vacuo*, for one hour to insure the complete removal of solvated THF. The yield of powder was 57% for $K_2[Yb(C_8H_8)_2]$ (67% for $K_2[Ca(C_8H_8)_2]$) from the first crop of crystals. The infrared spectra of $K_2[Yb(C_8H_8)_2]$ and

$K_2[Ca(C_8H_8)_2]$ are shown in figure 2.5. ^{1}H-NMR of $K_2[Yb(C_8H_8)_2]$ δ = 5.47 ± .03, singlet ($K_2[Ca(C_8H_8)_2]$ δ = 5.47 ± .03, singlet). Visible spectrum of $K_2[Yb(C_8H_8)_2]$ 504 nm (850). Satisfactory analyses of the powders were difficult to obtain, especially in the case of the ytterbium complex. Anal. $K_2[Yb(C_8H_8)_2]$: Calcd. for $C_{16}H_{16}K_2Yb$: C, 41.82; H, 3.51; K, 17.01. Found: C, 39.66; H, 3.64; K, 19.2. $K_2[Ca(C_8H_8)_2]$: Calcd. for $C_{16}H_{16}K_2Ca$: C, 58.85; H, 4.94; K, 23.94. Found: C, 58.47; H, 5.22; K, 23.4.

The slow cooling of a saturated solution of $K_2[Yb(C_8H_8)_2]$ or $K_2[Ca(C_8H_8)_2]$ in DME gave crystals of the complexes as DME adducts. The DME adducts of $K_2[Yb(C_8H_8)_2]$ and $K_2[Ca(C_8H_8)_2]$ were stable and gave satisfactory analyses for one DME molecule per potassium. Anal. $K_2[Yb(C_8H_8)_2]\cdot 2DME$: Calcd. for $C_{24}H_{36}O_4K_2Yb$: C, 45.06; H, 5.67; K, 12.22. Found: C, 44.79; H, 5.59; K, 12.4. $K_2[Ca(C_8H_8)_2]\cdot 2DME$: Calcd. for $C_{24}H_{36}O_4K_2Ca$: C, 56.88; H, 7.16; K, 15.43. Found: C, 57.11; H, 7.07; K, 16.07.

* Preparation of $K[Yb(C_8H_8)_2]$. In a procedure which is analogous to the procedure used to synthesis $K_2[Yb(C_8H_8)_2]$ and $K_2[Ca(C_8H_8)_2]$, the potassium salt of bis([8]annulene)ytterbate(III) was prepared by the addition of 0.88 g (8.4 mmoles) of cyclooctatetraene to a Dry-Ice/isopropanaol cooled liquid ammonia solution of 0.73 g (4.2 mmoles) of ytterbium metal and 0.16 g (4.2 mmoles) potassium metal. When the reaction was complete and the solvent had evaporated, a bright orange powder was left in

the reaction vessel. This powder turned bright blue when the reaction vessel was warmed with a heat gun and exposed to a vacuum. The crude yield of this powder was 1.50 g (86 %). Satisfactory analysis could not be obtained for $K[Yb(C_8H_8)_2]$, but the infrared spectrum of $K[Yb(C_8H_8)_2]$ (the major absorbances in the 600 to 1000 cm^{-1} region are given in Table III) is similar to the infrared spectra of the other bis-[8]annulene lanthanide salts, and and indicated that the crude material contained ammonia. Anal. Calcd. for $C_{16}H_{19}NKYb$: C, 40.33; H, 4.02; N, 2.94. Found: C, 37.79; H, 4.02; N, 2.19. λ_{max} of $K[Yb(C_8H_8)_2]$ in THF is 574 nm (1400).

A portion of this powder was dissolved in anhydrous, degassed THF to give a dark blue solution. When anhydrous, degassed hexane was allowed to diffuse into this solution dark blue crystals appeared. The crystals were isolated by filtration and washed with anhydrous, degassed hexane. The crystals were placed, *in vacuo*, for ca. one hour at room temperature to remove solvent. The dark blue powder changes to a lighter blue when heated to 100 °C sealed under one atm. of argon gas, probably from loss of THF of solvation. Analysis of the dark blue powder indicated that there are two THF molecules per potassium atom in the ytterbium(III) complex. Anal. Calcd. for $C_{24}H_{32}O_2KYb$: C, 51.06; H, 5.71. Found: C, 51.37; H, 6.01.

Another portion of $K_2[Yb(C_8H_8)_2]$ powder was crystallized from DME by allowing hexane to diffuse into a saturated solution of $K[Yb(C_8H_8)_2]$ in DME. Analysis indicated that the complex contained one DME molecule per potassium. Anal. Calcd. for $C_{20}H_{26}O_2YbK$: C, 47.05; H, 5.13; K, 7.66. Found: C, 46.51; H, 4.91; K, 8.27; N, 0.28.

* Preparation of $Yb(C_8H_8)$. Degassed, anhydrous C_8H_8 (0.32 g, 3.1 mmol) was added to a blue solution of 0.53 g (3.1 mmol) of ytterbium metal in mL of liquid ammonia. As the solution warmed, on orange precipitate began to appear. When all the ammonia had been removed a lavender solid was left behind. When a portion of this lavender solid was heated to 200 °C, it turned bright pink. The crude yield of the powder was .74 g (87 %). Infrared (nujol mull): 3322 w, 3229 w, 3038 w, 1835 w, 1720 w, 1590 w, 1310 m, 1301 w, 888 s, 674 vs. Anal. Calcd. for C_8H_8Yb (contaminated with 17 % $Yb(NH_3)_6$): C, 29.66; H, 3.43; N, 4.41. Found: C, 29.60, H; 3.38, N; 3.91.

* Preparation of $K_2[Yb(t\text{-}BuC_8H_7)_2]$. Anhydrous t-butyl-cyclooctatetraene (0.57 g, 3.6 mmol) was added to a blue solution of 0.14 g (3.6 mmol) potassium and 0.31 g (1.8 mmol) ytterbium metal in liquid ammonia at -78 °C. Five minutes after removing the Dry Ice bath, the reaction mixture was green and then underwent a rapid color change to orange and then back to

green. After the ammonia allowed to evaporate, a blue powder was left behind. When the blue powder was heated to 200 °C, *in vacuo*, it turned bright pink. The yield of the pink powder was 0.93 g (91 %).

A portion of the pink powder (0.73 g) was dissolved in 10 mL of anhydrous, degassed diglyme. The suspension was heated to 140 °C and filtered. When the solution cooled to room temperature, 50 mL of anhydrous, degassed hexane was carefully added via syringe such that two layers (a lower orange layer and an upper clear layer) formed. As the hexane slowly diffused into the digylme solution, large reactangular crystals formed (some crystals formed almost immediatly, but complete crystallization took three days). The solvent was removed by filtration and the crystals were washed three times with 50 mL of hexane. A second crop a crystals was grown from the filtrate and the hexane wash. The yield of crystals was 0.77 g (0.41 g 1st crop and 0.36 g 2nd crop) or 72 %. UV-vis: λmax(THF) = 521 nm. ^{1}H-NMR: (THF-*d8*) 5.26 m (7), 3.58 m (8), 3.46 s (6), 1.52 s (9). Anal. Calcd. for $C_{36}H_{60}O_6K_2Yb$: C, 51.47; H, 7.20. Found: C, 51.60; H, 7.39.

• Preparation of $Yb(C_5H_4-C_2H_4-C_8H_7)$. Ytterbium metal (0.26 g, 1.7 mmol) was dissolved in 40 mL of liquid NH_3(at -78 °C) to give a blue solution. After two minutes, a solution 0.34 g of (2-cyclopentadienylethyl)cyclooctatetraene in three mL of anhydrous, degassed THF was added to the ammonia solution via syringe.

The solution immediatly turned dark yellow with a dark precipitate forming. After five minutes, the solution grew darker in color and began to bubble vigorously. After fifteen minutes, the solution had a definite green color. After the ammonia was allowed to evaporate and the THF had been removed, *in vacuo*, a dark green powder was left in the reaction vessel. Anhydrous, degassed THF was added to a portion of this solid and the resulting dark green solution was filtered. Anhydrous, degassed pentane was allowed to diffuse into the dark green solution causing a dark green precipitate to appear. The solid was isolated by filtration and washed with pentane, and all traces of solvent were removed, *in vacuo*. The dark green solid was characterized as $Yb(C_5H_4-C_2H_4-C_8H_7)$ by its mass spectrum. Mass Spec.(peaks shown for ions which include ytterbium; *m/z* listed for the most abundant ytterbium isotope, Yb^{174}): 369 {$Yb(C_5H_4-C_2H_4-C_8H_7)$}, 343 {369 - C_2H_2}, 291 {369 - C_6H_6}, 265 {369 - C_8H_8}, 239 {265 - C_2H_2 and 343 - C_8H_8}, 213 {239 - C_2H_2 and 291 - C_6H_6}.

Reaction of Benzocyclooctatetraene with Potassium and Calcium. Benzocyclooctatetraene (0.31 g 2.1 mmoles) in 10 mL of dry, degassed THF was syringed into a 50 mL solution of 0.04 g (1.0 mmoles) calcium and 0.08 g (2.0 mmoles) potassium metal. After half of the THF solution was added, the solution turned from dark blue to dark red. After completion of the reaction, the removal of solvent, *in vacuo*, left 0.39 g (91% crude yield) of a light

orange, pyrophoric powder. This powder was dissolved in diglyme and a layer of hexane was placed on top of the red-orange diglyme solution. The slow diffusion of hexane into the diglyme solution caused a micro-fine yellow powder and red-orange platlets to form. The solvent was removed by filtration, and the mixed product was washed with hexane. The powder and the crystals were carefully separated by hand. Elemental analysis of the red-orange platelets suggest that they are $[K(diglyme)]_2benzoC_8H_6$. Calc. for $C_{24}H_{38}O_6K_2$: C, 57.57; H, 7.65; K, 15.61; O, 19.17. Found: C, 56.45; H, 7.94; K, 15.4; O (by difference), 20.21. Analysis of the yellow powder was consistent with $[Ca(diglyme)]benzoC_8H_6$. Calc. for $C_{18}H_{24}O_3Ca$: C, 65.82; H, 7.37; Ca-O, 26.81. Found: C, 63.62; H, 7.79; K, 0.97; Ca-O (by difference), 27.62.

Reaction of Potassium with $K[Yb(C_8H_8)_2]$. In an argon atmosphere glovebox, potassium metal (0.02 g, 0.5 mmol) was added to a solution of 0.35 g $[K(THF)_2][Yb(C_8H_8)_2]$ (0.62 mmol) in 100 mL of dry, degassed THF in a uranocene reactor.[45] The reactor with solution was removed from the glovebox, connected to a Schlenk line and the solution was heated at reflux under a slightly positive argon pressure. After two days of heating, no potassium remained and the solution was still blue , although a bright pink solid had formed (this solid was probably $Yb(C_8H_8)$). The solution degassed by freeze-thawing and taken into an argon atmosphere glovebox. A visible spectrum of the blue solution indicated only the starting material, and no $K_2[Yb(C_8H_8)_2]$. glovebox.

Appendix A: X-ray Analysis:

The crystal structures of both ytterbium(II) complexes reported in this chapter were solved by Dr. Allan Zalkin at Lawrence Berkeley Laboratory. With the exception of the ORTEP program, all computer programs used for the structural determinations were written by Dr. Zalkin for a CDC 7600 computer.

Structure of $[K(C_4H_{10}O_2)]_2[Yb(C_8H_8)_2]$. An irregular, orange-red single crystal fragment of $K_2[Yb(C_8H_8)_2]\cdot 2DME$ with maximum dimensions of 0.2 mm was sealed inside a quartz capillary in an argon atmosphere and examined with a modified Picker FACS-I Automated diffractometer equipped with a graphite monochromator and a Mo x-ray tube. Least squares refinement of the setting angles of 24 centered reflections ($27° > 2\theta > 20°$) using Mo Kα (λ = 0.71073 Å) radiation gave $\underline{a}$ = 9.346(4) Å , $\underline{b}$ = 9.775(4), $\underline{c}$ = 7.740(4) Å , α = 91.72(4)°, β = 109.16(4)°, γ = 86.22(4)°, and V = 666.5 $Å^3$ at 23 °C. The space group of the crystal is triclinic, P1, with one formula unit in the unit cell. The calculated density of the crystal (molecular weight of $[K(C_4H_{10}O_2)]_2[Yb(C_8H_8)_2]$ = 639.80) is 1.59 g cm^{-3}.

Intensities were collected to a maximum 2θ value of 50° using a θ - 2θ scan technique. Three standard reflections were measured at every 250th measurement; the three standards showed an isotropic decay of about 5% and the data were adjusted

accordingly. A total of 4729 intensities were measured and averaged to give 2361 unique data of which 2312 were used in the least squares with $F^2 > 1\sigma(F^2)$. The data were not corrected for absorption because of the difficulty of seeing the faces and measuring the crystal's irregular dimensions. The absorption coefficient calculates to 38 cm^{-1} and an error of approximately 5% in the intensities is estimated.

Trial positions for the ytterbium and potassium atoms were obtained from a three-dimensional Patterson function and were refined by least squares. An electron density map revealed all of the non-hydrogen atoms. All of the non-hydrogen atoms were refined with anisotropic temperature factors and the hydrogen atoms were included at their estimated positions, but not refined. The F magnitude was used in the full-matrix refinement.

The final weighted R factor[46] was 0.034 for 2312 data with $F^2 > \sigma(F^2)$, and the goodness of fit was 1.33. The assigned weights $w = (\sigma(F))^{-1}$, were derived from $\sigma(F^2) = [\underline{c} + (\underline{p}F^2)^2]^{1/2}$, where $\underline{c}$ is the variance due to counting statistics and $\underline{p} = 0.05$. An empirical extinction correction of the form $F_{corr} = F_{obs}(1 + \underline{k}I)$, where $\underline{k} = 2.13 \times 10^{-7}$, was applied to the data. Scattering factors were taken from literature sources[47] and anomalous scattering terms were applied.[48]

Table of Anisotropic Thermal Paramenters in

$[K(C_4H_{10}O_2]_2[Yb(C_8H_8)_2]$.

ATOM	B11	B22	B33
YB	3.848(16)	3.324(16)	3.317(16)
K	3.47(5)	3.57(5)	4.28(5)
O(1)	4.26(18)	3.39(16)	4.55(18)
O(2)	3.57(17)	3.62(17)	6.15(22)
C(1)	2.41(28)	3.78(24)	5.84(28)
C(2)	4.36(26)	4.66(27)	2.75(28)
C(3)	4.65(27)	4.57(27)	3.88(24)
C(4)	3.69(24)	2.75(21)	6.9(4)
C(5)	3.41(23)	3.07(22)	5.5(3)
C(6)	4.21(25)	4.51(26)	2.90(28)
C(7)	3.96(24)	4.50(26)	4.30(25)
C(8)	2.43(28)	3.72(24)	6.5(3)
C(9)	6.4(4)	4.4(3)	9.2(5)
C(10)	5.28(29)	3.93(25)	4.84(25)
C(11)	3.27(24)	5.7(3)	4.83(28)
C(12)	4.7(3)	5.4(3)	6.3(4)

ATOM	B12	B13	B23
YB	1.267(18)	1.163(11)	.594(18)
K	1.16(4)	.81(4)	.28(4)
O(1)	.87(14)	1.85(14)	.42(13)
O(2)	.84(14)	.88(15)	-.26(15)
C(1)	.92(18)	-.28(19)	-.32(21)
C(2)	2.16(23)	.13(18)	.61(19)
C(3)	1.98(23)	2.82(22)	2.38(21)
C(4)	.61(18)	1.87(24)	1.57(22)
C(5)	.46(18)	.56(21)	-1.81(28)
C(6)	1.76(22)	.98(18)	-.59(18)
C(7)	1.77(21)	2.74(21)	.89(28)
C(8)	.82(18)	2.14(21)	.82(22)
C(9)	-.58(28)	3.9(4)	-.3(3)
C(10)	1.42(22)	1.26(22)	.81(28)
C(11)	.98(22)	.37(21)	-.43(24)
C(12)	-1.18(27)	.47(27)	-.33(28)

Estimated Positional Paramenters for the Hydrogen Atoms in $[K(C_4H_{10}O_2]_2[Yb(C_8H_8)_2]$.

H(1)	.374	.011	.2789
H(2)	.2535	-.0968	.423
H(3)	.0733	-.2419	.3465
H(4)	-.0435	-.3442	.0944
H(5)	-.0522	-.3333	-.189
H(6)	.0583	-.2175	-.3334
H(7)	.2338	-.0719	-.2576
H(8)	.3674	.0203	-.0018
H(9)	.390	-.6917	.2988
H(10)	.4995	-.7861	.2097
H(11)	.3549	-.7033	.0743
H(12)	.7113	-.6623	.3875
H(13)	.6003	-.5698	.4700
H(14)	.817	-.4519	.4868
H(15)	.7735	-.4637	.2691
H(16)	.7616	-.2087	.2038
H(17)	.7854	-.2103	.4982
H(18)	.6360	-.1353	.3602

[a] These parameters were included at these calculated positions but not refined in the least-squares procedures. H(1-8) and H(9-18) were assigned isotropic thermal parameters of 8.0 and 10.0 respectively; the isotropic thermal parameters were also not refined. All C-H distances are between 0.98 and 1.00 Å.

Cyclooctatetraene Least Squares Plane.

Atom	Distances to Plane (Å)
C(1)	0.006
C(2)	-0.010
C(3)	-0.008
C(4)	0.011
C(5)	0.009
C(6)	-0.012
C(7)	-0.008
C(8)	0.012
Yb	-2.032
K	2.391

Plane equation with respect to crystallographic axes:

$$6.005X - 6.898Y - 0.425C = 2.032$$

Selected angles in $K_2Yb(C_8H_8)_2 \cdot (CH_3OCH_2CH_2OCH_3)$

C(1)-C(2)-C(3)	134.8(5)
C(2)-C(3)-C(4)	135.0(5)
C(3)-C(4)-C(5)	134.9(5)
C(4)-C(5)-C(6)	134.9(5)
C(5)-C(6)-C(7)	135.5(5)
C(6)-C(7)-C(8)	134.6(5)
C(7)-C(8)-C(1)	135.0(5)
C(8)-C(1)-C(2)	135.2(5)
O(1)- K -O(2)	92.8(2)
K -O(1)-C(9)	112.9(4)
K -O(1)-C(10)	114.0(3)
K -O(2)-C(12)	117.4(4)
K -O(2)-C(11)	118.1(4)
C(9)-O(1)-C(10)	111.4(5)
C(12)-O(2)-C(11)	113.9(5)
O(1)-C(10)-C(11)	109.6(5)
O(2)-C(11)-C(10)	109.0(5)

C-C Distances in cyclooctatetraene ligand

C(1)-C(2)	1.409(9)
C(2)-C(3)	1.400(10)
C(3)-C(4)	1.421(10)
C(4)-C(5)	1.409(9)
C(5)-C(6)	1.395(9)
C(6)-C(7)	1.413(9)
C(7)-C(8)	1.407(9)
C(8)-C(1)	1.408(9)

Appendix B: Structure of $[K(C_6H_{14}O_3)]_2[Yb(t\text{-}BuC_8H_7)_2]$

The crystals were sealed inside thin walled quartz capillaries under argon and mounted on a modified Picker FACS-I Automatic diffractometer equipped with a Mo-Kα x-ray tube and graphite monochromater. Sets of θ-2θ scan data were collected and corrected for crystal decay, absorption (analytical method)[49] and Lorentz and polarization effects. Experimental details are shown in Table 1.

The ytterbium and potassium atoms were located with 3-dimensional Patterson maps, and subsequent least-squares and electron density maps revealed the locations of the other atoms. All of the non-hydrogen atoms were refined with anisotropic temperature factors.

The positions of fourteen hydrogen atoms of the [8]annulene rings were also refined, but with isotropic temperature factors. The remaining hydrogen atom positions were included in the least-squares at their calculated locations and with an assigned isotropic thermal parameter, but not refined.

Atomic scattering factors of Doyle and Turner[50] were used and anomalous dispersion corrections were applied.[51] With the exception of the ORTEP program all of the computer programs used are written by Dr. Zalkin. Details of the refinements and the residuals follow.

Anisotropic Thermal Parameters.

ATOM	B11	B22	B33	B12	B13	B23
YB	3.297(16)	3.817(17)	2.788(15)	.143(21)	-.239(10)	.090(19)
K(1)	4.17(8)	5.30(11)	3.05(7)	.50(8)	.22(6)	-.27(8)
K(2)	3.89(8)	4.79(9)	3.20(7)	-.14(9)	.24(6)	.06(8)
O(1)	4.64(28)	5.8(4)	4.90(29)	.63(27)	.93(24)	.73(27)
O(2)	7.4(4)	5.3(3)	3.48(28)	-.1(3)	1.75(26)	-.38(27)
O(3)	8.9(5)	5.4(4)	5.5(4)	1.9(3)	1.6(3)	.1(3)
O(4)	4.43(26)	5.2(3)	4.77(27)	-.25(29)	.76(22)	.4(3)
O(5)	5.7(3)	4.9(3)	3.31(26)	-.18(27)	.90(23)	.40(25)
O(6)	7.3(4)	4.9(4)	6.2(4)	.6(3)	2.5(3)	.4(3)
C(1)	4.2(5)	3.8(5)	2.9(4)	-.1(4)	-.7(4)	2.3(4)
C(2)	3.2(4)	7.7(7)	1.8(4)	.3(5)	.6(3)	.9(4)
C(3)	4.5(5)	5.3(7)	3.2(5)	.9(5)	-.0(4)	-1.3(5)
C(4)	4.6(5)	4.2(6)	3.9(5)	.4(5)	-.2(4)	-1.6(4)
C(5)	4.4(5)	3.0(5)	3.6(5)	-.2(4)	-.6(4)	-.0(4)
C(6)	2.5(4)	3.9(5)	3.7(4)	-.8(4)	-.5(3)	.1(4)
C(7)	2.2(4)	4.8(5)	3.4(4)	.2(3)	.1(3)	.3(3)
C(8)	2.4(4)	3.6(5)	3.1(4)	.8(3)	-.5(3)	.7(3)
C(9)	4.9(4)	3.5(4)	4.7(5)	1.6(4)	-.1(4)	.1(4)
C(10)	5.7(5)	7.0(6)	9.7(7)	3.7(5)	-2.7(5)	-1.7(6)
C(11)	8.2(6)	6.7(6)	5.9(6)	1.5(5)	1.6(5)	-2.3(5)
C(12)	9.7(8)	4.1(6)	8.0(7)	.8(5)	.9(6)	.2(5)
C(13)	1.9(4)	6.0(6)	3.2(4)	-1.1(4)	.0(3)	.3(4)
C(14)	2.6(4)	5.3(6)	3.4(4)	.7(4)	-.2(3)	-.0(4)
C(15)	4.0(5)	3.5(6)	4.4(5)	2.5(5)	-1.4(4)	.9(4)
C(16)	5.0(5)	3.4(5)	3.5(4)	.1(4)	-.5(4)	1.5(4)
C(17)	3.9(4)	5.8(6)	2.2(4)	-.5(4)	.7(3)	.4(4)
C(18)	4.5(5)	4.4(5)	2.1(4)	-.6(4)	.7(3)	-.7(4)
C(19)	4.0(5)	3.4(5)	3.4(4)	-.9(4)	.1(4)	-.6(4)
C(20)	3.4(4)	4.3(5)	2.5(4)	-1.1(4)	-.1(3)	.3(3)
C(21)	4.3(4)	4.3(5)	4.5(5)	-1.6(4)	.4(4)	.6(4)
C(22)	6.1(6)	5.5(6)	8.4(7)	-1.8(5)	1.4(5)	-.1(5)
C(23)	7.6(6)	6.9(6)	5.4(5)	-2.3(5)	.8(4)	1.7(5)
C(24)	7.3(6)	4.2(6)	8.1(7)	-.3(5)	1.0(5)	.7(5)
C(25)	6.0(5)	7.3(6)	5.5(5)	-.8(5)	.0(4)	1.0(5)
C(26)	5.2(5)	5.6(6)	5.4(5)	.0(4)	1.9(4)	-1.0(4)
C(27)	5.7(5)	6.2(6)	4.4(5)	-.2(4)	1.2(4)	-1.2(4)
C(28)	9.9(7)	6.7(6)	3.9(4)	.9(6)	1.8(4)	-.2(5)
C(29)	12.0(9)	4.9(6)	7.9(7)	2.0(6)	5.7(7)	1.1(5)
C(30)	16.1(12)	6.0(7)	7.0(7)	.7(7)	1.5(7)	.7(6)
C(31)	7.1(6)	5.7(6)	5.6(5)	1.0(5)	-.1(5)	-1.0(5)
C(32)	4.8(4)	4.6(6)	6.2(5)	-.1(4)	1.3(4)	1.7(4)
C(33)	5.1(5)	6.5(6)	4.1(5)	.1(4)	1.0(4)	.8(4)
C(34)	6.4(5)	6.3(7)	4.0(4)	-1.1(5)	1.5(4)	-.9(4)
C(35)	6.3(6)	5.9(6)	5.7(5)	-.0(5)	2.0(5)	-1.3(5)
C(36)	14.2(10)	5.7(7)	5.6(6)	1.6(6)	2.4(6)	-.2(5)

Hydrogen Positional and Isotropic Thermal Parameters.

H(1)	C	.126(6)	.060(3)	.368(3)	2.1(14)
H(2)	C	.014(8)	.130(4)	.406(4)	5.5(23)
H(3)	C	-.003(9)	.242(4)	.403(4)	5.8(26)
H(4)	C	.090(12)	.313(6)	.357(6)	10.3(43)
H(5)	C	.244(8)	.320(4)	.305(4)	5.2(23)
H(6)	C	.374(8)	.248(4)	.278(4)	4.0(20)
H(7)	C	.395(8)	.149(4)	.265(4)	6.4(22)
H(8)	C	-.301(7)	.144(3)	.214(3)	3.3(17)
H(9)	C	-.292(8)	.252(4)	.228(4)	6.3(22)
H(10)	C	-.159(8)	.310(4)	.180(4)	4.1(21)
H(11)	C	-.018(7)	.315(4)	.120(4)	4.9(19)
H(12)	C	.093(9)	.231(4)	.079(5)	6.9(25)
H(13)	C	.095(9)	.127(4)	.088(4)	6.5(24)
H(14)	C	-.027(8)	.052(5)	.136(4)	6.6(25)
H(15)	C	.2734	.3383	.5291	10.000
H(16)	C	.3857	.3841	.5742	10.000
H(17)	C	.4902	.2878	.6293	10.000
H(18)	C	.348	.3025	.6457	10.000
H(19)	C	.2918	.200	.6637	10.000
H(20)	C	.4244	.166	.6517	10.000
H(21)	C	.2423	.0949	.6305	10.000
H(22)	C	.1679	.1419	.5701	10.000
H(23)	C	-.1907	.3329	-.0384	10.000
H(24)	C	-.3099	.3744	-.0841	10.000
H(25)	C	-.3985	.277	-.139	10.000
H(26)	C	-.2550	.2941	-.1524	10.000
H(27)	C	-.1873	.1902	-.1683	10.000
H(28)	C	-.3277	.1595	-.1635	10.000
H(29)	C	-.1497	.0836	-.1331	10.000
H(30)	C	-.0843	.1291	-.0696	10.000
H(31)	C	.4573	.0353	.3917	12.000
H(32)	C	.5085	.0669	.3294	12.000
H(33)	C	.4907	-.0101	.333	12.000
H(34)	C	.3599	.0660	.2108	12.000
H(35)	C	.2129	.0359	.1982	12.000
H(36)	C	.3404	-.0109	.2158	12.000
H(37)	C	.140	-.0187	.2936	12.000
H(38)	C	.236	-.0204	.3687	12.000
H(39)	C	.2745	-.0607	.3077	12.000
H(40)	C	-.3670	.0313	.1047	12.000
H(41)	C	-.4153	.0636	.1675	12.000
H(42)	C	-.3972	-.0135	.1647	12.000
H(43)	C	-.2590	.0638	.2853	12.000
H(44)	C	-.1116	.0344	.2966	12.000
H(45)	C	-.2384	-.0130	.2809	12.000
H(46)	C	-.0468	-.0226	.1950	12.000
H(47)	C	-.1528	-.0232	.1227	12.000
H(48)	C	-.1818	-.0637	.1859	12.000
H(49)	C	.4535	.4183	.4738	12.000
H(50)	C	.3482	.3735	.428	12.000
H(51)	C	.4926	.3651	.4235	12.000
H(52)	C	.1655	.0474	.4992	12.000
H(53)	C	.2554	.0078	.5619	12.000
H(54)	C	.3042	.0181	.4929	12.000
H(55)	C	-.3772	.4071	.018	12.000
H(56)	C	-.2584	.365	.0635	12.000
H(57)	C	-.4093	.3521	.0684	12.000
H(58)	C	-.1121	.033	-.0025	12.000
H(59)	C	-.1943	-.0035	-.0695	12.000
H(60)	C	-.2609	.0084	-.0058	12.000

Interatomic Distances

Atoms	Distance (Å)	Atoms	Distance (Å)
Yb-C(1)	2.733(8)	Yb-C(13)	2.788(8)
Yb-C(2)	2.710(8)	Yb-C(14)	2.758(8)
Yb-C(3)	2.762(10)	Yb-C(15)	2.735(8)
Yb-C(4)	2.786(10)	Yb-C(16)	2.746(8)
Yb-C(5)	2.747(9)	Yb-C(17)	2.766(8)
Yb-C(6)	2.758(8)	Yb-C(18)	2.737(8)
Yb-C(7)	2.791(8)	Yb-C(19)	2.767(8)
Yb-C(8)	2.821(7)	Yb-C(20)	2.836(8)
mean Yb-C	2.77(4)		
K(1)-C(1)	3.107(9)	K(2)-C(13)	3.101(9)
K(1)-C(2)	3.034(9)	K(2)-C(14)	3.087(9)
K(1)-C(3)	3.012(10)	K(2)-C(15)	3.102(10)
K(1)-C(4)	3.054(11)	K(2)-C(16)	3.066(9)
K(1)-C(5)	3.077(9)	K(2)-C(17)	3.021(9)
K(1)-C(6)	3.057(9)	K(2)-C(18)	3.027(9)
K(1)-C(7)	3.096(9)	K(2)-C(19)	3.105(9)
K(1)-C(8)	3.158(8)	K(2)-C(20)	3.178(8)
mean K -C	3.08(5)		
K(1)-O(1)	3.056(6)	K(2)-O(1)	2.857(6)
K(1)-O(2)	2.751(6)	K(2)-O(4)	2.984(7)
K(1)-O(3)	2.981(6)	K(2)-O(5)	2.762(6)
K(1)-O(4)	2.865(6)	K(2)-O(6)	3.020(7)
C(1)-C(2)	1.455(13)	C(13)-C(14)	1.429(12)
C(2)-C(3)	1.404(12)	C(14)-C(15)	1.396(13)
C(3)-C(4)	1.413(15)	C(15)-C(16)	1.426(14)
C(4)-C(5)	1.403(14)	C(16)-C(17)	1.418(13)
C(5)-C(6)	1.400(12)	C(17)-C(18)	1.412(11)
C(6)-C(7)	1.410(12)	C(18)-C(19)	1.415(11)
C(7)-C(8)	1.409(11)	C(19)-C(20)	1.412(12)
C(8)-C(1)	1.425(12)	C(20)-C(13)	1.427(12)
C(8)-C(9)	1.584(11)	C(20)-C(21)	1.549(11)
C(9)-C(10)	1.542(12)	C(21)-C(22)	1.581(12)
C(9)-C(11)	1.538(12)	C(21)-C(23)	1.522(12)
C(9)-C(12)	1.538(13)	C(21)-C(24)	1.536(13)
C(26)-C(27)	1.495(13)	C(32)-C(33)	1.485(13)
C(28)-C(29)	1.474(15)	C(34)-C(35)	1.493(13)
O(1)-C(25)	1.444(10)	O(4)-C(31)	1.445(10)
O(1)-C26)	1.441(10)	O(4)-C(32)	1.424(11)
O(2)-C(27)	1.437(10)	O(5)-C(33)	1.431(11)
O(2)-C(28)	1.420(12)	O(5)-C(34)	1.429(10)
O(3)-C(29)	1.388(11)	O(6)-C(35)	1.419(11)
O(3)-C(30)	1.422(14)	O(6)-C(36)	1.400(12)

Interatomic Angles

C(8)-C(1)-C(2)	135.7(9)	C(20)-C(13)-C(14)	138.0(10)
C(1)-C(2)-C(3)	136.9(11)	C(13)-C(14)-C(15)	136.2(10)
C(2)-C(3)-C(4)	135.0(12)	C(14)-C(15)-C(16)	134.3(10)
C(3)-C(4)-C(5)	132.5(11)	C(15)-C(16)-C(17)	134.1(10)
C(4)-C(5)-C(6)	135.4(10)	C(16)-C(17)-C(18)	133.6(10)
C(5)-C(6)-C(7)	137.7(10)	C(17)-C(18)-C(19)	137.9(10)
C(6)-C(7)-C(8)	136.8(10)	C(18)-C(19)-C(20)	136.7(9)
C(7)-C(8)-C(1)	129.9(9)	C(19)-C(20)-C(13)	129.1(9)
C(1)-C(8)-C(9)	115.8(8)	C(19)-C(20)-C(21)	117.1(9)
C(7)-C(8)-C(9)	114.3(8)	C(13)-C(20)-C(21)	113.8(8)
C(8)-C(9)-C(10)	108.5(8)	C(20)-C(21)-C(22)	108.5(8)
C(8)-C(9)-C(11)	110.7(7)	C(20)-C(21)-C(23)	111.6(8)
C(8)-C(9)-C(12)	115.3(8)	C(20)-C(21)-C(24)	115.2(8)
C(25)-O(1)-C(26)	110.7(7)	C(31)-O(4)-C(32)	112.2(8)
O(1)-C(26)-C(27)	107.7(8)	O(4)-C(32)-C(33)	109.5(8)
C(26)-C(27)-O(2)	108.0(8)	C(32)-C(33)-O(5)	109.4(8)
C(27)-O(2)-C(28)	113.6(8)	C(33)-O(5)-C(34)	113.9(7)
O(2)-C(28)-C(29)	110.0(8)	O(5)-C(34)-C(35)	108.5(8)
C(28)-C(29)-O(3)	109.1(11)	C(34)-C(35)-O(6)	109.0(9)
C(29)-O(3)-C(30)	111.2(10)	C(35)-O(6)-C(36)	112.3(9)

Deviations (Å) from Least Squares Planes

Plane 1: C(1)-C(8)

Atom	Distance
C(1)	-0.022
C(2)	-0.004
C(3)	0.025
C(4)	0.003
C(5)	-0.030
C(6)	0.007
C(7)	0.018
C(8)	0.003
C(9)	0.007
Yb	-2.054
K	2.456
H(1)	0.065
H(2)	0.119
H(3)	0.058
H(4)	-0.117
H(5)	-0.098
H(6)	0.124
H(7)	-0.028

Plane 2: C(13)-C(20)

Atom	Distance
C(13)	-0.022
C(14)	-0.011
C(15)	0.024
C(16)	0.009
C(17)	-0.024
C(18)	-0.005
C(19)	0.018
C(20)	0.011
C(21)	0.010
Yb	2.056
K	-2.468
H(8)	-0.199
H(9)	0.012
H(10)	0.006
H(11)	-0.120
H(12)	-0.108
H(13)	0.050
H(14)	0.118

Crystallographic Summary and Data Processing

a, Å	10.292(4)
b, Å	20.588(6)
c, Å	20.036(6)
alpha, deg	90.00(0)
beta, deg	103.28(4)
gamma, deg	90.00(0)
cryst syst	monoclinic
space group	P21/c
volume, $Å^3$	4131.9
d(calc), g/cm^{-3}	1.350
Z	4
temp (°C)	23.0
empirical formula	C(36)H(60)O(6)K(2)Yb(1)
fw	840.12
color	red
wavelength (Ka^1,Ka^2), Å	0.70930,0.71359
crystal size (mm)	0.130 x 0.160 x 0.360
abs coeff, cm^{-1}	16.50
abs corr range	1.19-1.39
cryst decay corr range	0.96-1.06
2θ limits, deg	4.1-45.1
hkl limits	h -11,11; k 0,22; l -21,21
scan width, deg	1.5 + 0.693 * tan(θ)
no. of standards	3
no. reflections between stds	250
no. scan data	10798
no. unique reflections	5413
R_{int}	0.030
no. non-zero weighted data	3212 (F^2 3σ)
p	0.040
extinction k	0.165E-06
max % extinction corr	11.8 %
no. parameters	462
R (non-zero wtd dat)	0.032
Rw	0.038
R (all data)	0.076
goodness of fit	1.34
max shift/esd in least-square	0.03
max/min in diff map	0.72,-0.76

Appendix C: Derivation of the Rate of Exchange at Coalescence

For general reading on dynamic NMR see:

Jackman, L.M.; Cotton, F.A. "Dynamic Nuclear Magnetic Resonance Spectroscopy," Academic Press, New York, N.Y., 1975.

Becker, E.D. "High Resolution Nuclear Magnetic Resonance," Academic Press, New York, N.Y., 1980.

Carrington, A.; McLachlan, A.D. "Introduction to Magnetic Resonance," Harper and Row, New York, N.Y., 1967.

When a two-site exchange is occuring between sites on the same molecule, equation 2.9 greatly simplifies. Since the exchange is first-order the expression simplifies as follows for the first order exchange process:

$$\text{rate} = k[X]$$

and

$$W_{1,2} = f_1 W_1 + (1-f_1)W_1 + f_1(1-f_1)4\pi(\delta v)^2/k$$

Since the line widths of the protons in the individual sites is considered to be small compared with the line width coalesced peak, then $W_1 \simeq W_2 \simeq 0$ and

$$W_{1,2} = f_1(1-f_1)4\pi(\delta v)^2/k$$

At coalescence, the population of both sites is assumed to be equal so that $f_1 = 1-f_1 = .5$ and $f_1(1-f_1) = 1/4$. The line width at coalescence is now given as;

$$W_{1,2} = \pi(\delta v)^2/k$$

Since the line width is related to the reciprocal of the transverse relaxation time as

$$W_{1,2} = 1/\pi T_{1,2}$$

then

$$1/\pi T_{1,2} = \pi(\delta v)^2/k$$

Upon rearrangement

$$1/T_{1,2} = \pi^2(\delta v)^2/k$$

At coalescence, the transverse relaxation time of the coalesced peak is the lifetime of the proton spin in one site then,

$$1/T_{1,2} = 1/\tau$$

and

$$1/\tau = 2k$$

then

$$2k = \pi^2(\delta v)^2/k$$

Rearranging and simplifying the equation above one obtains the simple equation for the rate of a chemical exchange at coalescence.

$$k = \pi(\delta v)/\sqrt{2}$$

When the exchange is occuring between two sites on different molecules, the mole fractions of each component and the total concentration of both species must be considered. For the ytterbium(III) species, the rate of exchange is still assumed to be faster than the transverse relaxation time of the paramagnetic species such that

$$1/\pi\tau_P = 1/T_{2P} << 1/\pi T_{1,2} = W_{1,2}$$

so again the line widths of the individual species are essentially 0 when compared with the line width of the coalesced peak.

In this case

$$W_{1,2} = f_1 f_2 \frac{4\pi(\delta v)^2}{kc}$$

Since $W_{1,2} = 1/\pi T_{1,2}$ then

$$1/T_{1,2} = f_1 f_2 \frac{4\pi^2(\delta v)^2}{kc}$$

At coalescence $1/T_{1,2} = 1/\tau_D = k[Yb(C_8H_8)_2^-]$ then

$$k[Yb(C_8H_8)_2^-] = f_1 f_2 \frac{4\pi^2(\delta v)^2}{kc}$$

Upon rearranging and simplifying the above equation one obtains equation 2.24

$$k_c' = \left(4\, f_{YbII} f_{YbIII} \frac{\pi^2(\delta v)^2}{c[Yb(C_8H_8)_2^-]}\right)^{1/2}$$

References and Notes

1. Cotton, F.A.; Wilkinson, G. "Advanced Inorganic Chemistry" 4th Ed., Wiley and Sons, New York, 1980.

2. Sullivan, G.O.; Carroll, P.K. *Phys. Rev. A.* 1982, 25, 275.

3. Forsberg, J.H.; Moeller, T. in: *Gmelin Handbook of Inorganic Chemistry, Part D6, Sc, Y, La-Lu, Rare Earth Elements*, 8th E.; Springer, Berlin, 1983.

4. Schumann, H. *Angew. Chem. Int. Ed. Eng.* 1984, *23*, 474.

5. Mikheev, N.B. *Inorg. Chim. Acta* 1984, *94*, 241.

6. Huheey, J. "Inorganic Chemistry," 2nd. Ed., Harper and Row, New York, 1978.

7. As given in reference 5.

8. Shannon, R.D. *Acta Crystal.* 1976, *A32*, 751.

9. Weast, R.C. "CRC Handbook of Chemistry and Physics" 60th Ed. CRC Press, Baca Raton, Florida, 1980.

10. Warf, J.C.; Korst, W. *J. Phys. Chem.* 1956, *60*, 1590.

11. Schroeder, R.L; Thompson, J.C.; Oertel, P.L. *Phys. Rev.* 1969, *178*, 298.

12. Fischer, E.O.; Fischer, H. *Angew. Chem. Int. Ed. Eng.* 1964, *3*, 132. Fischer, E.O.; Fischer, H. *J. Organometal. Chem.* 1965, *3*, 181.

13. Zerger, R.; Stucky, G. *J. Organometal. Chem.* 1974, *80*, 7.

14. Evans, W.J.; Hughes, L.A.; Hanusa, T.P. *J. Am. Chem. Soc.* 1984, *106*, 4270.

15. Hayes, R.G.; Thomas, J.L. *J. Am. Chem. Soc.* 1969, *91*, 6876.

16. DeKock, C.W.; Ely, S.R.; Hopkins, T.E.; Brault, M.A. *Inorg. Chem.* 1978, *17*, 625.

17. The infrared spectrum of $Yb(C_8H_8)$ is reported in reference 16.

18. Greco, A.; Cesca, S.; Bertolini, G. *J. Organometal. Chem.* 1976, *113*, 321.

19. The dipotassium salt of [8]annulene dianion has absorbances in the 1000 to 600 cm^{-1} region at 880 and 684 cm^{-1} as reported in Fritz, H.P., Keller, H. *Chem. Ber.* 1962, *95*, 158.

20. Dietrich, M.W.; Wahl, A.C. *J. Phys. Chem.* 1963, *38*, 1591.

21. Yang, E.S.; Chan, M.; Wahl. A.C. *J. Phys. Chem.* 1980, *84*, 3094.

22. Marcus, R.A. *J. Chem. Phys.* 1956, *24*, 966. Marcus, R.A. *J. Chem. Phys.* 1965, *43*, 679.

23. In equations 2.5, 2.6 and 2.7; Z is the bimolecular collision number ($\approx 10^{11}$ $M^{-1}s^{-1}$, D_{op} and D_s are the optical and static dielectric constants ($D_{op} = n_d^2$), e is the electronic charge, R^* is the distance between the reactant centers in the transition state (assumed to be the touching of two spheres), κ is the transmission coefficient (usually assumed as equal to 1), and ρ is the square root of the ratio of the mean square deviation in reaction distance to the mean square deviation in perpendicular distance above the reaction hypersuface and is usually assumed to be $\approx$ 1. See reference 21.

24. Rosenblum, M. "Chemistry of the Iron Group Metallocenes," Interscience, New York, 1965, p. 31.

25. For $Fe(Cp)_2I_3$: Bernstein, T.; Herbstein, F.H. *Acta Crys. Sect. B.* 1968, *24*, 1640.

26. Yang, E.S.; Chun, M.; Wahl, A.C. *J. Phys. Chem.* 1975, *19*, 2049.

27. Prepared by M. Miller, see: Miller, M. Ph.D. Thesis, University of California, Berkeley, 1978.

28. Halpern, M. unpublished results.

29. Prepared by R. Kluttz, see: Streitwieser, A., Jr.; Kluttz, R.Q.; Smith, K.A.; Luke, W.D. *Organometallics* 1983, *2*, 1873.

30. Mares, F.; Hodgson, K.; Streitwieser, A., Jr. *J. Organometal. Chem.* 1970, *24*, C68. Hodgson, K.; Mares, F.; Starks, D.; Streitwieser, A., Jr. *J. Am. Chem. Soc.* 1973, *95*, 8650.

31. Stevenson, G.R.; Forsch, B.E. *J. Phys. Chem.* 1981, *85*, 378.

32. Calderazzo, F.; Pappalardo, R.; Losi, S. *J. Inorg. Nucl. Chem.* 1966, *28*, 987.

33. Aleksanyan, V.T.; Garbusova, I. A.; Chernyshova, T.M.; Todres, Z.V. *J. Organometal. Chem.* 1981, *217*, 169.

34. Hocks, L.; Goffart, J.; Duyckaerts, G.; Teyssie, P. *Spectrochim. Acta* 1974, *30A*, 907. These authors comment that the band at 698 cm^{-1} in $U(C_8H_8)_2$ is unusually high for ring-metal-ring tilt.

35. Hodgson, K.O.; Raymond, K.N. *Inorg. Chem.* 1972, *11*, 3030.

36. Anderson, S.E. *J. Organometal. Chem.* 1974, *71*, 263.

37. Raymond, K.N.; Eigenbrot, C.W.,Jr. *Acc. Chem. Res.* 1980, *13*, 276; Baker, E.C.; Halstead, G.W.; Raymond, K.N. *Struct. Bonding* (Berlin) 1976, *25*, 23.

38. In this type of [8]annulene complex, Raymond employs a radius of 1.49 Å for a ring carbon atom; see reference 37.

39. See reference 8. Each [8]annulene dianion is considered to be a ten- electron donor so that each ring formally donates five electron pairs.

40. Schilling, B. unpublished results.

41. Pauling, L. "The Nature of the Chemical Bond," 3rd. Ed., Cornell University Preess, Ithaca, New York, 1960, p. 260.

42. Lyttle, M. Ph.D. Thesis, University of California, Berkeley, 1982.

43. Ytterbium(II) has a ground state configuration of $[Xe]4f^{14}$.

44. Estimated from the temperature-dependent ^{1}H-NMR spectrum of $K[Yb(C_8H_4Me_4)_2]$ as reported in; Metz, T. Masters Thesis, University of California, Davis, 1974.

45. Streitwieser, A., Jr.; Müller-Westerhoff, U.; Sonnichsen, G.; Mares, F.; Morell, D.G.; Hodgson, K.O. *J. Am. Chem. Soc.* 1973, 95, 8644.

46. $R = \Sigma| |F_o| - |F_c| | / \Sigma |F_o|$

47. For Yb, K, O, and C atoms: International Tables for X-ray Crystallography (1974), Vol. IV, Kynoch Press, Birmingham. For H atoms: Stewart, R.F.; Davidson, E.R.; Simpson, W.T. *J. Chem. Phys.* 1965, *42*, 3175.

48. Cromer, D.T.; Liberman, D. *J. Chem. Phys.* 1970, 53, 1891.

49. Templeton, L.K.; Templeton, D.H. *Abstract, American Crystallographic Association Procedings, Storrs, Conn.* 1973, *1*, 143.

50. Doyle, P.A.; Turner, P.S. *Acta Crystallogr.* 1968, *A24*, 390.

51. Cromer, D.T.; Liberman, D. *J. Chem. Phys.* 1970, 1891.

CHAPTER THREE

New Studies on Bis([8]annulene)cerium(IV)

Introduction

The synthesis of bis([8]annulene)uranium(IV) and other actinide(IV) organometallic compounds has led to considerable controversy on the nature of the ring-metal bond in f-block element organometallic complexes.[1] The description of ring-metal bond in bis([8]annulene)uranium(IV) as "ionic" or "covalent" is difficult, due, in part, to the difficulty in applying the simple, classical bond definitions to the uranium complex. The molecular orbital description for a covalent bond in the bis-([8]annulene complexes is the involvement of both metal and ligand orbitals in the ring-metal interaction. One type of interaction involving the uranium f and [8]annulene p orbitals was shown in Figure 1.1 (in chapter 1). The controversy for bis-([8]annulene)uranium(IV) is whether interactions, especially f-orbital interactions as the ones in Figure 1.1, are significant;

in other words, which, if any, physical properties or reactions of bis([8]annulene)uranium(IV) can be explained by the effect of a covalent ring-metal interaction.

As shown in the previous chapter, one method of ascertaining the orbital involvement in an f-block element organometallic complex's ring-metal bond is by comparison with similar "ionic" organometallic complex. The comparison of the ionic calcium complex, $K_2[Ca(C_8H_8)_2]$, in which it is very unlikely that d and f orbitals play a major role in bonding, with the analogous ytterbium(II) complex strongly suggests that in [8]annulene lanthanide(II) organometallic complexes, the ring-metal interaction is essentially ionic.

Comparison of Bis([8]annulene)actinide(IV) and Bis([8]annulene)-lanthanate(III) Complexes

The series of bis([8]annulene)lanthanate(III) complexes were synthesized to provide an "ionic" bis([8]annulene complex for comparison with the bis([8]annulene)actinide(IV) complexes.[2] It is well-established that the effect of f and d orbitals in lanthanide(III) chemistry is small.[3,4] A simple example of this is seen by the lack of effect of most ligand fields on the energies of the f-f transitions of the lanthanides.[4] As is the case for the bis([8]annulene)lanthanate(II) complex dianion, the relative "ionicity" of the bis([8]annulene)lanthanate(III) anions can be shown by comparison with non-f-block bis([8]annulene) complexes.

The similarity in properties and structure between bis([8]annulene)yttrate(III) anion and the bis([8]annulene)lanthanate(III) anions clearly suggests that f and d orbitals on the metals play no major role in the ring-metal bond in the bis([8]annulene)lanthanide(III) ions, since the 4f and 5d orbitals are energetically unfavorable for the fourth row element.[2]

The class of bis([8]annulene)lanthanide(III) complex anions is reviewed in chapter one of this work. These complexes are non-volatile and show high thermal stability; bis([8]annulene)-thorium(IV) and uranium(IV) can be sublimed at < 200°C, *in vacuo*. Unlike bis([8]annulene)uranium(IV), which has solubilities of 10^{-3} moles/liter in a variety of polar and non-polar solvents, the lanthanide(III) complexes are soluble only in polar ethereal solvents. The bis([8]annulene)lanthanate(III) anions also hydrolyze much more rapidly than bis([8]annulene)uranium(IV). Although solubilities, volatility and thermal stability are not sufficient to classify compounds as ionic or covalent, these properties are suggestive that the bis([8]annulene)lanthanate(III) complexes are highly ionic. The comparisons between bis([8]annulene)lanthanate(III) anions and bis([8]annulene)-uranium(IV) indicate that the lanthanide complexes are considerably more "salt-like" than bis([8]annulene)uranium(IV).[2]

A clear indication of the relative bond strengths of the lanthanide(III) and uranium(IV) complexes is shown by a ligand

exchange experiment. Bis([8]annulene)cerate(III) anion was shown to undergo rapid ligand exchange with uranium tetrachloride to form bis([8]annulene)uranium(IV).[2] This experiment indicates not only the relative thermodynamic stabilities of the bis([8]annulene)lanthanate(III) and -actinide(IV) complexes, but that the ligand exchange is kinetically rapid. Note that in the similar exchange experiment between bis([8]annulene)thorium(IV) and uranium tetrachloride, the exchange equilibrium also favors the formation of bis([8]annulene)uranium(IV), but the exchange is much slower.[5]

The ionic lanthanide(III) complexes are clearly more "salt-like" than the corresponding actinide(IV) complexes. Unfortunately, the comparison of a potassium bis([8]annulene)lanthanate(III) salt with a bis([8]annuene)actinide(IV) complex is poor, since in the former case, the bis([8]annulene) complex is an anion; in the latter, the sandwich moiety is neutral. The "salt-like" properties of the lanthanide(III) complexes could be due only to the effects of the ionic interaction between the potassium cation and the sandwich, and independent of the ring-metal interactions in the sandwich moiety. The bis([8]annulene)-lanthanide(III) anions are a poor choice for comparison with bis-([8]annulene)uranium(IV).

A far better lanthanide analogy for the actinide complexes is the bis([8]annulene)lanthanide(IV) complexes. Rösch and Streitwieser have carried out SCF-Xα calculations on the bis([8]annu-

lene)cerium(IV) complex.[6] Shown in Figure 3.1 are some of the results of their calculations.

In Figure 3.1, the orbital energy levels for the series $M(C_8H_8)_2$ are compared. One method of deducing the relative involvement of metal f-orbitals in the bis([8]annulene)complexes is by looking at the effects of the $e_{2u}(f)-e_{2u}(\pi)$ interaction on the relative orbital energy levels of the three complexes.

The SCF-Xα calculations indicate an unusually large HOMO-LUMO ($e_{2u}(\pi)-e_{3u}(f)$) for bis([8]annulene)thorium(IV). From examination of Figure 3.1, this large gap (relative to the cerium(IV) and uranium(IV) analogs) is partially due to the relatively higher energy of the $e_{3u}(f)$ orbital of bis([8]annulene)thorium. If the strong visible absorption of bis([8]annulene)thorium(IV) and -uranium(IV) is assigned as the charge transfer band, $e_{2g}(\pi)-e_{3u}(f)$, the calculated vs measured values for this gap are 3.03 eV vs 2.75 eV for bis([8]annulene)thorium(IV) and 1.97 vs 2.01 eV for bis([8]annulene)uranium(IV). Prior to this thesis, the optical spectrum of bis([8]annulene)cerium(IV) had not been reported, thus the calculated vs measured(assigned) $e_{2g}(\pi)-e_{3u}(f)$ energy difference could not be determined for this molecule.

The splitting of the metal orbitals, the $e_{2u}(f)$ and $e_{3u}(f)$, is indicative of an interaction of the metal e_{2u} and ligand e_{2u} orbitals. In Figure 3.2, the simplified cases of no ligand metal interaction and some ligand metal interaction is shown. In this simple example, the relative position of the $e_{3u}(f)$ orbital is

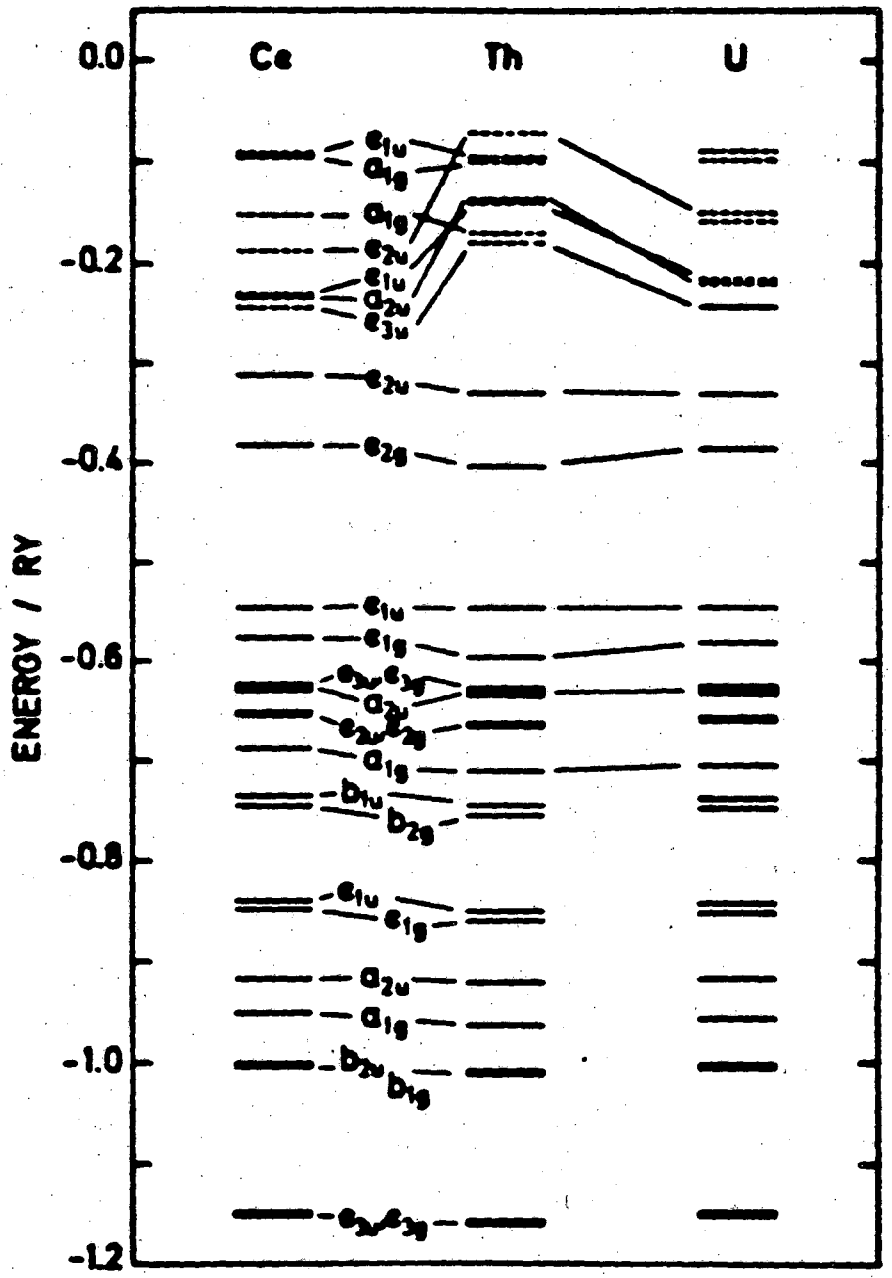

Figure 3.1: Orbital Energy Diagrams for $M(C_8H_8)_2$ (M=Ce,Th,U)

considered to be unaffected by any interaction with the ligand $e_{3u}(\pi)$; the ligand $e_{3u}(\pi)$ orbital is too high in energy.

Figure 3.2 clearly shows that the $e_{3u}(f)$-$e_{2u}(f)$ can be indicative of f-orbital interaction in the ring-metal bond; the greater interaction being indicated by the larger energy gap. Using the criterion of the $e_{3u}(f)$-$e_{2u}(f)$, one predicts that the order of f-orbital covalency is Ce < Th < U for the ring-metal interaction in $M(C_8H_8)_2$.

The electron populations of the $e_{2u}(\pi)$, $e_{2g}(\pi)$, $e_{1u}(\pi)$ and $e_{1g}(\pi)$ orbitals can also be used as a criterion for ring-metal interaction in the bis([8]annulene) complexes. All of these ligand orbitals have the proper symmetry to interact with metal d (the gerade) and f (the ungerade) orbitals. In Table 3.1, the sphere populations are shown for the e_2 and e_1 orbitals in the bis([8]annulene)complexes. In this table, the higher fraction of electrons in the metal sphere indicate a more covalent interaction, since any fraction of electrons in the metal sphere is from donation from the ligand.

As can be seen from Table 3.1, the sphere populations predict an order of covalent ring metal interaction for $M(C_8H_8)_2$ as Th < Ce ≃ U. Since the relative population distribution between ligand and metal for the e_{2g} and e_{1g} orbitals is roughly the same for all the complexes, then the difference in covalency is due to f-orbital interactions in the cerium(IV) and uranium(IV). This

Figure 3.2: Result of $e_{2u}(\pi)$-$e_{2u}(f)$ interaction on the $e_{2u}(f)$-$e_{3u}(f)$ energy gap in bis([8]annulene) sandwich complexes.

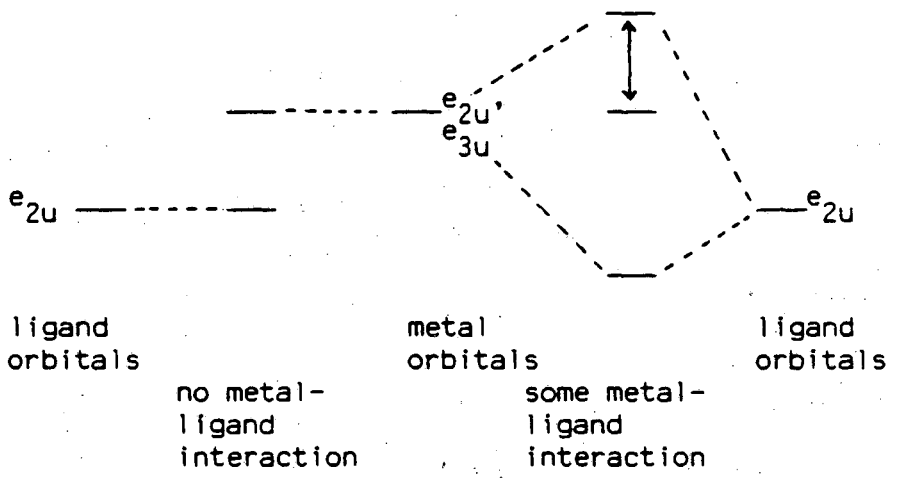

Table 3.1: Sphere Populations for $M(C_8H_8)_2$.[a]

	Ce		Th		U	
	M[b]	L[c]	M	L	M	L
e_{2u}	.321	.437	.203	.512	.328	.430
e_{2g}	.207	.408	.211	.403	.197	.411
e_{1u}	.065	.55			.104	.85
e_{1g}	.098	.58			.096	.58

(a) from ref. 6b.
(b) electrons in metal sphere.
(c) electrons in ligand sphere.

result is, of course the opposite of that predicted by the comparison of the $e_{2u}(f)-e_{3u}(f)$ energy differences.

Since the metal d-orbital involvement is roughly equal for the three complexes, one may also look at the $e_{2u}(\pi)-e_{2g}(\pi)$ energy difference as a measure of f-orbital covalency. In Figure 3.3, the qualitative result of an $e_{2u}(\pi)-e_{2u}(f)$ interaction on the $e_{2u}(\pi)-e_{2g}(\pi)$ gap is shown. In this example, the energy level of the $e_{2g}(\pi)$ is held constant.

Examination of Figure 3.3 indicates that an order of covalency Th < Ce < U is predicted by consideration of the $e_{2u}(\pi)-e_{2g}(\pi)$ energy difference.

The calculations of Rösch and Streitwieser indicate significant involvement of metal d and f orbitals bis([8]annulene)-uranium(IV) and d orbital involvement equal to that of the uranium complex in bis([8]annulene)thorium(IV); these conclusions are supported experimentally by the photoelectron spectra (PES) of the complexes.[7] Since the relativistic Xα calculations indicate some ligand-metal orbital interactions for bis([8]annulene)-uranium(IV) and -thorium(IV), it is important that the PES results agree with the relative energy level differences for the thorium and uranium complexes. Both calculation and experiment indicate a larger $e_{2u}-e_{2g}$ difference in bis-([8]annulene)thorium(IV) vs bis([8]annulene)uranium(IV). It now becomes important to observe whether the Xα calculations are as

<u>Figure 3.3</u>: Result of $e_{2u}(\pi)$-$e_{2u}(f)$ interaction on the $e_{2u}(\pi)$-$e_{2g}(\pi)$ energy gap in bis([8]annulene) sandwich complexes.

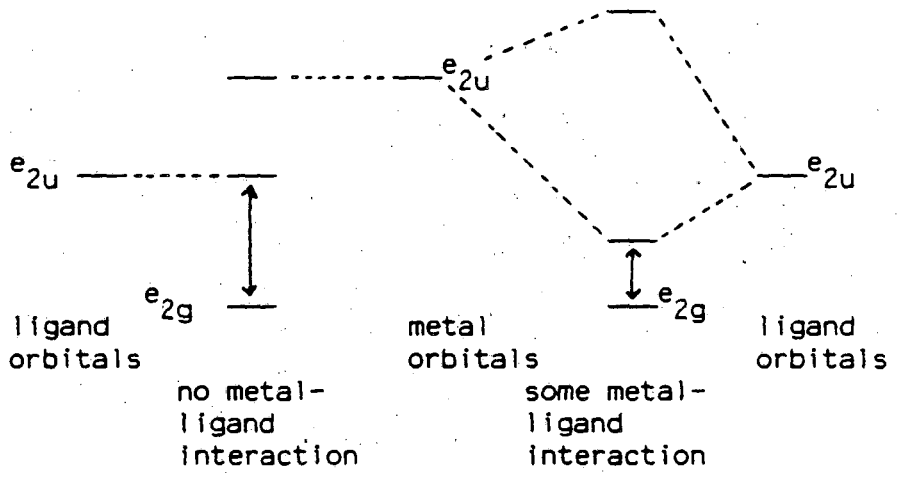

satisfactory in prediction of the relative orbital energy levels of bis([8]annulene)cerium(IV), especially since these calculations predict that the $e_{2u}(\pi)$-$e_{2g}(\pi)$ energy difference for the cerium(IV) complex is less than that of bis([8]annulene)-thorium(IV) and greater than that of bis([8]annulene)uranium(IV). It is interesting indeed that the relativistic SCF-Xα calculations indicate some f-orbital involvement in the ring-metal interaction in bis([8]annulene)cerium(IV).

Cerium(IV) Chemistry

Given that calculations can be carried out on bis([8]annulene)cerium(IV), the next question is, does the molecule exist? There are two reports of bis([8]annulene)cerium(IV) in the chemical literature. The first of these reports is by an Indian research group; Kalsotra, Multani and Jain,[8] and the second by an Italian research group; Greco, Cesca and Bertolini.[9] These reports are striking in that the method of synthesis, the physical properties and spectral characterization of the complex reported as bis([8]annulene)cerium(IV) differ in every detail. A brief backround on cerium(IV) chemistry and the attempts (one of them successful) in duplicating the literature preparations of bis([8]annulene)cerium(IV) follows.

Cerium is the only lanthanide element that has a tetrapositive oxidation state that exists in both aqueous solution and in

solids.[3] Praseodymium(IV) and terbium(IV) have also been shown to exist in solid compounds, but only as the oxides and fluorides.[3] Alkali metal fluorides of dysprosium(IV) and neodymium(IV) have also been reported;[10,11,12] however, reports of higher oxides of Dy and Nd are incorrect.[3,12]

All of the tetrapositive lanthanide ions are strong oxidizing agents; cerium(IV) complexes are employed in both organic (e.g., oxidations of ketones, alcohols and phenols) and inorganic chemistry as an oxidizing agent. The literature on oxidation by cerium(IV) is far too extensive to be reviewed here; shown below (3.1-3.3) are a few recent examples of synthesis or kinetic studies using oxidation by cerium(IV) in inorganic or organometallic systems.[13,14,15]

$$[(bpy)_2ClRu(py)](PF_6) \xrightarrow[Ce(IV)/ClO_4^- \text{ aq.}]{} [(byp)_2ClRu(py)](ClO_4)_2 \qquad [3.1]$$

$$U(IV) \xrightarrow[Ce(IV)/F^- \text{ aq.}]{} U(VI) \qquad [3.2]$$

$$Se(IV) \xrightarrow[Ce(IV) \text{ aq.}]{} Se(VI) \qquad [3.3]$$

The oxidation potential of Ce(IV) in aqueous, acidic conditions varies significantly depending on the type of acid and acid

strength. Shown in Table 3.2 are the values of the Ce(IV)/Ce(III) couple in various aqueous solutions.

Table 3.2: Oxidation Potential of Ce(IV)/Ce(III)

8M $HClO_4$	1.87 V[a]
1M $HClO_4$	1.70 V[b]
1M HNO_3	1.61 V[c]
1M H_2SO_4	1.44 V[d]
3M HCl	1.27 V[e]
catechol	-0.4 V[f,g]

(a) ref. 16. (b) ref. 17. (c) ref. 18. (d) ref. 19. (e) ref. 20. (f) basic solution (g) ref. 21.

As a result of the dependence of the Ce(IV)/Ce(III) couple on the aqueous medium, dilute solutions of manganese(II) perchlorate are oxidized to permanganate by Ce(IV) in dilute perchloric acid, but permanganate is reduced to manganese(II) by Ce(III) in dilute sulfuric acid.[12]

Work by Raymond[21] has indicated that the Ce(IV)/Ce(III) couple is negative in basic solution with catechol present as a complexing agent. Table 3.2 illustrates that the reduction potential of Ce(IV)/Ce(III) varies dependent on the complexing reagent in solution. The value of the Ce(IV)/Ce(III) couple can then be looked on as a function of the ratio of the stability constants of the Ce(IV) and Ce(III) complexes. Raymond's catechol results clearly show that the couple is driven toward Ce(IV) due to the strong complexation of Ce(IV) relative to Ce(III).

Due to the oxidation potentials of the tetravalent lanthanide ions, the existence of organometallic complexes involving lanthanide(IV) ions, such as cerium, with strongly reducing ligands, such as cyclopentadienyl anion or [8]annulene dianion have been thought to be unlikely. In support of this, the reaction of cerium metal atoms with cyclooctatetraene, *in vacuo*, gives only the cerium(III) complex, $Ce_2(C_8H_8)_3$,[22] whereas the reaction of cyclooctatetraene with uranium or thorium metal gives the bis-([8]annuene)actinide(IV) complex.[23] The lack of formation of bis-([8]annulene)cerium(IV) under the metal atomization conditions suggests that either the cerium(IV) complex cannot be formed at all, or that under the experimental conditions, the cerium(IV) complex is formed, but decomposes to the cerium(III) complex.

One of the major problems in the synthesis of cerium(IV) organometallic complexes, aside from the oxidation potential of cerium, is the availibility of cerium(IV) containing starting materials. For example, *Advanced Inorganic Chemistry*[3] lists only two binary solids which contain cerium(IV), CeO_2 and CeF_4. Complex anions which contain cerium(IV) are somewhat more common. One familar example of a cerium(IV) complex anion is the common oxidizing agent, ceric ammonium nitrate, $(NH_4)_2[Ce(NO_3)_6]$.

The cerium(IV) starting materials in the Indian and Italian preparations of bis([8]annulene)cerium(IV) are pyridinium hexachlorocerate(IV)[24] and cerium(IV) isopropoxide.[24]

Although ceric ion oxidizes concentrated HCl to Cl_2 in aqueous solution, the reaction of HCl with $Ce(OH)_4$ in absolute ethanol produces the complex anion $[CeCl_6]^{2-}$. This dianion can be isolated as the corresponding pyridinium salt. pyridinium hexachlorocerate(IV) can be made anhydrous at 120°C, *in vacuo*.[3]

[3.4]

$$Ce(OH)_4 + 6\ HCl \xrightarrow[EtOH]{} [H_2CeCl_6] + 4\ H_2O$$

[3.5]

$$[H_2CeCl_6] + 2\ C_5H_5N \longrightarrow (C_5H_5NH)_2CeCl_6$$

Reaction of the anhydrous pyridinium hexachlorocerate(IV) hexachloride with alcohols and ammonia in benzene give cerium(IV) alkoxides.[24]

[3.6]

$$(C_5H_5NH)_2CeCl_6 + 4\ ROH + 6\ NH_3 \xrightarrow[benzene]{} Ce(OR)_4 + 2\ C_5H_5N + 6\ NH_4Cl$$

Cerium(IV) isopropoxide can be crystallized as a mono-adduct of pyridine or isopropyl alcohol.[24]

False Reports of Cerium(IV) Organometallic Complexes

The first report of bis([8]annulene)cerium(IV) was in 1972 by Kalsotra, Multani and Jain. In fact, most of the cerium(IV) organometallic complexes have been reported by research groups involving Kalsotra. In all of their work, the Indian researchers employed pyridinium hexachlorocerate(IV) as a starting material. It has been noted that $CeCl_6^{2-}$ is a strong oxidizing agent and that the synthesis of cerium(IV) organometallics complexes from this starting material is doubtful.[25] The Indian group has reported cerium(IV) complexes with cyclopentadienide(Cp) (both $CeCp_4$[26] and $CeCp_3X$[27]), indenide,[28] fluorenide(Fl),[28] cycloheptatrienide[29] and [8]annulene dianion.[8] One is impressed both by the almost perfect chemical analyses and the physical descriptions of these complexes. For example, the cyclopentadienide complex, $CeCp_4$, and the bis([8]annulene)cerium(IV) complex analyze perfectly and are reported as stable to water and dilute acid, (although they decompose in hot conc. nitric acid!) properties which are incredible and totally inconsistent with any known [8]annulene complexes.

The work of Kalsotra, Multani and Jain on $CeCp_4$, not surprisingly, has been recently refuted. Deacon, Tuong and Vince[30] followed the Indian preparation and obtained only the known cerium(III) complex, $CeCp_3$.[31] There are reports of other work, namely the syntheses of $Ce(Fl)_4$[28] and $Ce(C_7H_7)Cl_2$,[29] by the

Indian researchers which could not be repeated.[25] In light of these reports, the work by Kalsotra, Multani and Jain on bis-([8]annulene)cerium(IV) was also doubted. Indeed, all of the attempts to duplicate the Indian work were unsuccesful; the reaction of [8]annulene dianion and di(pyridinium)cerium(IV) hexachloride does not lead to a singular characterizable organometallic complex. No material was obtained which matched the reported bis([8]annulene)cerium(IV) complex.

Bis([8]annulene)cerium(IV): Synthesis and Characterization

Greco, Cesca, and Bertolini reported bis([8]annulene)-cerium(IV) from the reaction of cerium(IV) isopropoxide, triethylaluminum and the solvent in cyclooctatetraene. This same synthetic method was employed by Wilke for the synthesis of $Ti(C_8H_8)_2$ and $Ti_2(C_8H_8)_3$.[32]

[3.7]

$$Ti(OR)_4 + Al(C_2H_5)_3 \xrightarrow[C_8H_8/80°C]{} Ti(C_8H_8)_2$$

[3.8]

$$Ti(OR)_4 + Al(C_2H_5)_3 \xrightarrow[C_8H_8/60°C]{} Ti_2(C_8H_8)_3$$

Unlike the work of Kalsotra, Multani and Jain, the Italian workers report a bis([8]annulene)cerium(IV) whose characteriza-

tion is completely consistent with what one would expect for the cerium complex. Their bis([8]annulene)cerium(IV) complex was decomposed by air, water and alcohols, had only one signal in the NMR which was consistent with the absence of a paramagnetic metal ion, and gave correct analysis and mass-spectrum for $Ce(C_8H_8)_2$. The crystal powder pattern of bis([8]annulene)cerium(IV) was reported by the Italian group; this pattern compares closely with the other patterns of bis([8]annuene)actinide(IV) complexes and suggests that the cerium(IV) complex is isostructural with the actinide(IV) complexes. Shown in Table 3.3 is the comparison of the x-ray powder patterns of the bis([8]annulene) f-block metal complexes.

The only questionable aspect of the Italian preparation of bis-([8]annulene)cerium(IV) is the synthesis of a cerium(IV) complex under reducing conditions; triethylaluminum is a sufficiently strong reducing agent to reduce cerium(IV) to cerium(III).

Upon following the procedures of the Italian group for the preparation of bis([8]annulene)cerium(IV), The product obtained is an air-sensitive, brown-black, microcrystalline compound, as reported. This compound has a single signal in ^{1}H-NMR at 5.9 ppm in THF-*d8* or at 5.75 ppm in toluene-*d8*. When the toluene solution of the complex was exposed to air, the brown solution became pale yellow and the ^{1}H-NMR contained only one peak at 5.61 ppm, which is the resonance for neutral cyclooctatetraene. The infrared

Table 3.3: X-ray powder pattern data on $M(C_8H_8)_2$ complexes[a,b]

Th[d]		Pa[d]		U[d]		Np[e]		Pu[e]		Ce[f]	
d[c]	I	d	I	d	I	d	I	d	I	d	I
6.78	s	6.67	s	6.70	s	6.73	s	6.73	s	6.75	s
6.27	m	6.26	m	6.29	m	6.30	m	6.28	s	6.21	s
5.47*	s	5.47	s	5.46*	s	5.49	s	5.47	s	5.45	s
5.29	w	5.26	m	5.25	w	5.26	v	5.25	m		
										4.61	v
4.41	w	4.38	m	4.36	w			4.37	m	4.35	v
4.05	w	4.04	m	4.03	w	4.01	v	4.04	m	4.02	m
3.61*	w	3.59	m	3.58*	w	3.60	v	3.57	m	3.58	m
				3.35	v			3.36	w	3.34	v
3.29	w	3.25	w	3.25*	w			3.24	m	3.24	w
3.23	w										
2.99*	w	2.98	w	2.98*	w			2.98	m	2.98	m
2.83	w	2.81	w	2.80	w			2.79	m	2.81	w
2.74*	w	2.73	w	2.73*	w			2.73	m	2.72	m

* Combined lines with d-spacing less that .04

(a) For comparison of x-ray data, any intensities(i) listed in the original papers as I+ or I- are listed in this Table as I.
(b) Calculated. Numerical intensities calculated are given as: within 30% of strongest band = s; 30-60% = m; 60-90% = w; 90% = v.
(c) in Å . (d) ref. 33. (e) ref. 34. (f) ref. 9.

spectrum of this brown-black microcystalline compound is the same as the one reported by the Italian group and is also similar to the infrared spectrum reported for bis([8]annulene)uranium(IV). Shown in Table 3.4 is a comparison of the infrared spectrum of $Ce(C_8H_8)_2$ and $U(C_8H_8)_2$ in the 600-1000 cm^{-1} region.

Table 3.4: Infrared spectra of $M(C_8H_8)_2$ M = Ce, U[a]

$Ce(C_8H_8)_2$[b]	$Ce(C_8H_8)_2$[c]	$U(C_8H_8)_2$[d]
692 vs	687 vs	698 vs
746 m	740 m	746 s
	770 w	777 m
790 w	785 w	792 m
902 s	896 s	900 s

(a) values in cm^{-1}. vs, very strong; s, strong; m, medium; w, weak.
(b) ref. 9. (c) this work. (d) ref. 35.

The mass spectrum of the microcystalline compound also verifies the Italian report; the parent and fragment peaks in the MS are exactly what one would expect for bis([8]annulene)-cerium(IV). Shown in Figure 3.4 is the comparison of the mass-spectrum of the cerium(IV) complex with the mass-spectrum of bis([8]annulene)uranium(IV).[36]

From the above data one can conclude that the cerium complex contains only one type of proton and is diamagnetic. The complex is also isostructural with bis([8]annulene)uranium(IV) as suggested by infrared and x-ray powder pattern data. The MS further

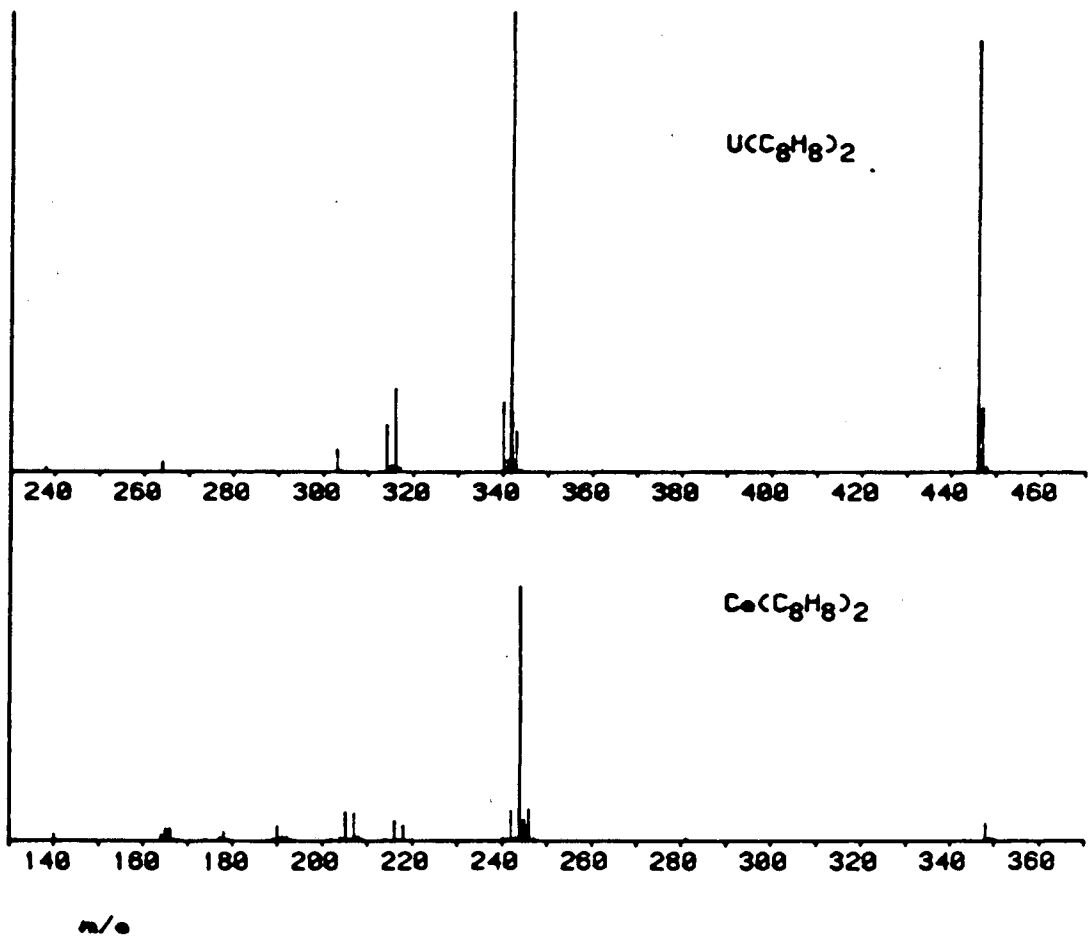

Figure 3.4: Mass Spectra of bis([8]annulene)uranium(IV) and -cerium(IV).

supports that the parent peak of the complex contains only one cerium ion and two C_8H_8 moieties. These results indicate that the report of bis([8]annulene)cerium(IV) by Greco, Cesca, and Bertolini is correct, and that the cerium(IV) complex is a bis-([8]annulene)uranium(IV) analog.

Bis([8]annulene)cerium(IV) is further characterized by this work. The brown-black complex can be sublimed, *in vacuo*, but with extensive decomposition to the green cerium(III) complex, $Ce_2(C_8H_8)_3$, due to the loss of cyclooctatetraene (3.9). This manner of reductive decomposition by loss of cyclooctatetraene is analogous to the thermal reduction of $K[Yb(C_8H_8)_2]$ to $K_2[Yb(C_8H_8)_2]$.

[3.9]

$$2\ Ce(C_8H_8)_2 \text{ ------> } C_8H_8 + Ce_2(C_8H_8)_3$$

This thermal instability of the cerium(IV) to the cerium(III) complex was predicted from results of the metal atomization experiment reported reported earlier in this chapter.

Rösch and Steitwieser report good agreement of the calculated $e_{2g}(\pi)$-$e_{3u}(f)$ charge transfer band for bis([8]annulene)-uranium(IV) and -thorium(IV) with the observed strong visible

absorptions of the actinide complexes. The calculated charge transfer band for bis([8]annulene)cerium(IV) could not, at that time, be compared with the actual compound, since the Italian group did not include visible spectra in their report of bis-([8]annulene)cerium(IV). The visible spectrum of bis([8]annulene)cerium is now known. In THF solution, bis([8]annulene)-cerium(IV) has a strong absorbance at 469 nm with $\varepsilon \approx 8000$. This absorption band is more intense than the band for bis([8]annulene)uranium(IV), which has an extinction coefficient $\varepsilon \approx 1800$.

Rösch and Streitwieser calculate a value of 1.92 eV for the difference in energy between the $e_{2g}(\pi)$ and $e_{3u}(f)$ in bis-([8]annulene)cerium(IV). If the strong absorption of the cerium(IV) complex is assigned as the $e_{2g}(\pi)$-$e_{3u}(f)$ charge transfer band, then the calculated vs observed value is 1.92 vs 2.63 eV. Not only does result indicate poor agreement between the calculation and experiment; the result also suggests that the calculations did not predict the trend in $e_{2g}(\pi)$-$e_{3u}(\pi)$ energy differences correctly (predicted trend Ce $\approx$ U $\ll$ Th; found U $\ll$ Ce $\approx$ Th).

A closer examination of the bis([8]annulene)cerium(IV) optical spectrum (Figure 3.5) indicates a shoulder on the broad peak at 469 nm. Rigsbee and Gronert, of this research group, have deconvoluted the bis([8]annulene)cerium(IV) spectrum and found that the shoulder is an absorption at 570 nm, $\varepsilon \approx 1000$. If this

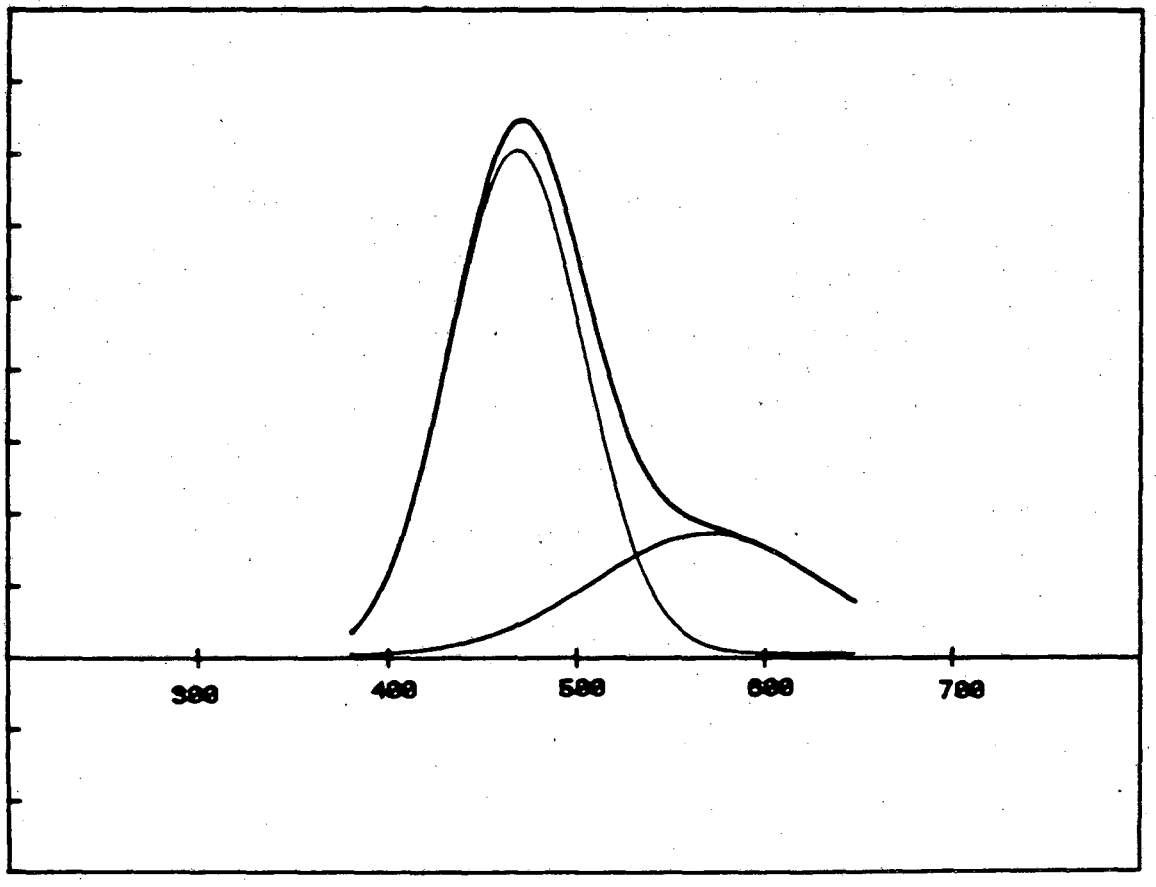

Figure 3.5: Visible Spectrum of Bis([8]annulene)cerium(IV) (with deconvuluted spectrum shown).

shoulder is assigned as the $e_{2g}(\pi)$-$e_{3u}(f)$ charge-transfer for bis([8]annulene)cerium(IV) then the measured value of 2.18 eV is in better agreement with the calculated value of 1.92 eV.

The structure of bis([8]annulene)cerium(IV), although not yet elucidated by single crystal x-ray diffraction, is the same as the structures of bis([8]annulene)uranium(IV) and -thorium(IV). Comparison of the calculated x-ray powder pattern from single crystal data for the bis([8]annuene)actinide(IV) complexes with the observed pattern for bis([8]annulene)cerium(IV), shown earlier in Table 3.2, clearly show that the lanthanide complex is isomorphous with the actinide(IV) complexes. Bis([8]annulene)-cerium(IV) clearly has little structural similarity with the group IVb complexes, $M(C_8H_8)_2$ M = Ti,[37] Zr.[38] Although the preparations of bis([8]annulene)cerium(IV) and the titanium(IV) complex are quite similar, their structures are radically different; the cerium(IV) complex is the symmetrical sandwich while the titanium(IV) complex structure shows that $Ti(C_8H_8)_2$ cannot be classified as a bis([8]annulene) complex, Figure 3.6, since in this structure one of the eight-membered rings is not planar.

The structure of bis([8]annulene)cerium(IV) is illustrative of the differences between d- and f-block bis([8]annulene) complexes. The smaller d-transition metals, which usually conform with the 18-electron rule,[4] cannot accomadate two ten-electron moieties in their coordination sphere, whereas for the larger

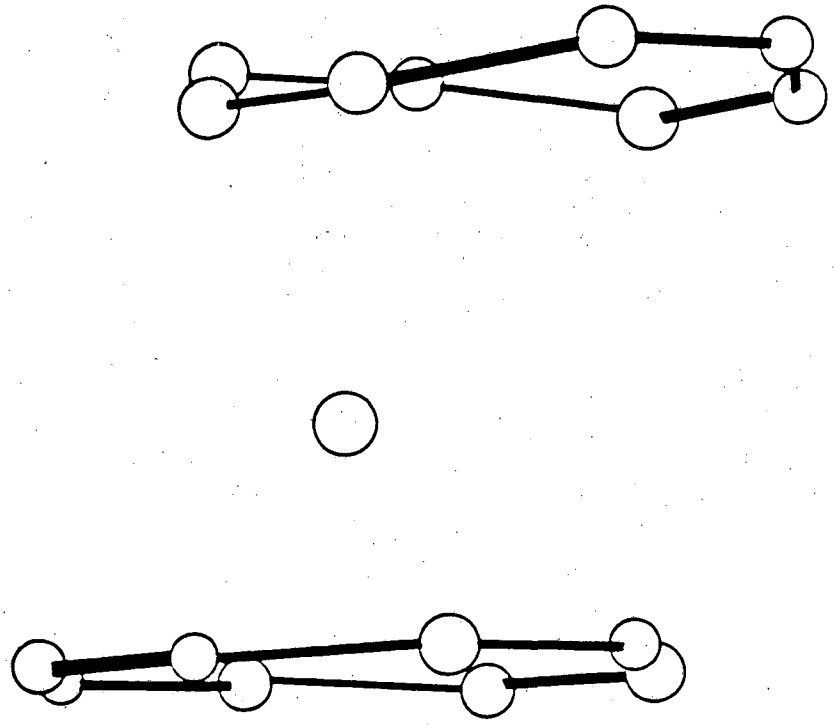

Figure 3.6: Structure of $Ti(C_8H_8)_2$ (hydrogen atoms omitted for clarity).

lanthanide(IV) and actinide(IV), for which there is no 18-electron rule[4], the coordination of two ten-electron ligands is not a problem.

The Nature of the Ring-Metal Interaction in bis([8]annulenecerium(IV)

The NMR, IR, MS, and x-ray powder patterns of bis([8]annulene)cerium(IV) are not indicative of the type of bonding in the cerium complex. Information on the nature of the ring-metal bond in the cerium(IV) complex must be elucidated in another manner. One indication of a thermodynamically stronger ring-metal bond in bis([8]annulene)uranium(IV) as compared with bis([8]annulene)-thorium(IV) is the aforementioned exchange reaction of bis-([8]annulene)thorium(IV) with uranium tetrachloride to form bis-([8]annulene)uranium(IV). The reverse reaction does not occur.

The calculations by Rösch and Streitwieser indicate that bis-([8]annulene)cerium(IV) is more ionic than the uranium(IV) analog and that the ranking of these complexes in order of increasing metal orbital involvement in the ring-metal interaction is $Th(C_8H_8)_2 \leq Ce(C_8H_8)_2 < U(C_8H_8)_2$. This ordering predicts that the cerium(IV) complex should have properties that are more similar to the bis([8]annulene)thorium(IV) complex than to the bis-([8]annulene)uranium complex; hence, bis([8]annulene)cerium(IV) should undergo exchange with uranium tetrachloride to form

bis([8]annulene)uranium(IV). Indeed, upon carrying out the bis-([8]annulene)cerium(IV):uranium tetrachloride exchange experiment in an NMR tube (thf-*d8*), the slow formation of bis([8]annulene)-uranium(IV) (days) can be monitored by the appearance of a singlet at -36 ppm and the disappearance of the bis([8]annulene)-cerium(IV) complexes resonance of 5.9 ppm. This experiment, unfortunately, is not as straightfoward as the analogous experiment involving the thorium(IV) species and does not indicate the relative stability of the bis([8]annulene)cerium(IV) complex as compared with bis([8]annulene)uranium(IV). One of the products of the balanced exchange reaction, shown below, is $CeCl_4$. Cerium tetrachloride is solution unstable, disproportionating to $CeCl_3$ and Cl_2. If the disproportionation occurs in the exchange reaction, then the reaction is not reversible and the disproportionation could be the driving force of the reaction.

[3.10]

$$Ce(C_8H_8)_2 + UCl_4 \xrightarrow[THF]{} U(C_8H_8)_2 + [CeCl_4]$$

Clearly, the simple ligand exchange experiment cannot be used to estimate the ring-metal bond strength for the cerium(IV) complex relative to the uranium and thorium complexes. It is important, however, that the exchange between bis([8]annulene)-cerium(IV) and uranium tetrachloride is relatively slow; this result is in direct contrast with the immediate reaction of bis-([8]annulene)cerium(III) anion with uranium tetrachloride.

Hydrolysis of bis([8]annulene)uranium(IV) to give a mixture of 1,3,5- and 1,3,6-cyclooctatrienes is a relatively slow reaction with a half-life of 20 hours in a 10^{-3} M solution of water in THF.[39] The hydrolysis of bis([8]annulene)thorium(IV) is rapid with a half-life of <60 seconds.[41] Since bis([8]annulene)-cerium(IV) is predicted to be more similar to the thorium(IV) complex, one expects a rapid hydrolysis for the cerium(IV) complex. Addition of a 10^{-3} M solution of bis([8]annulene)cerium(IV) in THF to a 10^{-3} M solution of water in THF decomposes at approximately the same rate as the bis([8]annulene)thorium(IV) complex. The Italian research group reported that the organic products of the reaction of bis([8]annulene)cerium(IV) with isopropyl alcohol were 80 % cyclooctatetraene, and 20 % 1,3,5- and 1,3,6-cyclooctatriene.[9] This result suggests that there is a redox reaction occuring in this experiment in addition to the simple alcoholysis, which would be one explanation of the faster reaction of bis([8]annulene)cerium(IV) than the actinide(IV) complexes, since electron transfer reactions are faster than proton transfer reactions. Moore, however, has carefully repeated the Italian work and found that the only organic products of this reaction were the expected mixture of trienes in a 80 to 20 ratio of 1,3,5- to 1,3,6-cyclooctatriene.[40] Additional work by Moore shows that the hydrolysis of bis([8]annulene)cerium(IV) also gives a mixture of 1,3,5- and 1,3,6-cyclooctatrienes.[40]

A sample of bis([8]annulene)cerium(IV) was given to Dr. Fragalá for the determination of its photo electron spectra. The PES results are are shown in Figure 3.7 and are tabulated in Table 3.5.[41]

In Table 3.6, the results from the PES are compared with the predictions from the calculations of Rösch and Streitwieser. It is difficult to calculate total energies for molecules such as bis([8]annulene)cerium(IV). The relative energies of orbitals can, however, be calculated with reasonable accuracy. Table 3.6 shows only relative energy levels; the energy of the e_{2g} orbital is set as zero with the other orbital energy levels listed relative to the e_{2g}.

The agreement of experimental to calculated values is remarkable. The calculations of Rösch and Streitwieser correctly assigned the ordering of the e_2 ligand orbitals in bis([8]annulene)thorium(IV) and -uranium(IV). This same ordering, $e_{2g}(\pi) > e_{2u}(\pi)$, was predicted and observed for the bis([8]annulene)cerium(IV) compound. The calculations also indicated that the $e_{2g}(\pi)$-$e_{2u}(\pi)$ splitting in bis([8]annulene)cerium(IV) should be smaller than the splitting of those same orbitals in bis-([8]annulene)thorium(IV) or -uranium(IV). Again, this prediction is verified by the experiment, although experimentally, the relative energy differences for the $e_{2g}(\pi)$-$e_{2u}(\pi)$ orbitals in uranium(IV) and cerium(IV) complexes are quite similar. In every

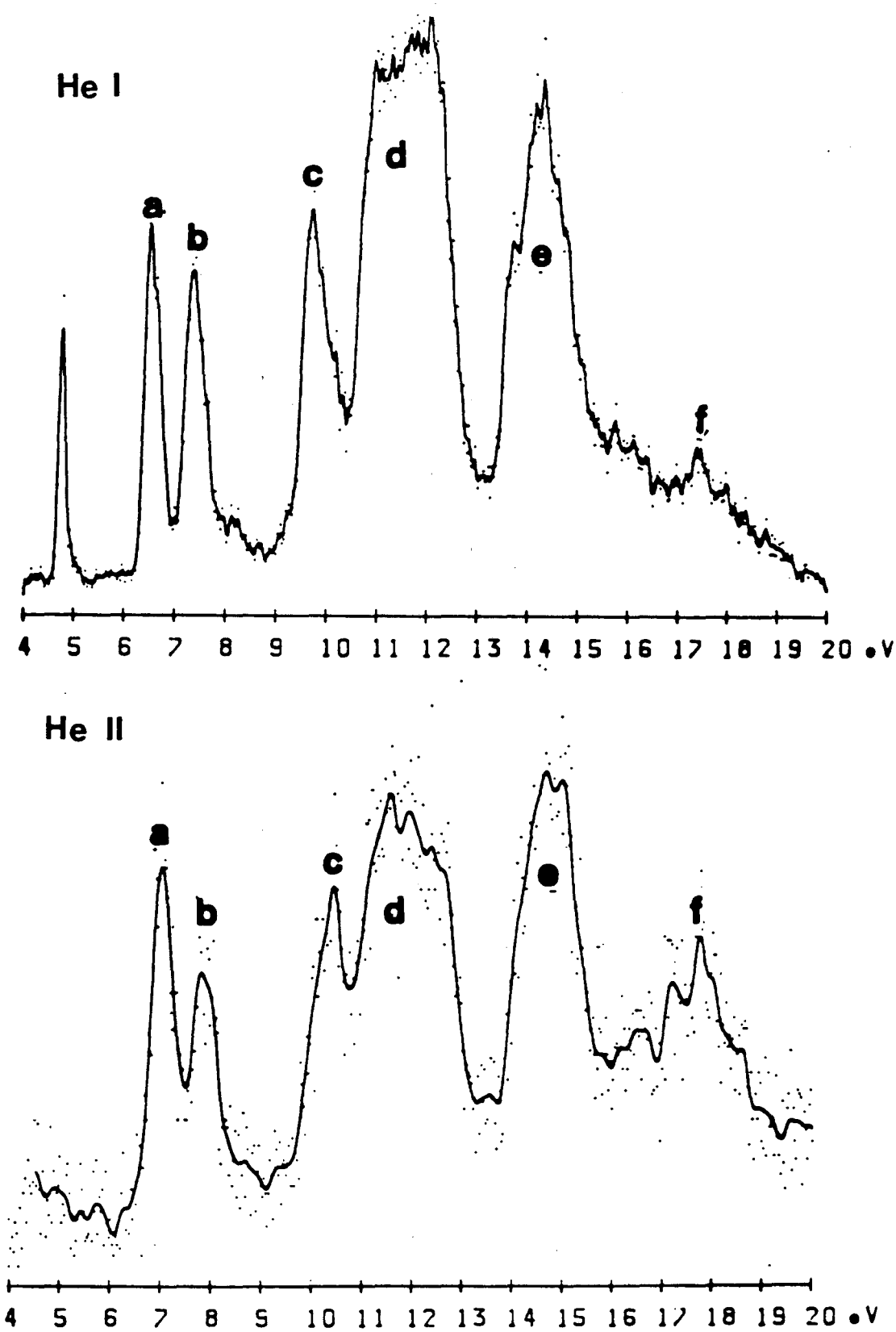

Figure 3.7: Photo-Electron Spectra of Bis([8]annulene)cerium(IV).

Table 3.5: Tabulated Data from the Photo-electron spectra of $Ce(C_8H_8)$.

band label	Ionization Energy (eV)	Assignment[a]
a	6.75	e_{2u}
a′	6.92	
b	7.68	e_{2g}
b′	7.81	
e	9.98	e_{1u}
e′	10.32	

(a) The band assignments are by Dr. Fragalà.

Table 3.6: Comparison of the calculated and measured ionization energy differences with respect to the ligand derived $e_{2u}(\pi)$ molecular orbital for $(C_8H_8)_2$ dimer (empty sandwich) and the series $M(C_8H_8)_2$, M = Ce, Th, U. Only the experimentally assigned peaks are shown.

Irred. rep.	$(C_8H_8)_2$	$Ce(C_8H_8)_2$		$Th(C_8H_8)_2$		$U(C_8H_8)_2$	
		calc.	exp.	calc.	exp	calc.	exp
$e_{3u}(f)$						-0.82	-0.70
$e_{2u}(\pi)$	0	0	0	0	0	0	0
$e_{2g}(\pi)$	0.62	0.89	0.90	0.98	1.12	0.71	0.95
$e_{1u}(\pi)$	4.16	3.11	3.15	2.91	3.11	2.86	3.05
$e_{1g}(\pi)$	3.62	3.53	3.50	3.58	3.86	3.37	3.66

instance, the calculations of Rösch and Streitwieser correctly predict the relative energies of the orbitals in bis([8]annulene)cerium(IV) as compared with the bis([8]annuene)actinide(IV) complexes. Although some of the closeness in fit of the calculated to experimental results for bis([8]annulene)cerium(IV) is undoubtedly fortuitous, the results clearly support the relativistic SCF-Xα methods for assigning the relative orbital energy levels in bis([8]annulene) complexes.

Further Studies on bis([8]annulene)cerium(IV)

The verification of the Italian work on bis([8]annulene)-cerium(IV) suggests many other studies involving cerium(IV) organometallics. One important study is the synthesis of other cerium(IV) organometallic complexes. Since it was generally believed that cerium(IV) complexes with π-anions could not exist, there is only one method contained in the literature for the synthesis of cerium(IV) organometallic methods, that of Greco, Cesca and Bertolini.[9] In addition to the synthesis of bis-([8]annulene)cerium(IV), these authors also reported the synthesis of $Cp_3Ce(O\text{-}i\text{-}C_3H_7)$ in low yield (4%) from the reaction of bis(cyclopentadienyl)magnesium(II) with cerium(IV) isopropoxide.[9] It is doubtful that any of the reports of cerium(IV) organometallic complexes from $(C_5H_5NH)_2CeCl_6$ are correct.

The Italian preparation of bis([8]annulene)cerium(IV) is not a general one. Since this method employs cyclooctatetraene as a solvent, the preparation of cerium(IV) complexes with substituted [8]annulene ligands is prohibitively expensive, both in man-hours and money. Many of the mono-alkyl-substituted cyclooctatetraenes are prepared from cyclooctatetraene (≈ $1/gram, BASF), typically in 40-70% yield.[42] With other [8]annulene ligand systems additional problems arise. For example, bis(1,3,5,7-tetramethyl-[8]annulene)cerium, because of its symmetry and potential comparisons with the known uranium(IV) analog, is a desirable derivative to obtain. Unfortunately, 1,3,5,7-tetramethylcyclooctatetraene is difficult to synthesize (see chapter 1) and a solid at room temperature. Clearly, an alternative synthesis to the Italian method is needed.

The chemical oxidation of the bis([8]annulene)cerate(III) anion is a potential method for the synthesis of bis([8]annulene)cerium(IV) complexes. The synthesis of cerium(IV) organometallic complexes by the oxidation of cerium(III) organometallic complexes is unprecedented. The are many methods for the oxidation of cerium(III) to cerium(IV). Some of the oxidizing agents employed in the cerium(III) oxidation include Ag^{2+},[43] MnO_4^-,[44] $S_2O_8^{2-}$,[45] $HO_2^{\cdot}$,[46] $NO_3^{\cdot}$,[47] BrO_3^-,[48] Cu^{3+},[49] and ClO_2^-.[50] All of this work is in aqueous medium, and most of the oxidations were carried out at a pH < 7. Bis([8]annulene)cerium(IV) and bis-([8]annulene)cerate(III) hydrolyze rapidly in water;

therefore, the oxidation of bis([8]annulene)cerium(III) anion in aqueous medium is not feasible.

One possible oxidizing agent, in addition to those listed above, for bis([8]annulene)cerium(IV) is the nitrosyl cation. Nitrosyl salts, such as the chloride, have been employed as oxidizing agents in a variety of systems.[51] Nitrosyl tetrafluoroborate is commercially available; the following reaction was envisioned for the oxidation of bis([8]annulene)-cerium(III) anion.

[3.11]

$$K[Ce(C_8H_8)]_2 + NOBF_4 \xrightarrow[THF]{} Ce(C_8H_8)_2 + KBF_4 + NO$$

An oxidation method, like the one shown above, should be applicable for the synthesis of any bis([8]annulene)cerium(IV) complex.

Results

Prior to the attempts to oxidize the bis([8]annulene)-cerate(III) anion, a very simple "test-tube" experiment was carried out. A solution of bis([8]annulene)cerate(III) in THF was briefly exposed to air. The solution turned brown and had an absorbance in it visible spectrum that corresponded to that of the bis([8]annulene)cerium(IV) complex. This result suggested that the oxidation of cerium(III) complexes is feasible.

The first step toward the synthesis of bis([8]annulene)-cerate(IV) was an improvement in the synthesis of bis([8]annulene)cerate(III) anion. The literature method[2] is by the addition of a suspension of lanthanide trichloride in THF to a solution of 1.5 equivalents of [8]annulene dianion and 0.5 equivalents of cyclooctatetraene in THF. The removal of solvent left a green powder which was purified by Soxhlet extraction with THF. The yield by this method was 51.2%. The major drawback in this method is that the lanthanide trichloride is added to the reducing solution of the dianion. The bis([8]annulene)ytterbate(III) anion could not be made by this method; presumably due to the reduction of the ytterbium(III) by the dianion.[2]

A superior method is the dropwise addition of the dianion solution to the suspension of lanthanide trichloride. In this manner of addition, the lanthanide trichloride is never exposed to an excess of the reducing dianion. The effect of this is clearly seen in the successful synthesis of bis([8]annulene)-ytterbate(III) anion. By this method, bis([8]annulene)ytterbate(III) was synthesized in greater than 40% yield. The yield of bis([8]annulene)cerate(III) by this method was 63%.

The dropwise addition of the dianion solution to the suspension of lanthanide trichloride indicates how rapidly the reaction

occurs. As the dianion solution is added to the suspension of lanthanide chloride, the solution changed color, pale yellow-green for Ce or robin's egg blue for Yb. After approximately one-third of the dianion solution was added there was an immediate color change, which corresponds to the color of the respective bis([8]annulene)lanthanate(III) complex. The addition method is essentially a titration; the dianion reacts immediately with the lanthanide trichloride, probably to form the intermediate mono-ring complex (for cerium, the mono-ring complex is yellow-green), which subsequently reacts with more [8]annulene dianion to form the bis(complex. The abrupt color change occurs at the time in the reaction when the concentration of the mono-ring sandwich is sufficient to compete with unreacted lanthanide trichloride for the [8]annulene dianion.

The chemical oxidation of bis([8]annulene)cerate(III) anion was accomplished by the addition of nitrosyl tetrafluoroborate to a solution of the sandwich anion in THF. The best isolated yield at this time is only 3%. In a series of simple experiments, where an oxidizing agent was added to a THF solution of bis([8]annulene)cerate(III) in a glass cuvette and the formation of bis([8]annulene)cerium(IV) was monitored by visible spectroscopy, benzoyl peroxide,[52] peroxidisulfate,[52] bromine, and ceric ammonium nitrate were tested as potential oxidizing agents. Bis([8]annulene)cerium(IV) was not detected in any of these

experiments, but the oxidizing agent did decompose the bis-([8]annulene)cerate(III) anion in every case.

One problem in the oxidation reaction is the possibility of further oxidation by the oxidizing agent. For example, the reduced product from the nitrosyl cation oxidation reaction is nitric oxide, which is itself an oxidizing agent. Another example is the oxidation of bis([8]annulene)cerate(III) anion with oxygen; in this reaction, the first reduced product is presumably potassium oxide, which is, again, an oxidizing agent. In order to determine the stoichiometry of the reaction of bis([8]annulene)-cerate(III) with nitrosyl tetrafluoroborate, an experiment was carried out using one-half equivalents of oxidizing agent to one equivalent of sandwich complex. After completion of the reaction, only 20% of starting material remained. This experiment shows that nitrosyl tetrafluoroborate functions as at least a two-step oxidizing agent.

Rigsbee[53] has recently measured the Ce(IV)/Ce(III) couple in THF for the bis([8]annulene) sandwich complexes and found that the value of the reduction couple is -1.3 ± .1 V. This result indicates significant stablilization of the tetravalent state of cerium by complexation with two [8]annulene rings. The cyclic-voltametry work by Rigsbee indicates that the oxidizing agents used thus far are too strong, so that the [8]annulene complex is decomposed. In the examples where no bis([8]annulene)cerium(IV)

was observed, the oxidizing agent was a two electron oxidizing agent. The negative value of the Ce(IV)/Ce(III) couple suggests that weaker, one electron, oxidizing agents should be used for the oxidation of bis([8]annulene)cerate(III) to bis([8]annulene)-cerium(IV).

Electron Exchange in the Bis([8]annulene)cerium(III)/(IV) System

Since the electron exchange reaction between bis([8]annulene)-ytterbate(III) anion and bis([8]annulene)ytterbate(II) dianion was known, it was postulated that the same type of reaction would occur between bis([8]annulene)cerium(IV) and bis([8]annulene)-cerium(III) (3.15).

$$Ce(C_8H_8)_2 \underset{-e^-}{\overset{+e^-}{\rightleftharpoons}} [Ce(C_8H_8)_2]^- \qquad [3.15]$$

In THF-*d8*, bis([8]annulene)cerium(IV) exhibits a sharp signal at 5.9 ppm which can be assigned as the ring proton resonance. For the bis([8]annulene)cerate(III) complex, no resonance can be found that can be attributed to the ring protons. When the solutions of bis([8]annulene)cerate(III) and -cerium(IV) were mixed, a broad resonance was observed which was shifted upfield relative to the position of the resonance for bis([8]annulene)cerium(IV). As this solution was cooled, the peak broadens such that at -70° C, the peak was no longer detectable. Through the course of the reaction, no peak was observed at 5.9 ppm.

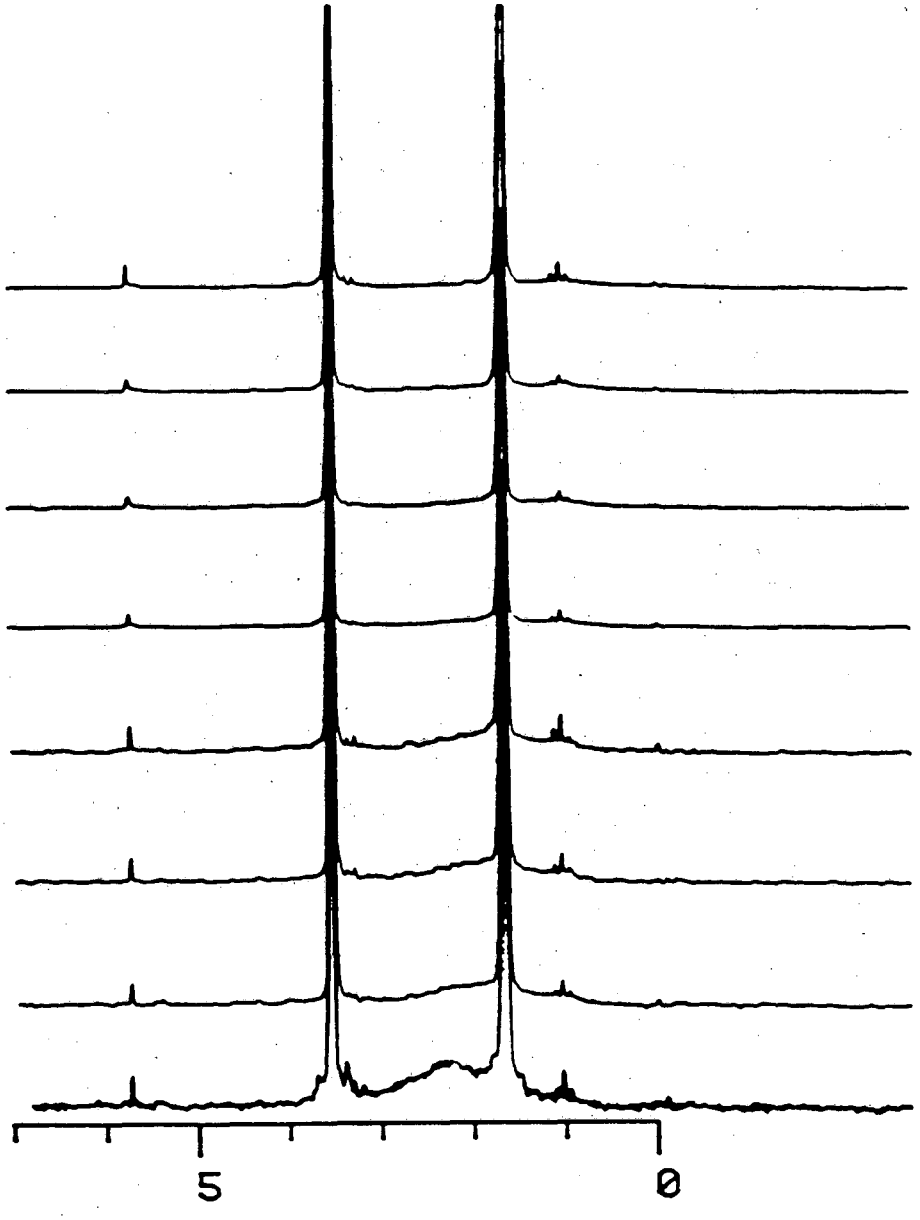

Figure 3.8: ^{1}H-NMR of Bis([8]annulene)cerate(III) and -cerium(IV)
T = -70 - 30°C

At this time, no further NMR experiments on the bis([8]annulene)cerate(III)/(IV) system have been attempted, but it is postulated from the behavior of the mixed system experiment described above, that electron exchange similar to that seen in the ytterbium(II)/ytterbium(III) system is occuring between bis-([8]annulene)cerate(III) and -cerium(IV). However, in the cerium system, the exchange is never slow enough such that a resonance is observed for the diamagnetic species. This does not imply that the electron exchange in the bis([8]annulene)cerium(III)/(IV) system is occuring at a faster rate. If the ring proton resonances (which is not observed for $[Ce(C_8H_8)_2]^-$) for the diamagnetic and paramagnetic species are, for example, 20 ppm apart, then the rate of reaction at coalescence would be $\approx 10^4$ $moles^{-1}s^{-1}$ (from equation 2.19). It is possible, therefore, that the bis([8]annulene)cerium(III)/(IV) system cannot be cooled to a low enough temperature to observe coalescence. The study of the electron exchange in bis([8]annulene) systems is clearly a candidate for future research.

Experimental

Preparation of $(C_5H_6N)_2CeCl_6$. Hydrogen chloride gas was added to an ice-cooled suspension of 8.32 g (40.0 mmol) of $Ce(OH)_4$ in 250 mL of absolute ethanol until the solution was saturated with HCL gas. The suspension was stirred over the next 20 hrs to allow the reaction to occur. Over this time, the yellow suspension was replaced with an orange solution. At the end of 20 hrs, the solution was filtered and 7.30 mL (90.6 mmol) of pyridine (dried over Sieves 3Å) was carefully added. The addition of pyridine caused a vigorous reaction and the precipitation of a yellow solid. Hydrogen chloride gas was then bubbled through the solution until no more yellow solid precipitated. The bright yellow solid was collected by suction filtration and dried, *in vacuo*, at 120 °C for three hours. The yield of the yellow powder was 16.6 g (80.1 % based on $Ce(OH)_4$. Anal. Calcd. for $C_{10}H_{12}N_2CeCl_6$: C, 23.41; H, 2.36; N, 5.46; Cl, 41.46. Found: C, 23.50; H, 2.43; N, 5.43; Cl, 42.46.

* Preparation of $Ce(O\text{-}i\text{-}C_3H_7)_4 \cdot i\text{-}C_3H_7OH$. To a solution of 0.42 g of $(C_5H_6N)_2CeCl_6$ (0.8 mmol) in 50 mL of benzene was added 0.13 mL of anhydrous 2-propanol. Anhydrous ammonia gas was bubbled into this solution causing a white precipitate to appear (this ppt. is NH_4Cl). The solution was filtered and the removal of the solvent from the yellow filtrate left a yellow powder. This powder was crystallized from anhydrous 2-propanol by cooling a saturated

room temperature solution to 0 °C in a refrigerator. The crystals were collected on a Schlenk filter. The analysis and NMR of this complex indicated that some Ce was present in the trivalent state (the proton resonances of the alkoxy moiety were broadened) and that there was some pyriding present in the complex. Yield of yellow crystals 0.9 g (30 %). Anal. Calcd. for $C_{15}H_{36}O_5Ce$: C, 41.27; H, 8.31. Found: C, 42.21; H, 7.84; N, 1.15.

* Preparation of $Ce(C_8H_8)_2$: Method A. Anhydrous, degassed C_8H_8 (5 mL) was added via syringe to 0.49 (1.1 mmol) of $Ce(O\text{-}i\text{-}C_3H_7)_4 \cdot i\text{-}C_3H_7OH$ in a 25 mL round-bottom flask equiped with a condensor, septum and argon inlet in the three ₹-14/20 necks. To the stirring yellow solution was added 2.3 mL of 25 % $Al(C_2H_5)_3$ in toluene. After the addition of the triethylaluminum, the septum was replaced with a stopper. The reaction vessel was then heated over a two hour period to 140 °C and held at this temperature for one hour. The solution turned very dark brown over this time. After one hour, the solution was allowed to cool to room temperature over a period of three hours. When the solution had cooled, the stopper was replaced with a Schlenk filter and the solution was filtered. Black needles were collected on the glass frit. The crystals were washed with 30 mL of hexane. The yield of crystals was 0.15 g (38.5 % based on the cerium alkoxide). ^{1}H-NMR: toluene-*d8*, 5.75 (s); tetrahydrofuran-*d8*, 5.90 (s). UV-Vis: λmax = 471 nm, ε = 7900 ± 400. Mass spec. (listed as *m/z*, relative abundance): 348, 1.6 {$Ce(C_8H_8)_2$}; 244, 27.6

{$Ce(C_8H_8)$}; 242, 3.4; 218, 2.2; 207, 3.0; 205, 3.1, 104, 9.2. Infrared (nujol mull; major peaks in range 600-1000 cm^{-1}): 688, vs; 740, m; 785, w; 897, s. Anal. Calcd. for $C_{16}H_{16}Ce$: C, 55.15; H, 4.63. Found: C, 53.32; H, 4.84.

* Preparation of $Ce(C_8H_8)_2$: Method B. Potassium bis([8]annulene)-cerium(III) (0.77 g 2.0 mmol) was dissolved in 200 mL of dry, degassed THF in a 500 mL rb Schlenk flask. The solution was then cooled in a -78°C Dry Ice/2-propanol bath. To the bright green solution was added, under argon purge, 0.21 g (1.8 mmol) of $NOBF_4$, which had been weighed into a Schlenk addition flask in an argon atmosphere glovebox. Over the next three minutes, the reaction mixture began to turn brown. The cold temperature bath was then removed and over the next 5 minutes, the reaction mixture turned dark brown. After fifteen minutes, the solent was removed, *in vacuo*, leaving 0.80 g of a brown, pyrophoric powder. This powder was extracted with toluene in a Soxhlet extractor giving a dark brown solution of toluene. The removal of solvent from this solution gave 0.03 ± .01 g of a black powder. ^{1}H-NMR: toluene-*d8*, 5.75 (s); exposure of this solution to air decolorized the solution and ^{1}H-NMR of the quenched material gave a singlet at 5.61 ppm, which is the chemical shift for cyclooctatetraene in toluene-*d8*. IR: (nujol mull, absorbances between 600-1000 cm^{-1}) 687, 740, 769, 782, 896.

Reaction of $K[Ce(C_8H_8)_2]$ with 1/2 eq. $NOBF_4$. A reaction identical to the previous reaction was carried by adding 0.13 g (1.1 mmol) of $NOBF_4$ to a room-temperature THF solution of 0.85 g (2.2 mmol) of $K[Ce(C_8H_8)_2]$. Removal of the solvent from this reaction mixture left 0.85 g of a brown-green powder. This powder was extracted with toluene. The powder and extraction thimble were placed in THF and hot filtered (60°C). The removal of solvent from the green filtrate left 0.15 g of $K[Ce(C_8H_8)_2]$, which was identified by infrared spectra.

* Preparation of $K[Ce(C_8H_8)_2]$. Anhydrous THF (70 mL) was added to a 250 mL round-bottom Schlenk flask which contained 0.63 g (16.2 mmol) of potassium metal which had been cut and weighed in a glovebox. The flask was then warmed with a water bath and stirred when the potassium metal melted (63 °C) thus creating small beads of potassium metal. When the beads formed, stirring was stopped and the flask was immediately placed in a room temperature water bath to keep the beads from melting together. When the THF had cooled to room temperature, 0.85 g (8.16. mmol) of cyclooctatetraene was added to the flask via syringe. The reaction of the potassium metal took three hours, the completion of the reaction indicated by the disappearance of the potassium metal. The now dark brown THF solution of dianion was added dropwise, by cannula, to a suspension of 1.00 g (4.1 mmol) of anhydrous $CeCl_3$ in 30 mL of anhydrous, degassed THF in a 500 mL round-bottom Schlenk flask. After ≈ one-third of the dianion solution was added, a

lime green color appeared in the reaction flask. After all the dianion solution was added (ca. 20 min), the suspension was heated to 60 °C and filtered, to give a dark green filtrate, leaving a lime green powder behind in the flask. The dark green filtrate was placed in a -78 °C refrigerator and overnight, large green crystals formed at the bottom of the solution. The solvent was filtered from these crystals at -78 °C and the crystals were then allowed to warm to room temperature. As the crystals warmed they fell apart to give a lime green powder. The powder was washed three times with 50 mL hexane and heated with a heat gun to insure the removal of all traces of solvent. The yield of this powder was 0.64 g. A second crop of crystals was grown by cooling the filtrate and hexane wash from the first crop to -78 °C. The yield of crystals from the second crop was 0.10 g. Overall yield was 0.74 g (47% based on $CeCl_3$).

In a similar experiment, 2.98 g of cyclooctatetraene, 2.23 g of potassium and 3.52 g of $CeCl_3$ were reacted by the procedure described above. At the end of the reaction, the solvent was removed, *in vacuo*, and the crude, brown-green powder was Soxhlet extracted with THF to give 3.47 g (62.7%) of the cerium(III) sandwich complex.

In both of the purification methods (crystallization or extraction) the bright green powder obtained was heated at 200°C, *in vacuo*, for ≈30 min to remove all traces of solvent.

The infrared spectra of these powders indicated that they contained no THF. Infrared (only the region 600-1000 cm^{-1} listed): 675 vs, 739 m, 775 w, 890 s. UV-Vis: λmax(THF) 690 nm. Anal. Successful analysis of the unsolvated cerium complex (as shown by the absence of THF absorbances in the infrared region) proved to be impossible. Calcd. for $C_{16}H_{16}KCe$: C, 49.59; H, 4.16. Found: C, 40.47; H, 3.81.

$K[Ce(C_8H_8)_2]$ can be crystallized from diglyme as its diglyme adduct. Analysis of $[K(diglyme)][Ce(C_8H_8)_2]$ was better, but still unsatisfactory. Anal. Calcd. for $C_{22}H_{30})_3KCe$: C, 50.65; H, 5.80; K, 7.49. Found: C, 48.02; H, 5.98; K, 9.15.

* Preparation of $K_2(C_8H_8)\cdot(C_4H_{10}O_2)_2$. Degassed, anhydrous C_8H_8 (0.49 g, 4.7 mmol) was added via syringe to a dispersion of 0.37 g (9.4 mmol) of potassium metal in 70 mL of anhydrous, degassed THF in a Schlenk tube. The reaction began immediately,

but took ca. two hours to go to completion (as indicated by the disappearence of the potassium). The solution was Schlenk filtered, and the solvent was removed from the filtrate, *in vacuo*. The pale purple solid obtained was dissolved in boiling, anhydrous, degassed DME and the resulting solution was filtered. The filtrate was allowed to cool to room temperature and then was place in a refrigerator overnight. The solution was filtered leaving large, clear, white crystals with a faint purple color. The purple color was removed by washing the crystals three times with pentane (note that the first pentane wash had a purple color). The yield of the white crystals was 0.75 g (44 %) Anal. Calcd for $C_{16}H_{28}O_4K_2$: C, 53.00; H, 7.78. Found: C, 52.91; H, 7.55. Potassium analysis was attempted on this complex, but it was not successful: Calcd. K, 21.56. Found: K, 28.5.

References and Notes

1. For example see: Streitwieser, A. Jr.; Klutz, R.Q.; Smith, K.A.; Luke, W.D. *Organometallics* 1982, *2*, 1873. and Raymond, K.N.; Eigenbrot, C.W. *Acc. Chem. Res.* 1980, *13*, 276.

2. Hodson, K.O.; Mares, F.; Starks, D.F.; Streitwieser, A., Jr. *J. Am. Chem. Soc.* 1973, *95*, 8650.

3. Cotton, F.A.; Wilkinson, G. "Advanced Inorganic Chemistry," 4th Ed., Wiley & Sons, New York, 1980, chapter 23.

4. Huheey, J. "Inorganic Chemistry," 2nd Ed., Harper and Row, Pub., New York, 1978, chapter 16.

5. Le Vanda, C.; Streitwieser, A., Jr. *Inorg. Chem.* 1981, *20*, 656.

6. a) Rösch, N.; Streitwieser, A., Jr. *J. Am. Chem. Soc.* 1983, *105*, 7237. b) Rösch, N. *Inorg. Chim. Acta* 1984, *94*, 297.

7. a) Clark, J.P.; Green, J.C. *J. Organometal. Chem.* 1976, *112*, C14. Clark, J.P.; Green, J.C. *J. Chem. Soc. Dalton Trans.* 1977, 505. b) Fragalà, I.; Condorelli, G.; Zanella, P.; Tondello, E. *J. Organometal. Chem.* 1976, *122*, 357.

8. Kalsotra, B.L.; Multani, R.K.; Jain, B.D. *Chem. Ind. [London]* 1972, 339.

9. Greco, A.; Cesca, S.; Bertolini, G. *J. Organometal. Chem.* 1976, *113*, 321.

10. Varga, L.P.; Asprey, L.B. *J. Chem. Phys.* 1968, *48*, 139.

11. Varga, L.P.; Asprey, L.B. *J. Chem. Phys.* 1968, *49*, 4674.

12. Johnson, D.A. *Adv. Inorg. Radiochem.* 1977, *20*, 1.

13. Johnson, E.C.; Callahan, R.W.; Eckberg, R.P.; Hatfield, W.E.; Meyer, T.J. *Inorg. Chem.* 1979, *18*, 618.

14. Michaille, P.; Kikindai, T. *J. Inorg. Nucl. Chem.* 1977, *39*, 493.

15. Dikshitulu, L.S.A.; Vani, P.; Hanumantha Rao, V. *J. Inorg. Nucl. Chem.* 1981, *43*, 1261.

16. Smith, F.R.; Getz, C.A. *Ind. Eng. Chem. Anal. Ed.* 1938, *10*, 191, from ref. 12.

17. Sherril, M.S.; King, C.B.; Spooner, R.C. *J. Am. Chem. Soc.* 1943, *65*, 170.

18. Noyes, A.A.; Garner, C.S. *J. Am. Chem. Soc.* 1936, *58*, 1265.

19. Kunz, A.H. *J. Am. Chem. Soc.* 1931, *53*, 98.

20. Rao, G.P.; Murthy, A.R.V. *J.Phys. Chem.* 1964, *68*, 1573.

21. Sofen, S.R.; Cooper, S.R.; Raymond, K.N. *Inorg. Chem.* 1979, *18*, 1611.

22. DeKock, C.W.; Ely, S.R.; Hopkins, T.E.; Brault, M.A. *Inorg. Chem.* 1978, *17*, 625.

23. Starks, D.F.; Streitwieser, A., Jr.; *J. Am. Chem. Soc.* 1973, 95, 3423.

24. Bradley, D.C.; Chatterjee, A.K.; Wardlaw, W. *J. Chem. Soc.* 1956, 2260.

25. Bagnall, K.W. *NATO Advan. Study Inst. C* 1979, *44*, 221.

26. Kalsotra, B.L.; Anand, S.P.; Multani, R.K.; Jain, B.D. *J. Organometal. Chem.* 1971, *28*, 87.

27. Kalsotra, B.L.; Multani, R.K.; Jain, B.D. *Isreal J. Chem.* 1971, *9*, 569. Kalsotra, B.L.; Multani, R.K.; Jain, B.D. *J. Chinese Chem. Soc. [Taipei]* 1971, *18*, 189. Kalsotra, B.L.; Multani, R.K.; Jain, B.D. *J. Inorg. Nucl. Chem.* 1972, *34*, 2265. Kalsotra, B.L.; Multani, R.K.; Jain, B.D. *J. Inorg. Nucl. Chem.* 1973, *35*, 311. Kapur, S.; Kalsotra, B.L.; Multani, R.K.; Jain, B.D. *J. Inorg. Nucl. Chem.* 1973, *35*, 1689. Kapur, S.; Kalsotra, B.L.; Multani, R.K. *J. Inorg. Nucl. Chem.* 1973, *35*, 3966. Kapur, S.; Multani, R.K. *J. Organometal. Chem.* 1973, *63*, 301. Kapur, S.; Kalsotra, B.L.; Multani, R.K. *J. Inorg. Nucl. Chem.* 1974, *36*, 932. Kapur, S.; Kalsotra, B.L.; Multani, R.K. *J. Chinese Chem. Soc. [Taipei]* 1972, *19*, 197.

28. Kalsotra, B.L.; Multani, R.K.; Jain, B.D. *Current Sci. [India]* 1972, *41*, 155. Kalsotra, B.L.; Multani, R.K.; Jain, B.D. *Inorg. Nucl. Chem.* 1972, *34*, 2679.

29. Kalsotra, B.L.; Mulatani, R.K.; Jain, B.D. *J. Organometal. Chem.* 1971, *31*, 67.

30. Deacon, G.B.; Tuong, T.D.; Vince, D.G. *Polyhedron* 1983, *2*, 969.

31. Birmingham, J.M.; Wilkinson, G. *J. Am. Chem. Soc.* 1956, *78*, 42.

32. Breil, H.; Wilke, G. *Angew. Chem.* 1966, *78*, 942; *Angew. Chem. Int. Ed. Eng.* 1966, *4*, 898.

33. Starks, D.F.; Parsons, T.C.; Streitwieser, A., Jr.; Edelstein, N. *Inorg. Chem.* 1974, *13*, 1307.

34. Karraker, D.G.; Stone, J.A.; Jones, E.R., Jr.; Edelstein, N. *J. Am. Chem. Soc.* 1970, *92*, 4841.

35. Hocks, L.; Goffart, J.; Duyckaerts, G.; Teyssie, P. *Spectrochim. Acta* 1974, *30A*, 907.

36. Agafonov, I.L.; Shushunov, N.F.; Gaivoronskii, P.E.; Spirina, T.L.; Leonov, M.R.; Il'yushchenkov, V.A.; Solov'eva, G.V.; Gramoteeva, N.I. *Radiokhimiya* 1981, *23*, 62.

37. a)Dierks, H.; Dietrich, H. *Angew. Chem.* 1966, *78*, 943; *Angew. Chem. Int. Ed. Eng.* 1966, *4*, 899. b) Dietrich, H.; Soltwisch, M. *Angew. Chem. Int. Ed. Eng.* 1969, *8*, 765.

38. Brauer, D.J.; Krüger, C. *J. Organometal. Chem.* 1972, *42*, 129.

39. Lyttle, M.H. *Doctoral Thesis* University of California, 1983.

40. Moore, R.M., unpublished results.

41. Fragalá, I.; Ciliberto, B.; Rösch, N., Streitwieser, A., Jr.; Kinsley, S.A.; manuscript in preparation.

42. Miller, J.T.; DeKock, C.W.; Brault, M.A. *J. Org. Chem.* 1979, *44*, 3508.

43. a) Gonzalez-Perez, G. *Acta Salmanticensia Cienc.* 1973, *45*, 135, taken from *Chem. Abst.* 1974, *80*, 152423e. b) Erin, E.A.; Kipytov, V.V.; Vityutuev, V.M. *Radiokhimiya* 1976, *18*, 514, taken from *Chem. Abst.* 1976, *85*, 186130a.

44. Rao, G.G.; Naidu, P.P. *Z. Anal. Chem.* 1964, *206*, 360.

45. Fronaeus, S.; Ostman, C.O. *Acta Chem. Scand.* 1955, *9*, 902.

46. Samuni, A.; Czapski, G. *Israel J. Chem.* 1970, *8*, 551.

47. Martin, T.W.; Glass, R.W. *J. Am. Chem. Soc.* 1970, *92*, 5075.

48. Yoshida, H.; Nagai, H,; Onishi, H. *Bunseki Kagaku* 1966, *15*, 513, taken from *Chem. Abst.* 1966, *65*, 12916d.

49. Bisi, C.; Clerici, A. *Gazz. Chim. Ital.* 1963, *93*, 1438, taken from *Chem. Abst.* 1964, *60*, 11586a.

50. Rybka, J.S.; Kurtz, J.L.; Neubecker, T.A.; Margerum, D.W. *Inorg. Chem.* 1980, *19*, 2791.

51. For a review article entitled "Nitrosonium Salts in Inorganic Synthesis" see: Mocella, M.T.; Okamoto, M.S.; Barefield, E.K. *Syn. React. Inorg. Metal-Org. Chem.* 1974, *4*, 69.

52. Experiment performed by John Rigsbee.

53. Rigsbee, J.; Moran, K., unpublished results.

CHAPTER FOUR

Vibrational Spectra of Bis-[8]annulene Complexes

Introduction

Although the determination of a molecule's structure from vibrational spectra (Raman and infrared) is difficult and truly feasible only for simple molecules, information on a molecule's structure and bonding can be obtained from careful interpretation of vibrational spectra. For example, Lippincott[1] correctly assigned the structure of ferrocene as a D_{5d} sandwich complex from the analysis of the Raman and infrared spectra of $Fe(C_5H_5)_2$ and $Fe(C_5D_5)_2$.

The assignment of spectra by normal coordinate analysis[2] has never been reported for the 8-fold symmetric lanthanide and actinide sandwich complexes; this type of analysis is difficult and tedious for a molecule with as many atoms as bis([8]annulene)uranium(IV). Although not assigned by normal coordinate analysis, the vibrational spectra of bis([8]annulene)thorium(IV) has been assigned in two different studies.[3,4] The method used

for these assignments was the comparison of the vibrational spectra of the [8]annulene complex with the assigned vibrational spectra of other sandwich complexes involving planar hydrocarbon ligands (e.g. ferrocene[1] and bis(benzene)chromium(0)[5]). Shown in Table 4.1 is the vibrational spectra of bis([8]annulene)-thorium(IV) and the assignments reported.

Inspection of Table 4.1 reveals that the major differences in the assignments in the two reports are the assignment of a very strong infrared absorption at 695 cm^{-1} and a strong infrared absorption at 744 cm^{-1}. Goffart *et al.*[3] assign the former as a ring-metal tilt (E_{1u}) and the latter as the out-of-plane hydrogen bending (ρ(CH),A_{2u}), whereas Aleksanyan *et al.*[4] assign the former as the out-of-plane hydrogen bending (ρ(CH),A_{2u}) and the latter as the ring-carbon stretching (ν(CC),A_{2u}). The assignment of the band at ≈695 cm^{-1} as an out of plane ring-hydrogen bending is consistent with an earlier assignment.[6]

The assignment by Goffart [3] has been used to determine information on the ring-metal bond in ([8]annulene)actinide complexes. Since the very strong infrared vibration of dipotassium [8]annulene dianion at 675 cm^{-1} is assigned as ρ(CH),A_{2u} Goffart *et al.* interpret the shift of this vibration to ≈740 cm^{-1} in bis-([8]annulene)thorium(IV) and -uranium(IV) as indicative of covalent bonding; in their words, "the normal 'out of plane' vibrations are more difficult when metal orbitals interact with

Table 4.1: Vibrational Spectrum of Bis([8]annulene)thorium(IV) (from reference 4).

$Th(C_8H_8)_2$ (cm^{-1}) (only assigned bands shown)		Assignment	
Infrared	Raman	ref 3.	ref.4
250 vs	242 s	$\nu(M-L)_{as}$	
	391 m		$\gamma(CCC)E_{2g}$
695 vs		$\nu(M-L)_{tilt}E_{1u}$	$\rho(CH)A_{2u}$
742 s	726 w	$\rho(CH)$ } A_{2u},E_{1u}	$\rho(CH)E_{2u},E_{1g}$
775 s	775 s	$\rho(CH)$	$\nu(CC)A_{2u},A_{1g}$
895 s	901 vw	$\beta(CH)E_{1u}$	$\beta(CH)E_{1u},E_{1g}$
1315 m	1320 vw	$\nu(CC)A_{2u},E_{1u}$	$\nu(CC)E_{1u},E_{1g}$
	1505 w		$\nu(CC)E_{2g}$
2920 m	2928 vw	$\nu(CH)$	
	2982 w	} A_{2u},E_{1u}	$\nu(CH)E_{2g}$
3005 m		$\nu(CH)$	$\nu(CH)E_{1u},E_{1g}$
	3022		$\nu(CH)A_{2u},A_{1g}$

vw=very weak; w=weak; m=medium; s=strong; vs=very strong

ring orbitals." It is clear that the correct assignment of the infrared spectra of bis([8]annulene) complexes in the 600-900 cm^{-1} is important, since, if Aleksanyan *et al.* are correct, a shift of the $\rho(CH),A_{2u}$ from 675 cm^{-1} to 695 cm^{-1} is less dramatic and more easily rationalized without invoking arguements involving ring-metal orbital overlap.

As shown in Chapter Two, the infrared spectra of $K_2[Yb(C_8H_8)_2]$ and $K_2[Ca(C_8H_8)_2]$ suggest that the assignment by Aleksanyan is consistent with the spectra of [8]annulene complexes and also indicates that the assignment by Goffart *et al* is incorrect. Following is an interpretation of the infrared spectra in the 600-1000 cm^{-1} region for [8]annulene complexes, by a method which is similar to the method used by Aleksanyan for the assignment of the vibrational spectra of bis([8]annulene)thorium(IV) and bis-([8]annulene)lanthanate(III) anion. This method illustrates that similarities should be observed in the infrared spectra of [8]annulene dianion complexes.

Vibrational Modes of [8]annulene Complexes

The method of determining the normal vibrations for a molecule from group theory is outlined in textbooks[2,7] and will not be presented here. Given in Table 4.2 are the Mulliken symbols[8] for the irreducible representations for the infrared and Raman allowed vibrational modes for a series of [8]annulene complexes

Table 4.2: Infrared and Raman allowed vibrational modes for [8]annulene complexes.

Complex	$M_2C_8H_8$	MC_8H_8	$M(C_8H_8)_2$	$M'[M(C_8H_8)_2]$	$M_2'[M(C_8H_8)_2]$
Sym.	(D_{8h})	(C_{8v})	(D_{8h})	(C_{8v})	(D_{8h})
Γ_{Raman}	$3\ A_{1g}$	$4\ A_1$	$4\ A_{1g}$	$8\ A_1$	$5\ A_{1g}$
	$2\ E_{1g}$	$5\ E_1$	$5\ E_{1g}$	$12\ E_1$	$5\ E_{1g}$
	$4\ E_{2g}$	$6\ E_2$	$6\ E_{2g}$	$12\ E_2$	$6\ E_{2g}$
Γ_{IR}	$2\ A_{2u}$	$4\ A_1$	$4\ A_{2u}$	$8\ A_1$	$5\ A_{2u}$
	$4\ E_{1u}$	$5\ E_1$	$6\ E_{1u}$	$12\ E_1$	$7\ E_{1u}$

$M_2C_8H_8$ (D_{8h}), MC_8H_8 (C_{8v}), $M(C_8H_8)_2$ (D_{8h}), $M'[M(C_8H_8)_2]$ (C_{8v}) and $M_2'[M(C_8H_8)_2]$ (D_{8h}). It should be noted here that the character tables[9] used in this study differ from the character tables used previously, specifically in the labelling of the B_1 and B_2 representations. Inspection of the D_{8h} and C_{8v} character tables shows that this difference has no effect on the assignment of the vibrational spectra, since the B_1 and B_2 modes are neither Raman nor infrared active.

In order to assign the "ligand only" vibrational modes for the [8]annulene complexes, the following manipulations are performed. First, the vibrational modes for a "free" [8]annulene dianion are determined. In Table 4.3, the active normal vibrational modes and their assigments are given for "free" [8]annulene dianion.

Table 4.3: Infrared and Raman Correlation Chart for "free" [8]annulene dianion (D_{8h}).[a] complexes.

frequency	Assignment	
3011 s	A_{1g}+	ν(CH)
737 s	A_{1g}+	ν(CC)
710 w	E_{1g}+	ρ(CH)
2979 m	E_{2g}+	ν(CH)
1492 m	E_{2g}+	ν(CC)
not found	E_{2g}+	β(CH)
343 m	E_{2g}+	γ(CCC)
675 vs	A_{2u}‡	ρ(CH)
2994 s	E_{1u}‡	ν(CH)
1295 w	E_{1u}‡	ν(CC)
880 s	E_{1u}‡	β(CH)
inactive	E_{2u}	ρ(CH)
inactive	E_{2u}	χ(CCC)

a) from ref. 4. vs=very strong; s=strong; m=medium; w=weak.
+=Raman active. ‡=Infrared active.

The assignment of the infrared and raman bands is consistent with the assignments in other planar, cyclic hydrocarbons.[4,10] The normal vibrational modes for the free [8]annulene differ from $K_2C_8H_8$ by A_{1g}, E_{1g}, A_{2u}, and E_{1u}. Accordingly, these vibrations can be assigned as vibrations that involve displacement of the entire ring relative to the metal atoms.[4,10] The ring-metal vibrations can be viewed as not involving the vibrations or bending of the ligand CH or CC bonds.[10]

To determine the assignment of the ligand only vibrations for the other types of [8]annulene complexes, one needs only to consider the effects of changes in symmetry and/or presence of a second [8]annulene ligand in a sandwich type arrangement.

First, consider the changes in the vibrational modes of a "free" [8]annulene in a C_{8v} environment. Removal of the eight perpendicular C_2 axes and inversion center from the D_{8h} point group results in the loss of the classification of gerade or ungerade. For example, the A_{2u} and A_{1g} representations in the D_{8h} point group are both A_1 in the C_{8v} point group. This idea is easily illustrated by the consideration of a p-type orbital. In the D_{8h} point group, the p_z orbital is symmetric with respect to rotation by $2\pi/n$ about the principal axis (A), anti-symmetric about a perpendicular C_2 axis (2) and is anti-symmetric with respect to the inversion center (ungerade, u). In the C_{8v} point group, the p_z orbital is symmetric with respect to rotation by $2\pi/n$ about the principal axis (A), but since in C_{8v} symmetry there are no perpendicular C_2 axes, then the p_z orbital is sym-

metric with respect to a vertical plane of symmetry (1).[11] The is no inversion center in C_{8v} symmetry. The other changes in symmetry are shown in Table 4.4. If the results of simply considering the effects of restricting the free [8]annulene to C_{8v} symmetry are compared with the results from Table 4.2, it is seen that the only differences can be assigned as displacement of the entire ring and metal atoms. Therefore, by consideration of only the changes in the Mulliken symbols for the normal vibrational modes as a the [8]annulene dianion goes from D_{8h} to C_{8v} geometry, the correct normal modes of vibration for a "free" [8]annulene dianion in C_{8v} symmetry has been determined.

When a free D_{8h} [8]annulene dianion is placed in a sandwich arrangement with another free [8]annulene dianion the following changes occur. Although the symmetry of the sandwich is still D_{8h}, the horizontal plane of symmetry does not contain an [8]annulene ring. The consequence of this change is that there is a doubling of all observed normal vibrations for the molecule. For example, the A_{1g} modes of two independent [8]annulene rings become one A_{1g} and one A_{2u} mode in the sandwich arrangement. Again, this point is more easily demonstated by considering the addition of atomic orbitals. If one considers the addition of two s-type orbitals (A_{1g}) in a molecule with D_{8h} symmetry, the addition of two positive orbitals results in a new orbital that is still A_{1g}, whereas the addition of a positive s-type orbital with a negative s-type orbital gives a new orbital that has the same symmetry properties of the p_z orbital, which as shown earlier, is A_{2u} in the D_8 symmetry. Similar consideration of the other vibra-

tional modes leads to the result shown in Table 4.4. Again, the vibrational modes obtained by adding two [8]annulene differs from the result obtained for $M(C_8H_8)_2$ only by modes which can be assigned to the displacement of the entire ring and metal atoms.

The last column of Table 4.4 contains the result of constricting the bis([8]annulene) sandwich to C_{8v} symmetry. Thus, by considering only the allowed vibrational modes of a "free" [8]annulene dianion, the "ligand only" vibrational modes have been generated for the sandwich complexes.

What are the consequences of this treatment? First, ligand vibrations that appear in the infrared spectra of dipotassium [8]annulene, should also appear in the sandwich complexes. If the band is strong for the dianion, it should also be strong for the sandwich complex. Second, some of the bands which appear only in the Raman spectrum of [8]annulene dianion (specifically the A_{1g} and the E_{1g}) should appear in the infrared spectra of the sandwich complex (as A_{2u} and E_{1u}).

Table 4.4: Infrared and Raman Correlation Chart for [8]annulene complexes.

Mono([8]annulene)		Bis([8]annulene)		Assignment
D_{8h}	C_{8v}	D_{8h}	C_{8v}	
A_{1g}^{+}	$A_1^{+\ddagger}$	A_{1g}^{+} A_{2u}^{+}	$A_1^{+\ddagger}$ $A_1^{+\ddagger}$	ν(CH)
A_{1g}^{+}	$A_1^{+\ddagger}$	A_{1g}^{+} A_{2u}^{+}	$A_1^{+\ddagger}$ $A_1^{+\ddagger}$	ν(CC)
$A_{2g}^{\bullet}$	$A_2^{\bullet}$	$A_{2g}^{\bullet}$ A_{1u}	$A_2^{\bullet}$ A_2	
$E_{1g}^{\bullet}$	$E_1^{\bullet}$	$E_{1g}^{\bullet}$ $E_{1u}^{\ddagger}$	$E_1^{\bullet}$ $E_1^{+\ddagger}$	
E_{1g}^{+}	$E_1^{+\ddagger}$	E_{1g}^{+} $E_{1u}^{\ddagger}$	$E_1^{+\ddagger}$ $E_1^{+\ddagger}$	ρ(CH)
E_{2g}^{+}	E_2^{+}	E_{2g}^{+} E_{2u}	E_2^{+} E_2^{+}	ν(CH)
E_{2g}^{+}	E_2^{+}	E_{2g}^{+} E_{2u}	E_2^{+} E_2^{+}	ν(CC)
E_{2g}^{+}	E_2^{+}	E_{2g}^{+} E_{2u}	E_2^{+} E_2^{+}	β(CH)
E_{2g}^{+}	E_2^{+}	E_{2g}^{+} E_{2u}	E_2^{+} E_2^{+}	γ(CCC)
$A_{2u}^{\bullet}$	$A_1^{\bullet}$	A_{1g}^{+} $A_{2u}^{\bullet}$	$A_1^{+\ddagger}$ $A_1^{\bullet}$	
$A_{2u}^{\ddagger}$	$A_1^{+\ddagger}$	A_{1g}^{+} $A_{2u}^{\ddagger}$	$A_1^{+\ddagger}$ $A_1^{+\ddagger}$	ρ(CH)
$E_{1u}^{\bullet}$	$E_1^{\bullet}$	E_{1g}^{+} $E_{1u}^{\bullet}$	$E_1^{+\ddagger}$ $E_1^{\bullet}$	
$E_{1u}^{\ddagger}$	$E_1^{+\ddagger}$	E_{1g}^{+} $E_{1u}^{\ddagger}$	$E_1^{+\ddagger}$ $E_1^{+\ddagger}$	ν(CH)
$E_{1u}^{\ddagger}$	$E_1^{+\ddagger}$	E_{1g}^{+} $E_{1u}^{\ddagger}$	$E_1^{+\ddagger}$ $E_1^{+\ddagger}$	ν(CC)
$E_{1u}^{\ddagger}$	$E_1^{+\ddagger}$	E_{1g}^{+} $E_{1u}^{\ddagger}$	$E_1^{+\ddagger}$ $E_1^{+\ddagger}$	β(CH)
E_{2u}	E_2^{+}	E_{2g}^{+} E_{2u}	E_2^{+} E_2^{+}	ρ(CH)
E_{2u}	E_2^{+}	E_{2g}^{+} E_{2u}	E_2^{+} E_2^{+}	χ(CCC)

•=translation or rotation. +=Raman active. ‡=Infrared active.

Applications

The Structure of $K_2[M(C_8H_8)_2]$.

The D_{8h} symmetry of the class $K_2[M(C_8H_8)_2]$ was predicted by infrared spectra prior to the determination of the structure of $[K(C_6H_{14}O_3)]_2[Yb(C_8H_8)_2]$ by single crystal x-ray diffraction.[12] In Table 4.5, the infrared spectrum of $K_2[Yb(C_8H_8)_2]$ is compared with both the infrared and Raman spectra of $K_2C_8H_8$ in the 600-1000 cm^{-1} range.

As predicted, the strong infrared bands of dipotassium [8]annulene are observed in the infrared of dipotassium bis-([8]annulene)ytterbium(II). Also, the band in the Raman spectrum of dipotassium [8]annulene at 737 cm^{-1} (A_{1g}) is present in the infrared spectrum of dipotassium bis([8]annulene)ytterbium(II) (A_{2u}). Thus, the infrared spectrum of $K_2[M(C_8H_8)_2]$ in the 600-1000 cm^{-1} region is exactly what one would predict from consideration of the free ligand vibrations.

Since the infrared spectra of $K_2[Yb(C_8H_8)_2]$ and $K_2[Ca(C_8H_8)_2]$ are identical, then it is also obvious that the strong band at ≈680 cm^{-1} cannot be due to any vibrational mode involving the metal, since the position of this band is not affected by the change of the central metal atom. Any infrared active vibration involving the central metal should occur at vastly different

Table 4.5: Comparison of the vibrational spectra of $K_2C_8H_8$ with the infrared spectrum of $K_2[Yb(C_8H_8)_2]$ in the 600-1000 cm^{-1} range.

$K_2C_8H_8$		$K_2[Yb(C_8H_8)_2]$	Assignment
Raman	Infrared	Infrared	
	675 vs	683 vs	ρ(CH) A_{2u}
710 w		not observed[a]	ρ(CH) E_{1g},E_{1u}
737 s		740 m	ν(CC) A_{1g},A_{2u}
	880 s	888 s[b]	β(CH) E_{1u}

(a) Region obscured by Nujol absorbance. (b) split peak 879,888.

frequencies due to the difference in mass between calcium and ytterbium. Comparison of the infrared spectra of bis([8]annulene)uranium(IV) and bis([8]annulene)ytterbate(II) dianion (Table 2.6) clearly indicates that the strong band at ≈690 cm^{-1} in the infrared spectrum of the actinide complex is also the out-of-plane hydrogen bending, $\rho(A_{2u})$.

The structure of $Yb(C_8H_8)$ Polymer

Although $Yb(C_8H_8)$ is not crystalline, its structure can be deduced from its infrared spectrum. In Table 4.6, the infrared spectrum of $Yb(C_8H_8)$ is compared with both the infrared spectrum and the Raman spectrum of $K_2C_8H_8$ in the 600-1000 cm^{-1} range.

In this case, the Raman active bands in the [8]annulene dianion do not appear in the infrared spectrum of $Yb(C_8H_8)$. The results in table 4.4 predict that the Raman band at 737 cm^{-1} (A_{1g}) should appear in the infrared spectrum of $Yb(C_8H_8)$ (assuming C_{8v} symmetry) as A_1. This does not happen.

Since the infrared spectra of $K_2C_8H_8$ and YbC_8H_8 are identical (except for minor shifts in observed frequencies of the vibrations), it is then assumed that these complexes have similar structures. The only way that $Yb(C_8H_8)$ can have the same structure as $K_2C_8H_8$ is for YbC_8H_8 to exist as a polymer, as shown in Figure 4.1.

<u>Table 4.6</u>: Comparison of the vibrational spectra of $K_2C_8H_8$ with the infrared spectrum of $Yb(C_8H_8)$ in the 600-1000 cm^{-1} range.

$K_2C_8H_8$		$Yb(C_8H_8)$	Assignment
Raman	Infrared	Infrared	
	675 vs	678 vs	ρ(CH) A_{2u}
710 w			ρ(CH) E_{1g}
737 s			ν(CC) A_{1g}
	880 s	888 s	β(CH) E_{1u}

Figure 4.1: Proposed Polymeric Structure for $Yb(C_8H_8)$.

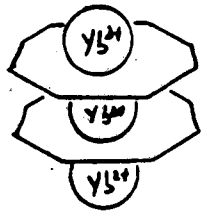

The Structure of $K[Ln(C_8H_8)_2]$

The crystal structure of $[K(C_6H_{14}O_3][Ce(C_8H_8)_2]$ indicates that the [8]annulene rings are in a staggered conformation making the symmetry of the bis([8]annulene)cerium(IV) anion D_{8d}. However, since the barrier to ring rotation in the solid is essentially 0 kcal/mole,[13] then it is not unexpected, depending on the infrared sample preparation, that the rings could exist in an eclipsed conformation, making the symmetry of the sandwich anion D_{8h} and the symmetry of the molecule C_{8v}. If $K[Ln(C_8H_8)_2]$ exists in C_{8v} symmetry, then one would predict that there would be pairs of vibrations. As a case in point, consider the ρ(CH) A_{2u} of dipotassium [8]annulene. This molecular vibration can be depicted

as shown in Figure 4.2. The addition of two of these vibrations (and still maintaining D_{8h} symmetry) gives an A_{1g} and an A_{2u} vibrational mode for the sandwich complex. The A_{1g} should appear at higher energy relative to the A_{2u}. In C_{8v} symmetry, both of these vibrations become A_1 and should occur as a pair of vibrations in the infrared of C_{8v} $K[Ln(C_8H_8)_2]$. There are no pairs of vibrations in the infrared spectra of the class $K[Ln(C_8H_8)_2]$ (Table 4.7).

As is the case for $Yb(C_8H_8)$, $K[Ln(C_8H_8)_2]$ can obtain D_{8h} by forming a polymer like the one shown in Figure 4.3. This polymer has the same symmetry properties of bis([8]annulene)uranium(IV) and bis([8]annulene)ytterbium(II) dianion, so it is not unexpected that solvent-free $K[Ln(C_8H_8)_2]$ should have the same infrared spectra as the D_{8h} sandwich complexes. Since the classes $M(C_8H_8)_2$, $K[M(C_8H_8)_2]$ and $K_2[M(C_8H_8)_2]$ all appear to have similar symmetry, the changes in infrared spectra as a result of changes in the central metal atom can be studied.

Figure 4.2

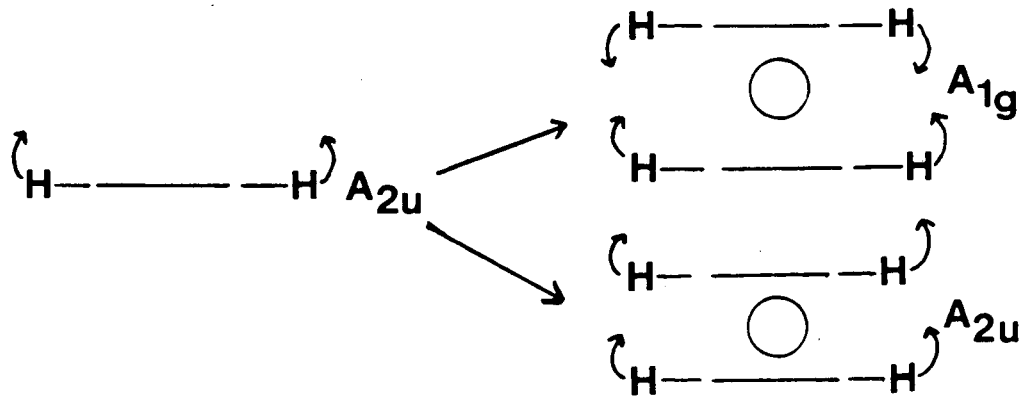

Table 4.7: Infrared Spectra of $K[Ln(C_8H_8)_2]$ in the 600-1000 cm^{-1} range (Nujol mulls).

Ln = La[a]	Ce	Pr	Yb
680 vs	675 vs	680 vs	690 vs
740 m	740 m	740 m	741 s
771 w	773 w	775 w	770 w
892 s	890 s	890 s	899 s

(a) from reference 4b.

Figure 4.3: Proposed Polymeric Structure for $K[Ln(C_8H_8)_2]$.

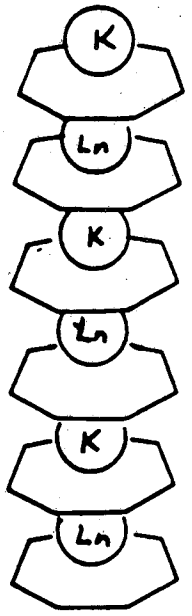

Effect of the Central Metal on the Infrared Spectra (600-1000 cm^{-1}) of [8]Annulene Complexes

The infrared spectra of $Ce(C_8H_8)_2$ and $K[Ce(C_8H_8)_2]$ are shown in Figure 4.4. As predicted, the two infrared spectra are almost identical. The only major differences in the two spectra in the 600-1000 cm^{-1} region are the positions of the strong bands. Table 4.8 lists the positions of the infrared bands for the bis-([8]annulene) complexes of cerium(IV) and cerium(III), along with the infrared spectra of the bis([8]annulene) complexes of ytterbium(III) and ytterbium(II).

In the pair of complexes involving different oxidation states of the same element, the shift of the bands assigned as CH bending is toward higher energy as the oxidation state increases. However, the band assigned to carbon-carbon vibration appears to be unaffected by the change in central metal atom oxidation state. The best explanation for these shifts is from the change in ionic radius of the central metal atom. The higher oxidation state for a given atom has a smaller ionic radius for a given coordination number. Assuming that the metal-ring carbon distance is determined by the addition of the ionic radii of the metal atom (coordination number 10) to the ionic radii of carbon in [8]annulene dianion results in the ring-ring distance becoming smaller as the formal oxidation state of the central metal atom increases. As suggested by figure 4.2, the out of plane CH

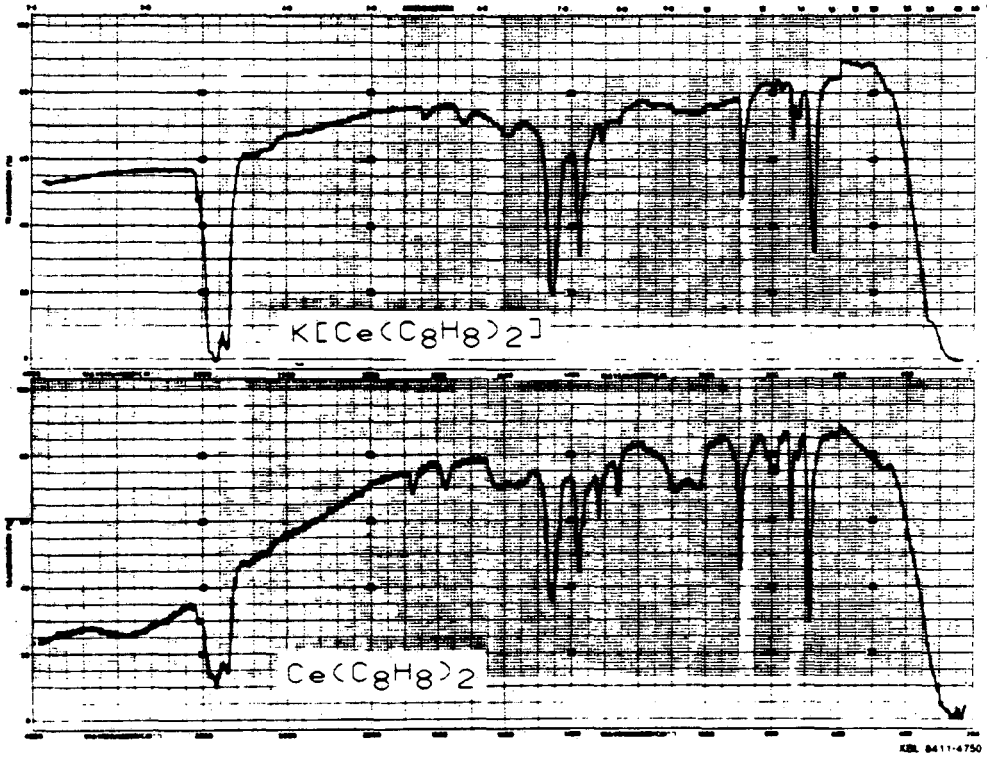

Figure 4.4: Infrared Spectra of $Ce(C_8H_8)_2$ and $K[Ce(C_8H_8)_2$ (Nujol mulls)

bending (A_{2u}) should be greatly affected by the intra-ring distance. It also follows that the CH bending modes should be more affected than the CC modes by intra and inter molecular forces.

The above arguements suggest that any differences in energies for the infrared absorptions in the free ligand can be rationalized by changes in the inter-ring distance; which, as shown by Raymond,[14] are determined by the ionic radii of the central metal atom and not by covalent interactions. Of course, the preparation of infrared samples can affect the infrared spectrum of a compound, but within the constraint of similar spectra indicating similar geometries, the energies of the free-ligand vibrations indicate nothing about ligand-metal orbital overlap in the bis-([8]annulene) complexes.

Table 4.8: Infrared Spectra of Bis([8]annulene) Sandwich Complexes with varying oxidation states of the central metal atom.

Ce(C8H8)2	K[Ce(C8H8)2]	K[Yb(C8H8)2]	K2[Yb(C8H8)2]	
687 vs	675 vs	690 vs	683 vs	ρ(CH)
740 m	740 m	741 s	740 m	ν(CC)
770 w	773 w	770 w		
785 w				
896 s	890 s	899 s	888 s[a]	β(CH)

(a) split peak 879,888.

Conclusion

The infrared spectra of [8]annulene sandwich complexes in the 600-1000 cm^{-1} region can be indicative of an eclipsed arrangement of the [8]annulene rings. The vibrations in this region involve only CH an CC movement, not ring-metal displacements, as suggested by Goffart. For two [8]annulene sandwich complexes involving same central metal atoms in different oxidation states, the position of the ρ(CH),A_{2u} and the β(CH), E_{1u} are expected to occur at a higher frequency for the molecule with the central metal atom in the higher oxidation state. The shifts in frequency in the bands in the 600-1000 cm^{-1} range can be explained in terms of the ionic radii of the central metal atom. Thus, no conclusions on the amount of ring-metal orbital interactions in bis([8]annulene) sandwich complexes can be drawn by consideration of their infrared spectra in the 600-1000 cm^{-1} range.

References and Notes

1. Lippincott, E.R.; Nelson, R.D. *Spectrochim. Acta* 1958, *10*, 307.

2. See; Cotton, F.A. "Chemical Applications of Group Theory" Wiley and Sons, New York, N.Y., 1963.

3. Hocks, L.; Goffart, J.; Duyckaerts, G.; Teyssié *Spectrochim. Acta* 1974, *30A*, 907.

4. (a) Aleksanyan, V.T.; Garbuzova, I.A.; Chernyshova, T.M.; Todres, Z.V. *J. Organometal. Chem.* 1980, *201*, 1. (b) Aleksanyan, V.T.; Garbuzova, I.A.; Chernyshova, T.M.; Todres, Z.V. *J. Organometal. Chem.* 1981, *217*, 169.

5. (a) Brunvoll, J.; Cyvin, S.J.; Schäffer, L. *J. Phys. Chem.* 1971, *54*, 1517. (b) Brunvoll, J.; Cyvin, S.J.; Schäffer, L. *J. Organometal. Chem.* 1971, *27*, 69.

6. Karraker, D.G.; Stone, J.A.; Jones, E.R., Jr.; Edelstein, N. *J. Am. Chem. Soc.* 1970, *92*, 4841.

7. Jolly, W.L. "The Synthesis and Characterization of Inorganic Compounds," Prentice-Hall, Englewood Cliffs, N.J.

8. Name after R.S. Mulliken. See ref. 2, p. 71.

9. Salthouse, J.A.; Ware, M.J. "Point Group Character Tables and Related Data" Cambridge Univ. Press, Cambridge, G.B., 1971.

10. Fritz, H.P. *Adv. in Organometal. Chem.* 1964, *1*, 240.

11. For further discussion of the assignment of Mulliken symbols to irreducible representations, see ref. 2, chap. 4.

12. Kinsley, S.A.; Streitwieser, A., Jr. *LBL Report #15018* 1981.

13. Anderson, S.E. *J. Organometal. Chem.* 1974, *71*, 263.

14. Raymond, K.N.; Eigenfrot, C.W., Jr. *Acc. Chem. Res.* 1980, *13*, 276; Baker, E.C.; Halstead, G.W.; Raymond, K.N. *Struct. & Bonding* (Berlin) 1976, *25*, 23.

This report was done with support from the Department of Energy. Any conclusions or opinions expressed in this report represent solely those of the author(s) and not necessarily those of The Regents of the University of California, the Lawrence Berkeley Laboratory or the Department of Energy.

Reference to a company or product name does not imply approval or recommendation of the product by the University of California or the U.S. Department of Energy to the exclusion of others that may be suitable.

TECHNICAL INFORMATION DEPARTMENT
LAWRENCE BERKELEY LABORATORY
UNIVERSITY OF CALIFORNIA
BERKELEY, CALIFORNIA 94720